STUDIES ON DISSOLUTION OF SOLID IN LIQUIDS

by

CHU-DUC-KHAI

DEPARTMENT OF METALLURGICAL ENGINEERING

INDIAN INSTITUTE OF TECHNOLOGY, KANPUR

JULY, 1987

STUDIES ON DISSOLUTION OF SOLID IN LIQUIDS

A Thesis Submitted
In Partial Fulfilment of the Requirements
for the Degree of

MASTER OF TECHNOLOGY

by
CHU-DUC-KHAI

to the

DEPARTMENT OF METALLURGICAL ENGINEERING

INDIAN INSTITUTE OF TECHNOLOGY, KANPUR

JULY, 1987

STUDIES ON DISSOLUTION OF SOLID IN LIQUIDS

By : CHU DUC KHAI
ROLL : 8510606

Name of student: CHU DUC KHAI ROLL NO. 8510606
Department : Metallurgical Engg. Programme : M.Tech.
Title of the thesis: Studies on dissolution of solid in liquids.
Thesis supervisor: Dr. S.C. KORIA.

ABSTRACT

An experimental study is conducted to study the dissolution of solid additive in gas stirred steel melts by using a low temperature mass transfer system. Influence of gas flow rate, position of introduction of the additive, aspect ratio of the bath, centre and off centr injection on the rate of dissolution of additive are investigated.

It is found that an increase in gas injection rate increases the rate of dissolution. Location of the gas injecting nozzle and introduction of additive, temperature of the bath, aspect ratio of the bath, different types of additive are all found to influence the rate of dissolution. A cubic rate law is found to describe the process of dissolution.

In this thesis, the above results are presented. About the organization of the thesis contents chapter 1 deals with introduction. In chapter 2 simulation criteria are discussed. Chapter 3 describes the experimental part of the thesis. Experimental observations and results are presented in chapters 4 and 5. Discussions of results constitute the chapter 6. The applications of results are discussed in chapter 7. In chapter 8 and 9 conclusions and suggestion for further work are given.

C O N T E N T S

Chapter 4

Chapter 5

EXPERIMENTAL RESULTS

Chapter 6

DISCUSION OF RESULTS

Chapter 7

APPLICATION TO INDUSTRIAL SYSTEMS

LIST OF TABLE

LIST OF FIGURES

AKNOWLEDGEMENTS

The author is deeply indebted to his thesis supervisor, Dr. S.C. Koria who not only initiated the problem but also rendered invaluable guidance and encouragement at every stage through out the course of this work.

This association with Dr. S.C. Koria has been highly rewarding and memorable.

The author also extends his warm gratitude to Professor T.R. Ramachandran (I.I.T. KANPUR), for his advice and encouragement.

The author takes this opportunity to thank all faculty members, staff of workshop, graphic arts and T.V. Central Section for their constant help during the experimental investigation.

- CHU DUC KHAI

C E R T I F I C A T E

Certified that the work presented in this thesis has been carried out under my supervision and that the work has not been submitted elsewhere for a degree.

Dr. [illegible]
Assistant Professor,
Department of Water Resources Engg.
Indian Institute of Technology, KANPUR

SYNOPSIS

An experimental study is conducted to study the dissolution of solid additive in gas stirred steel melts by using a low temperature mass transfer system. Influence of gas flow rate, position of introduction of the additive, aspect ratio of the bath, centre and off centre injection on the rate of dissolution of additive are investigated.

It is found that an increase in gas injection rate increases the rate of dissolution. Location of the gas injecting nozzle and introduction of additive, temperature of the bath, aspect ratio of the bath, different types of additive are all found to influence the rate of dissolution. A cubic rate law is found to describe the process of dissolution.

In this thesis, the above results are presented. About the organization of the thesis contents chapter 1 deals with introduction. In chapter 2 simulation criteria are discussed. Chapter 3 describes the experimental part of the thesis. Experimental observations and results are presented in chapters 4 and 5. Discussions of results constitute the chapter 6. The applicationsof results are discussed in chapter 7. In chapter 8 and 9 conclusionsand suggestions for further work are given.

CHAPTER I

INTRODUCTION

1.1 GENERAL

Ferro-alloys and metallic materials are very commonly added to steel-melts for deoxidation, alloying, desulphurization inclusion shaping etc. at various stages of steelmaking. A number of techniques are employed in the practice to add the solid additives to steel melt e.g.[1-5].

(a) directly in the steelmaking plant (open hearth furnace or converter);

(b) to the metal jet tapped from the steelmaking plant;

(c) into the bulk of metal in the ladle;

(d) to the metal jet following from the ladle into a mould or continuous casting machine;

(e) into a ladle placed in a vacuum chamber.

In all above techniques it is important that the additive should be dissolved and incorporated homogeneously in to large volumes of steel melt during the time of treatment.

It is an established fact that mixing and metal circulation play an important, often dominant role in determining the rate of dissolution[1-5]. Among the various methods induction stirring,

vacuum circulation of achieving mixing of liquid, gas injection is very widely employed to homogencize the steel bath with reference to concentration and temperature stratifications[1-5].

It is thought that during gas purging of molten steel in ladles, additions of metallic materials and ferro-alloys could also be made in order to extend gas injection procedure to alloying of liquid steel, composition adjustment etc. purposes[6]. It is with this objective the present investigation is undertaken to collect the experimental data on the rate of dissolution of the solid additive.

1.2 DISSOLUTION OF SOLID

1.2.1 Theoretical background

A most basic reaction of solid with liquid is the dissolution of solid into liquid, when the solubility exists. At the moment a solid contacts with a liquid, the dissolution of the solid into the liquid occurs. A theoretical basis for the kinetics of dissolution of solids in liquids has been formulated from the studies of the dissolution of inorganic and organic salts in water and non-aqueous solvents[7-10]. Similar studies have also been reported in metal system[11-19].

The over-all rate of dissolution is governed by the relative magnitudes of two separate rates, namely - the rate at which atoms solvate from the solid surface into the liquid layer immediately adjacent to the solid, and the rate at which solutes

diffuse from the liquid layer into the bulk of the liquid. By considering these two processes, the following relation for the rate of dissolution may be derived[15].

$$n = n_s \left\{ 1 - \exp \left[- \frac{k_s(D/\delta)}{k_s-(D/\delta)} \cdot \frac{A}{V} \cdot t \right] \right\} \tag{1}$$

$$\text{or} \quad \frac{dn}{dt} = \frac{k_s(D/\delta)}{k_s-D/\delta} \frac{A}{V} (n_s - n) \tag{2}$$

All the symbols and their meaning are given in Table 1. The above mentioned relation can be indicated by the following expression[15].

$$n = n_s \left\{ 1 - \exp \left[- k \frac{A}{V} t \right] \right\} \tag{3}$$

$$\text{or} \quad \frac{dn}{dt} = k \frac{A}{V} (n_s - n) \tag{4}$$

Here k is the dissolution rate constant

$$k = \frac{k_s(D/\delta)}{k_s-D/\delta} \tag{5}$$

If the dissolution process is controlled by the interface the rate constant is given by[15].

$$k = k_s \tag{6}$$

On the other hand, if the dissolution process is controlled by the diffusion, the rate constant is given by

$$k = \frac{D}{\delta} \tag{7}$$

TABLE - 1 Symbols and their Meanings

1	A	Dissolving area of the additive
2	A_o	Initial area of the additive
3	a	area of the nozzle
4	C	concentration
5	c_s	Saturation concentration of the additive
6	d	diameter of the nozzle
7	D	diameter of the vessel
8	g	acceleration due to gravity
9	H	bath height
10	k	constant in equation 7 (dissolution rate constant)
11	m_o	initial mass of the model additive
12	m_t	mass after time t
13	N_D	distribution number for gas injection
14	N_{Fr}	modified Froude number
15	N_{Re}	Reynold's number
16	Q	gas injection rate
17	r	radial coordinate
18	r_n	radial position of the nozzle at the base of the vessel
19	t	time in minutes
20	u	superficial gas injection velocity
21	Z	axial location distance
22	$\rho_g \rho_l$	densities of gas and liquid
23	μ_g	viscosity of gas
24	δ	

TABLE - 1 Symbols and their Meanings

1	A	Dissolving area of the additive
2	A_o	Initial area of the additive
3	a	area of the nozzle
4	C	concentration
5	c_s	Saturation concentration of the additive
6	d	diameter of the nozzle
7	D	diameter of the vessel
8	g	acceleration due to gravity
9	H	bath height
10	k	constant in equation 7 (dissolution rate constant)
11	m_o	initial mass of the model additive
12	m_t	mass after time t
13	N_D	distribution number for gas injection
14	N_{Fr}	modified Froude number
15	N_{Re}	Reynold's number
16	Q	gas injection rate
17	r	radial coordinate
18	r_n	radial position of the nozzle at the base of the vessel
19	t	time in minutes
20	u	superficial gas injection velocity
21	Z	axial location distance
22	$\rho_g \rho_l$	densities of gas and liquid
23	μ_g	viscosity of gas
24	δ	

Equation 1 or 2 has been derived assuming that the area solid/liquid interface during dissolution is invariant[15]. When the area is variable, it is necessary to modify the dissolution rate equation by taking the change of area into account[8,9].

1.2.2 Literature review

Many investigators have studied the dissolution of solid in liquid using low or high temperature mass transfer system[7-10]. In a low temperature mass transfer system dissolution of acid in water is mostly investigated[7-10]. Whereas in high temperature dissolution of metallic materials or ferro-alloys in molten metal bath are studied[1-5,11-19]. They have determined the mass transfer coefficient from the measurement of dissolution vs. time data by using equations 2 or 4 and assuming a constant surface area of the solid[7-10,11-19]. This assumption is probably acceptable in many situations (where the solubility is extremely small e.g. dissolution of benzoic acid in water), but in others (where solubility is appreciable) it may not have been valid. Various empirical correlations are proposed to calculate the mass transfer coefficient. A list of

Except where the solid surface presented to the action of the liquid is plane, there is a constant change in its area, and thereby a slowing down of the rate of dissolution, for it is almost an axiom in chemical philosophy that the rate of chemical action is directly proportional to the surface exposed to that action[9].

Several attempts have been made by many investigators theoretically[8] and experimentally to take into account the effects of changing surface area of the solid on the rate of dissolution. Brian and Hales have presented a theoretical analysis of the above problem by solving equation of continuity for mass or heat diffusion numerically for a sphere in a steady unidirectional viscous fluid flow[8]. Guthrie and Stubb have applied a correction factor to their rate data using Brian and Hales correlation and determined a true mass transfer coefficient for melting dissolution of scrap in in a steel bath[5]. Other investigators have derived rate expresions for the dissolution of solid by taking into account the reducing rate of the cylinder radius[13,16,18]. Height of the cylinder was assumed to be constant[13,16-18]. The resulting equations to calculate dissolution rate constant are, although fundamental in nature, but too much complicated for practical use.

1.3 FACTORS INFLUENCING THE DISSOLUTION OF SOLID

The rate at which a given mass of a solid dissolves in a liquid depends on the following factors[9]:

(1) The specific surface of the particles of the solid or their average surface per unit weight.

(2) The shape characteristics of the particles, which determine the specific surface in that as they approach those of a sphere the specific surface approaches a minimum. Therefore for fast rates, the particles should be angular, sharp, and fagged as possible.

(3) The diffusion coefficient of the solid for the given liquid. Other things being equal the rates of solution of two different solids in the same liquid should vary directly as their diffusion coefficients.

(4) The agitation of the liquid in contact with the surface of the solid.

(5) The temperature affects the rate of solution in two ways, it changes the solubility and it increases the actual velocity itself through its kinetic influence.

(6) The concentration of the dissolved solid already in solution.

(7) The viscosity of the liquid. This affects the rate of diffusion and must be taken into account while comparing the rate of dissolution in two different mass transfer systems.

(8) The relative density relationships of the solid, liquid and solution will have much to do with the rate of solution. For instance, the formation of currents of the more dense solution may cause motion of the liquid in the neighbourhood of the solid.

1.4 HYDRODYNAMIC CONDITIONS OF THE BATH

Among the list of the above factors, agitation in the liquid strongly influences the rate of dissolution. Agitation in the liquid can be provided either by natural convection or forced convection i.e. by gas injection[1-5], electromagnetic field or by mechanical means. Gas injection is more commonly used to stirr the metallurgical liquid systems[1-5].

Many investigators have studied the submerged injection of gases in liquids theoretically and experimentally[12,20-23]. The aim was to determine the velocity fields in the liquid caused by gas injection[12,20-23]. It is generally accepted that the velocity of the liquid induced by gas injection strongly depends upon bath height and location of gas injecting nozzle[12,20-23]. For a centrally located single nozzle liquid velocity is highest at the top surface of the bath and near the Plume, whereas it is lowest at the bottom of the bath[12,20-23]. A quantitative relationship to calculate the liquid velocity induced by a centrally gas injecting nozzle at the top surface of the bath has been proposed by many investigators[12,20-23]. The liquid velocity at the top surface of the bath can be calculated with reasonable accuracy[12,20-23]. No such relationships are available in the literature to calculate the velocity at the bottom of the bath. Similarly for off-centre location of the nozzle no empirical relationship could be found in the literature to calculate the liquid velocity in the bath.

The appropriate relationships are given in the discussion part of the thesis.

1.5 OBJECTIVES OF THE PRESENT INVESTIGATION

The present investigation is undertaken with the following objectives:

(I) to collect the experimental data on the rate of dissolution of solid of changing surface area in the liquid and to describe the process of dissolution by a rate law,

(II) to find out the most favourable position of introduction of the additive in the liquid for a given location of the gas injecting nozzle,

(III) to determine optimum gas injections rate with reference to dissolution of the solid.

(IV) to determine the liquid velocity induced by gas injection at various locations in the liquid.

Chapter 2

SIMULATION CRITERIA

In the actual practice ferro-alloys and metallic materials (here after called 'additives') are added in steel melts at around 1600^{o}C[4,6,24]. These additives are denser and lighter than steel melt[4,6,14]. The present study concerns with the dissolution of dense solid additives in gas stirred melts. These additives sink in the bath unless they are not otherwised added.

According to Guthrie and Coworkers the mass transfer kinetics is slower than heat transfer kinetics for dissolution of an additive with melting point and density higher than liquid steel[1-4]. Under such circumstances the term dissolution indicates a process of transformation of the solid into its dissolved and distributed products[1-4]. From this it follows that dissolution process of additives under steelmaking conditions can be simulated by a low temperature mass transfer system. Such a system is easier to handle in the laboratory than large quantity of liquid steel.

In the present investigation the oxalic acid compacts (model additive) are dissolved in water (model bath[6]). Model bath dimensions and gas flow rates are determined by calculating the various dimensionless numbers relevent to submerged injection of gasses in steel melts[20-22,25-28]. The aspect ratio of the bath governs whether the bath is shallow or deep and determines the assimilation of agitation energy suplied to the bath[25,27]. In a deep bath the assimilation of a given energy is more efficient than in a shallow bath[25-27]. Its similarity generates similar flow

fields in the model bath and steel melts contained in industrial ladles[20-22].

Diameter of the model nozzle to inject the gas is determined by calculating the distribution number defined as[25,26].

$$N_D = \frac{d}{D} \tag{8}$$

All the symbols and their meanings are given in Table 1, its similarily ensures a similar distribution of gas within the model and industrial vessels[25,26].

Model gas flow rate is determined by the modified Froude number. Froude number is defined as[20-23,28]

$$N_{Fr} = \frac{\rho_g u^2}{\rho_l g H} \tag{9}$$

This number compares the gas dynamic pressure at the nozzle exit with the hydrostatic pressure at the same point. Its similarity ensures the same behaviour of gas at the exit of a nozzle submerged in the model liquid and steel melt[23,28]. The superficial velocity u is given by

$$u = \frac{Q}{A} = \frac{4Q}{\pi d^2} \tag{10}$$

From equation 9 and 10 one obtains after simplification

$$N_{Fr} = 0.0826 \frac{Q}{H.d^4} \cdot \frac{\rho_g}{\rho_l} \tag{11}$$

Reynolds number determines whether the flow of gas is laminar or turbulent. It is calculated by[25]

$$N_{Re} = \frac{d.u.\rho_g}{\mu.g} \qquad (12)$$

All these numbers are calculated using the data of liquid steel/solid additive system[20,22,24] and compared in Table 2 with the values of the present investigation. A closed similarity between the two excepted distribution numbers is self evident.

A higher distribution number at constant vessel diameter means larger diameter of the nozzle in the model investigation. Since gases are normally injected in steel melts in the bubbling mode[20-23,28], a larger diameter of the nozzle will further ensure a bubbling mode of injection in the present investigation. Therefore a higher distribution number in the model investigation should not affect the flow pattern induced in the liquid and hence dissolution process, by a rising gas liquid plume.

TABLE 2: Comparison of Characteristic parameters of gas injection in steel melts with model investigation.

	Numberical definition	Industrial ladle	Model Investigation	Significance
ect io	$\frac{H}{D}$	0.95-1.2	0.95-1.5	Shallow or deep bath and assimilation of energy supply to the bath.
tribution ber	$\frac{d}{D}$	4.33×10^{-3}	6.67×10^{-3} [φ]	distribution of gas in the vessel
ified ude ber	$\frac{\rho_g u^2}{\rho_l gH}$	0.96-1.3	0.185 to 14.69	governs the discontinuous or continuous presence of gas at the exit of the nozzle submerged in the liquid.
nold's ber	$\frac{du\rho_g}{\mu g}$	10^5	3.5×10^3 to 14×10^4	Laminar or turbulent jet
e itive	density	Some additives have density higher than liquid steel e.g.Mo,W,Cr, Mn, etc.	Oxalic acid	Signifies buoyant non-buoyant addition.

higher distribution number is deliberately employed in order to inject the gas in the bubbling mode corresponding to the actual practice.

Chapter 3

EXPERIMENTAL

.1 EXPERIMENTAL SETUP

The apparatus used in the experiment is shown in Fig.1. The ystem includes a perspex glass vessel (14 cm ϕ x 40 cm high), a ozzle (1 mm ϕ), a gas bottle and capillary flow meter[6]. The bottom f the vessel is made detachable in order to be able to fix the nozzle t any radial position[6]. The flow rate of nitrogen gas is measured by calibrated capillary flowmeter. Temperature of the bath is measured y a thermometer.

Nitrogen is introduced either through the bottom or top of he vessel.

In order to determine the liquid velocity at various locations n the bath, the dissolving solid is plunged by a cage-wire arrangement.

.2 CHOICE OF MASSTRANSFER SYSTEM

Following the process of dissolution of solids with melting oint higher than liquid steel (solids after an initial period of eating to steel bath temperature simply dissolve in large volumes f liquid steel and as such dissolution represents a process of ransformation of solid into its dissolved product) a low temperature ass transfer system such as dissolution of acid in water is selected or this investigation. Such a system is easier to handle in the aboratory than large quantities of liquid steel.

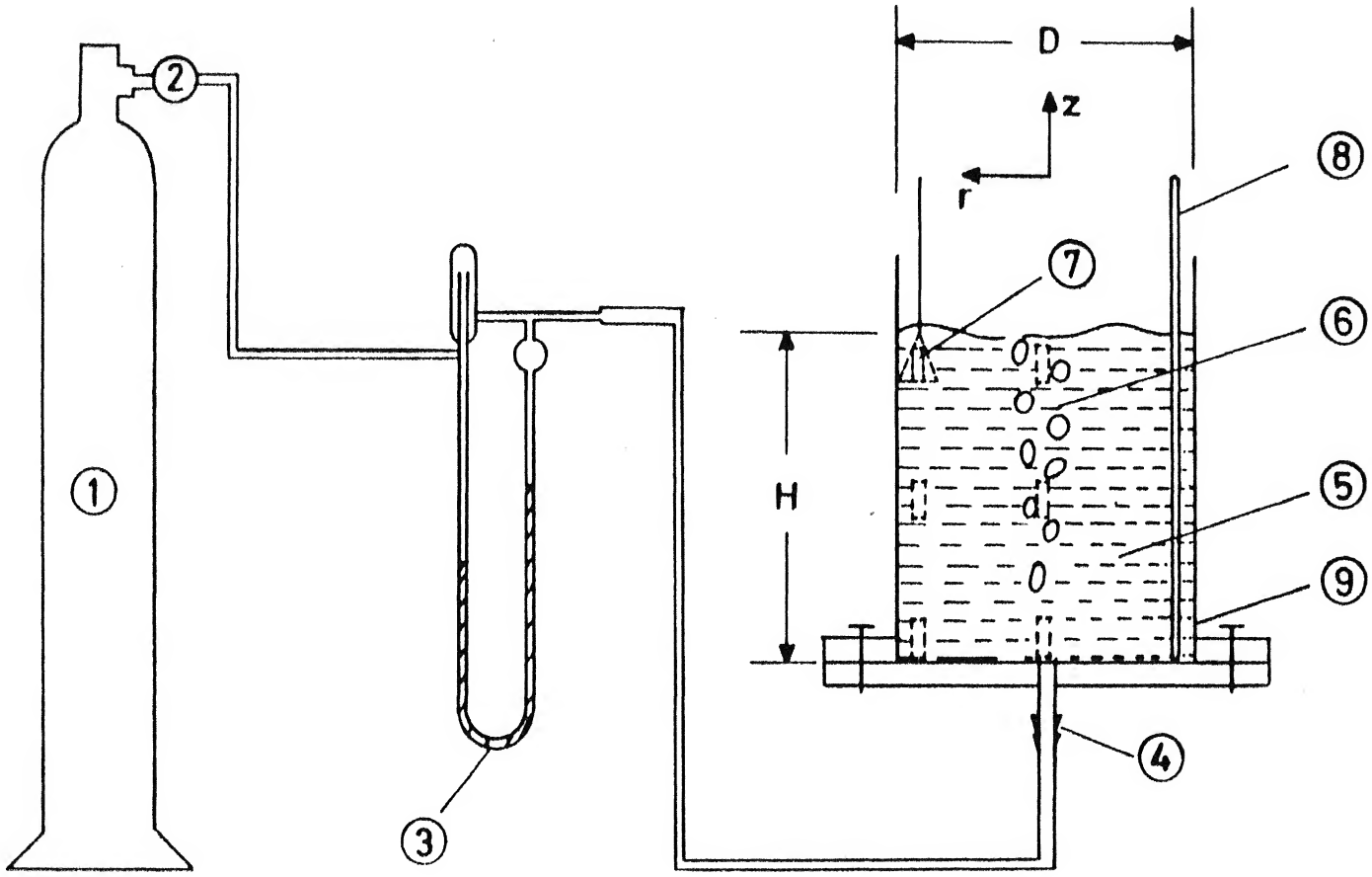

① Gas bottle

② Pressure regulator

③ Differential manometer cum flow meter

④ Model nozzle

⑤ Model bath

⑥ Bubble plume

⑦ Model additive

⑧ Thermometer

⑨ Model vessel

Fig. 1. Experimental arrangement to investigate the dissolution of solid additive in gas stirred liquid bath.

Based on the above consideration and noting that dissolution of the solid often follows with change in its surface area, acids of different solubility in water are used. These acids are oxalic acid, succinic acid, boric acid and benzoic acid.

Cylindrical compact (mass 10g; diameter = 2.33 cm and height = 1.58 cm) of the above acids are made at a pressure of 6.9×10^7 N/m^2 and used in the present investigation. The actual mass of the compact is varies from 9.62 g to 10.14 g and height from 1.52 mm to 1.60 mm.

3.3 EXPERIMENTAL METHOD

In the experiments the amount of solid dissolved in water is determined as a function of time. In preliminary investigations several methods are tried to determine the amount of solid dissolved in liquid[6]. In one method this amount is determined by measuring the initial weight and weight of the solid after drying at a dissolution time t[6]. This method has not given accurate results because of the problems associated with drying of the acids used in this investigation (when the additive is dried in the owen, it may undergo varying amounts of decomposition so this process had not been for estimation purpose).

In another method the amount dissolved is determined by titrating a known volume of the liquid after dissolution. Finally the amount dissolved is also determined by measuring the diameter and height of the compact as a function of time (By diameter and height of the compact is determined Multiplying this volume by the density of the acid compact, weight of the remaining solid is obtained.

Substraction of this weight from initial weight gives the amount of acid dissolved in liquid.).

Both the above methods are compared in Fig.2 . Both the methods have given comparable results.

In the experimental programme of this investigation the amount of acid dissolved is determined by measuring the dimensions of the compact as a function of dissolution time. This method is simple and is free from subjective errors in comparison to titration method.

3.4 EXPERIMENTAL PROCEDURE

Experiments are performed in accordance with the objectives of the present investigation.

The experimental procedure consists of measurement of the amount of acid dissolved in water as a function of time. Water of desired volume is taken in the vessel and the gas flow rate is adjusted to a known value. The cage with the model additive is then introduced into the agitated liquid. After a definite interval of time the additive is withdrawn from the vessel and its dimensions are measured. In this way the experiments are performed.

The following variables are included in this study:

(1) Gas flow rate: it is determined by the modified Froude number simulation and varied from 1 NL/min to 8.9 NL/min.

(2) Aspect ratio of the bath: it is varied from 0.9 to 1.5.

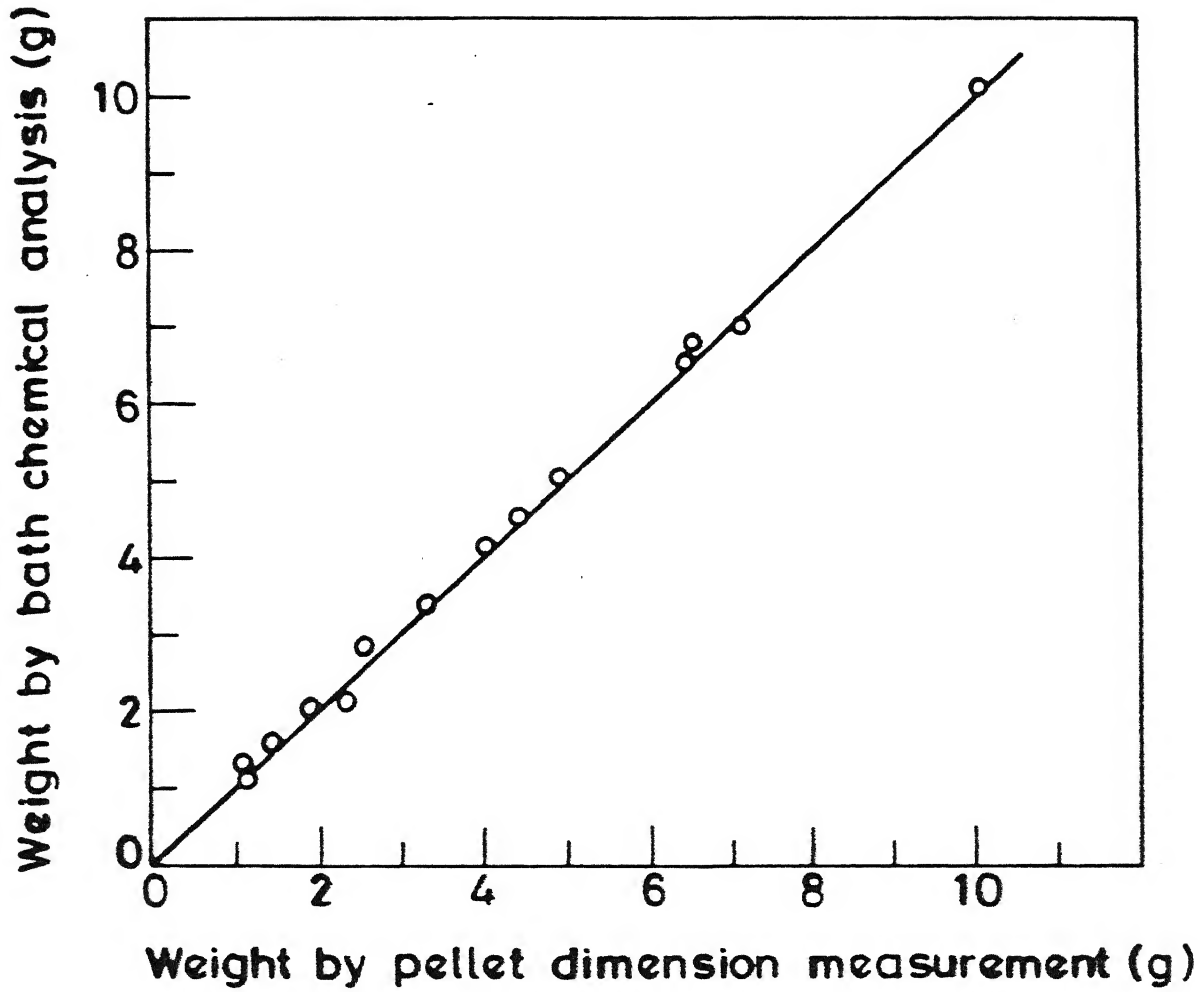

Fig. 2. Comparison of the amount dissolved determined by two independent methods, namely chemical analysis and dimensionaly measurement.

3. Location of the nozzle at the base and top of the vessel. For both the locations of the nozzle gas is injected either at the centre or off-centre of the vessel. For the off-centre injection of gas nozzle is radially moved upto 0.7 times vessel radius.

4. Introduction of the additive into the bath. Main positions are in the plume and annulus zone. In each position the additive is plunged at three different heights of the bath (see Fig.1) for bottom injection of gas.

   In top injection of gas the additive is kept either at top surface or bottom of the bath.

   Position of the additive is varied for both centre and off-centre injection of gas.

   These experiments are performed to determine indirectly the liquid velocity at that particular position of the additive.

5. Different types of additive: Four different types of acid are used. Oxalic, Succinic, boric and benzoic acid.

Chapter 4

VISUAL OBSERVATIONS

The visual observations have shown considerable difference in the behaviour of the model additive during the dissolution period[6]. This behaviour is observed to depend upon the position of the additive in the bath. For example, when the additive is plunged in the gas liquid plume (see Fig.3) a strong interaction between the gas bubble and the additive is observed. This has resulted in considerable oscillatory type of movement of the additive during the entire course of the dissolution period. A similar observation is also made for the additive when it is plunged in the top surface of the annulus zone ($r \simeq R$, $Z = H$ in Fig.3). Method of injection i.e. centre or off-centre injection has not been found to change the above observations.

However, method of injection has been found to influence considerably the behaviour of the additive lying at the bottom of the annulus zone($r \simeq R$ and $Z=0$ in Fig.3)[6]. Injection of gas through centre of the base of the vessel has resulted in no movement of the additive dissolving from the position referred to above. The additive remained almost still during the entire dissolution period. An increase in gas injection rate does not change the above behaviour. This shows the presence of relatively quiscent areas in the bottom layers of annulus zone as reported by many investigators.

Off-centre injection experiments have shown a considerable improvement in the behaviour of the additive dissolving from the bottom of the annulus zone. In these experiments the additive is not found to remain still during the dissolution period as compared to centre injection. This observation shows that off-centre injection imparts considerable agitation to the quiscent areas than centre injection.

The above reported behaviour is valid for top and bottom injection of gas.

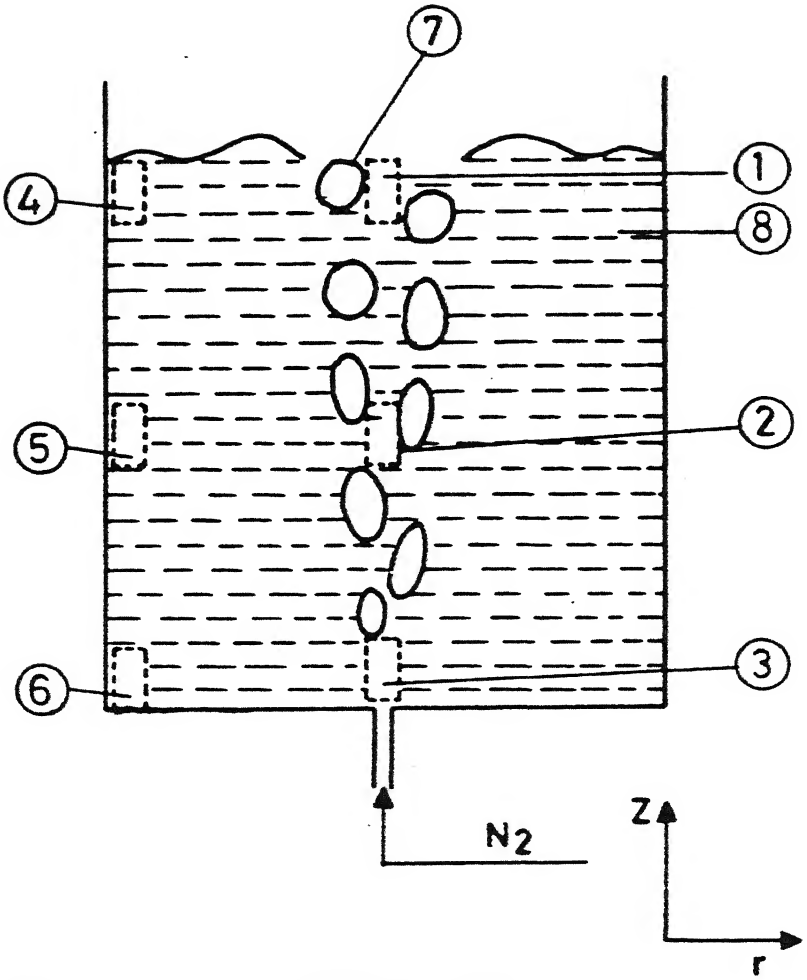

Plume zone	Annulus zone	
1. r = 0, Z = H	4. r = R, Z = H	7. Bubble plume
2. r = 0, Z = H/2	5. r = R, Z = H/2	8. Model bath
3. r = 0, Z = 0	6. r = R, Z = 0	

Fig. 3. Locations of introduction of the additive in term of cylindrical coordinate system.

Chapter 5

EXPERIMENTAL RESULTS

All the experimental results are given in Appendix-A and reported in Figs.4 to 18 in terms of the fractional mass dissolved, defined as equal to $\frac{m_o - m_t}{m_o}$.

5.1 Influence of gas flow rates

Fig.4 shows the fractional mass of model additive dissolved in water as a function of time for different gas flow rate. Experimental arrangement and the location of additive are shown in the figure. A zero flow rate indicates absence of stirring. An increase in gas flow rate increases the fractional mass of acid dissolved in water irrespective of the bcation of additive in the bath. Figure 5 evaluates the optimum gas flow rate required for the present investigation. In this figure the fractional mass dissolved is plotted as a function of gas flow rate for 10 and 20 min. Between 2.2 Nl/min to 8.9 Nl/min the fractional mass dissolved appears to level-off. Consider the dissolution of the additive in 10 min, when it is introduced at the surface of the annulus zone ($r \simeq R$ and $Z = H$). Fractional mass dissolved (in percent) increases from 16 pct. to 52 pct. by increasing the flow rate from zero to 2.2 Nl/min. Between 2.2 Nl/min and 8.9 Nl/min the increase in fractional mass dissolved is only from 52 pct. to 62 pct. Similar observations can be made in the figure 4 at other locations and dissolution time.

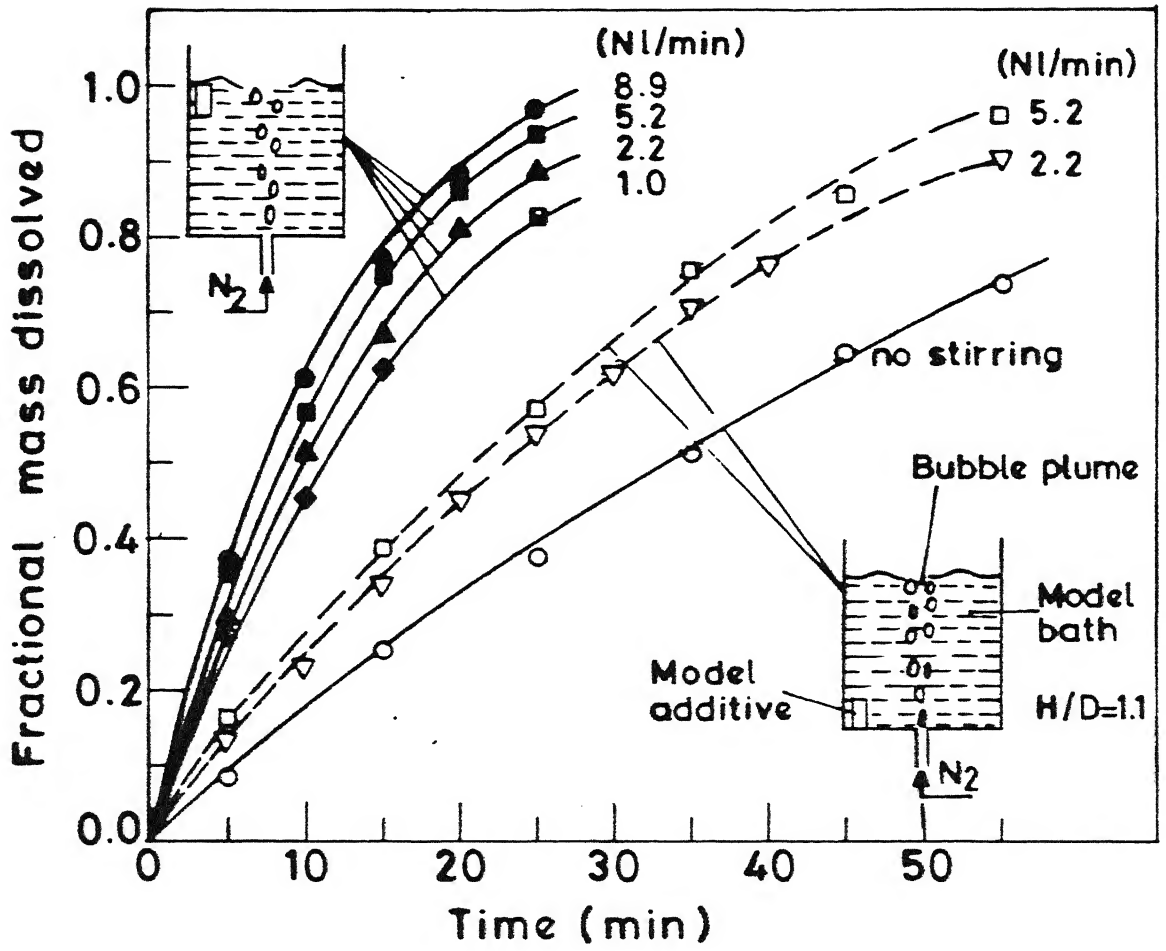

Fig. 4. Variation of fractional mass dissolved with time at different gas flow rates.

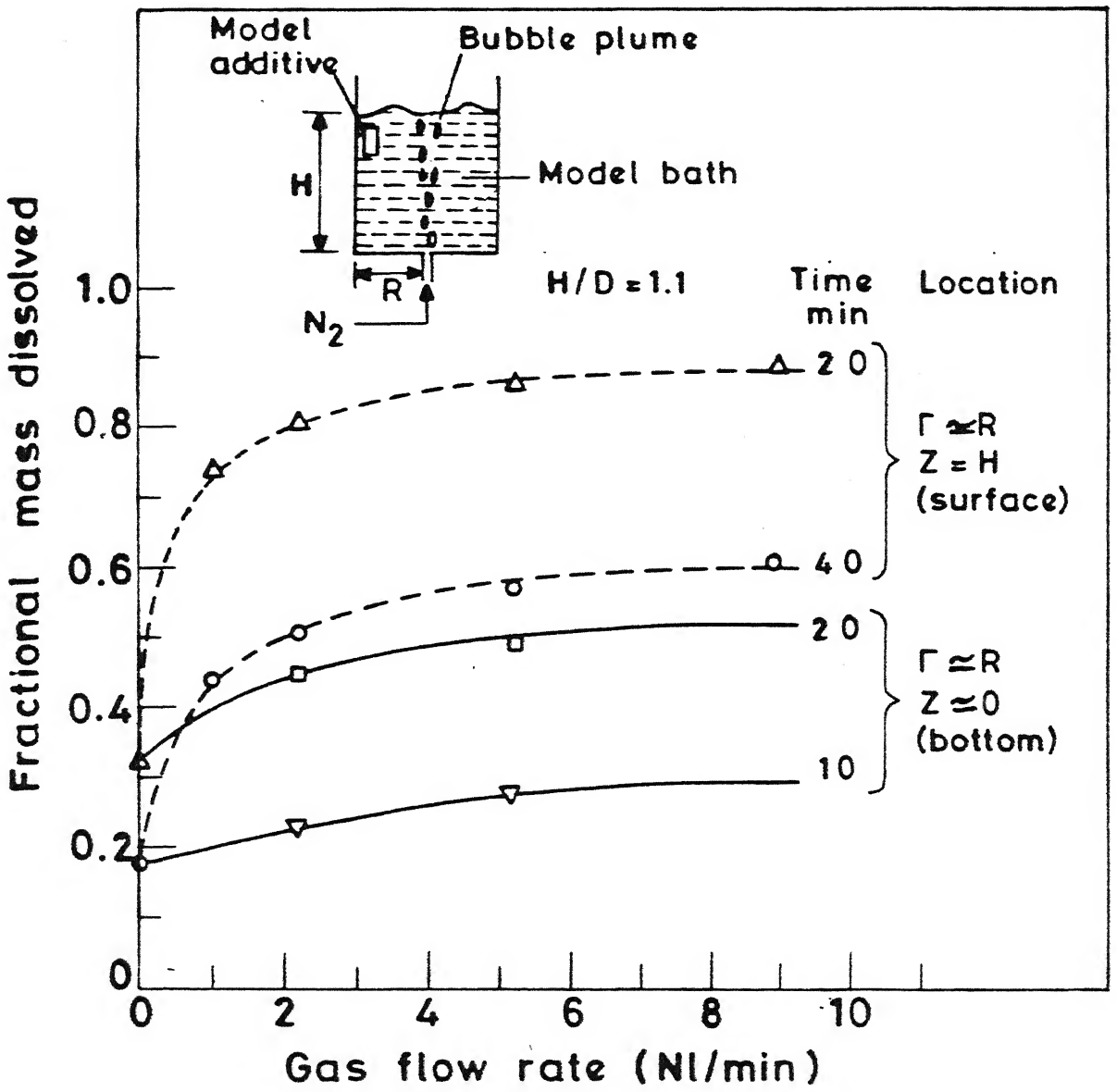

Fig. 5. Variation of fractional mass dissolved in a 2.5 L model bath as a function of gas injection rate.

From the above results it follows that gas injection rates beyond 2.2 Nl/min do not influence the fractional mass of acid dissolved in water significantly. In the subsequent experiments the gas injection rate is kept constant to 5.2 Nl/min.

5.2 Influence of aspect ratio of bath:

Fig.6 shows the fractional mass dissolved as a function of time for various aspect ratios of the bath. The location of the additive is shown on the figure. It can be seen in the figure that fractional mass dissolved with time does not vary significantly within the limits of aspect ratio of the present investigation.

Fig.7 clearly shows the above observation. There, the influence of aspect ratio of the bath on the fractional mass dissolved of an additi located at $r \simeq R$, $Z = H$ and $r \simeq R$, $Z = 0$ at constant gas injection rate through centre of the base of the vessel. At both locations of the additiv the fractional mass dissolved increases slightly with the increase in the aspect ratio of the bath (e.g. fractional mass dissolved in 10 min. increas from 54 pct. to 60 pct. for the locations of the additive $r \simeq R$, $Z = H$. Similar observations can be made at other time and location.).

These results show that aspect ratio of the bath has no significant influence on the dissolution of the additive. This observation indirectly suggests that the recirculating velocity in the liquid induced by a centrally rising gas-liquid plume is not significantly influenced by increase in bath height with in the limits of the present investigation. The results reported by other investigators corroborate the above derived observation[20-22].

In all the subsequent experiments the aspect ratio of bath is : $\frac{H}{D} = 1.1$

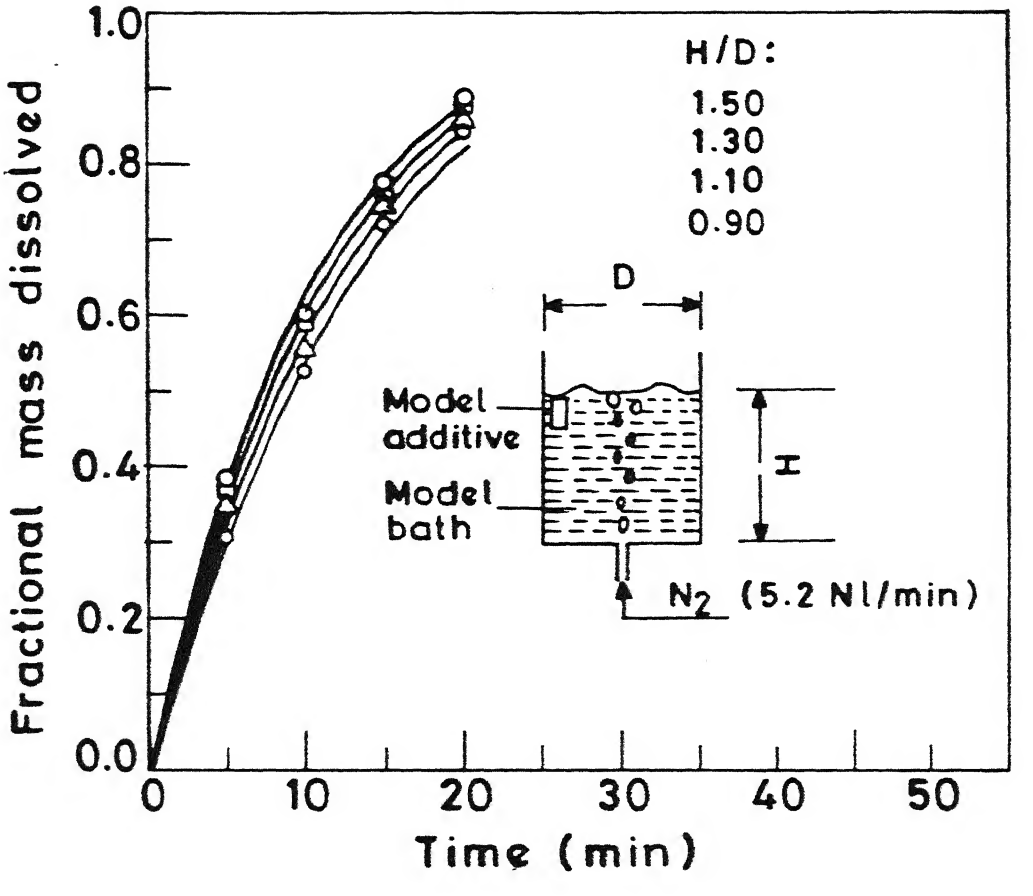

Fig. 6. Variation of fractionl mass dissolved with time at different aspect ratios of bath.

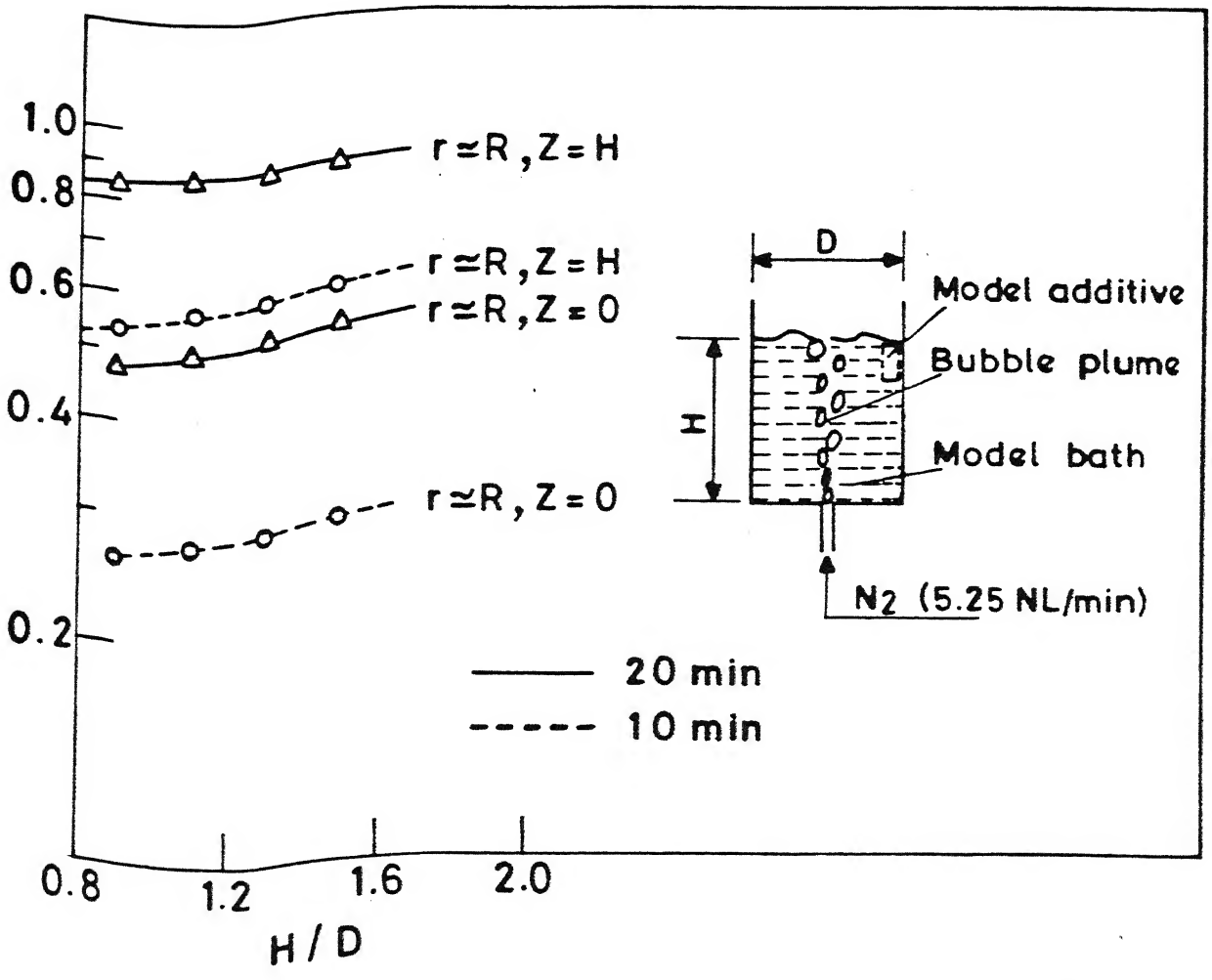

Fig. 7. Variation of fractional mass dissolved as a function of aspect ratio of bath.

5.3 Bottom Injection

5.3.1 Influence of off-center injection

Figure 8 shows the influence of off-center injection relative to center injection in term of fractional mass dissolved against time at different gas location of injection rate. The additive is shown on the figure. An off-center injection increases the fractional mass dissolved of additive more than center injection.

Fig. 9 evaluates the influence of the off-centre injection on fractional mass dissolved in 10 min. (by dotted line) and 20 min.. (By solid line). The gas injection rate is kept constant to a value of 5.25 Nl/min. Location of introduction of the additive and other experimental details are shown in the Fig.9. Off-centre injection is expressed by the ratio of the radial distance of the nozzle (r_n) to radius of the vessel (R). The ratio $r_n/R = 0$ expresses the injection of gas through centre of the base of the vessel.

Fig.9 shows that as r_n/R increases from 0 i.e. central injection towards 1 i.e. off-centre injection, the fractional mass dissolved of an additive introduced at the location $r \simeq R$, $Z = H$ (top surface of the annulus zone) decreases slightly (fractional mass dissolved (in pct.) in 10 min. decreases from 56 pct. for central injection to 52 pct. for off-centre injection at $r_n/R=0.7$). It is interesting to note that off-centre injection of gas considerably improves the dissolution of the additive at the location $r \simeq R$ and $Z = 0$ i.e. bottom of the annulus zone of the bath (the fractional mass dissolved in pct. in 20 min. increases from 48 pct. for central injection to as high as 70 pct. for off-centre injection at $r_n/R=0.7$.

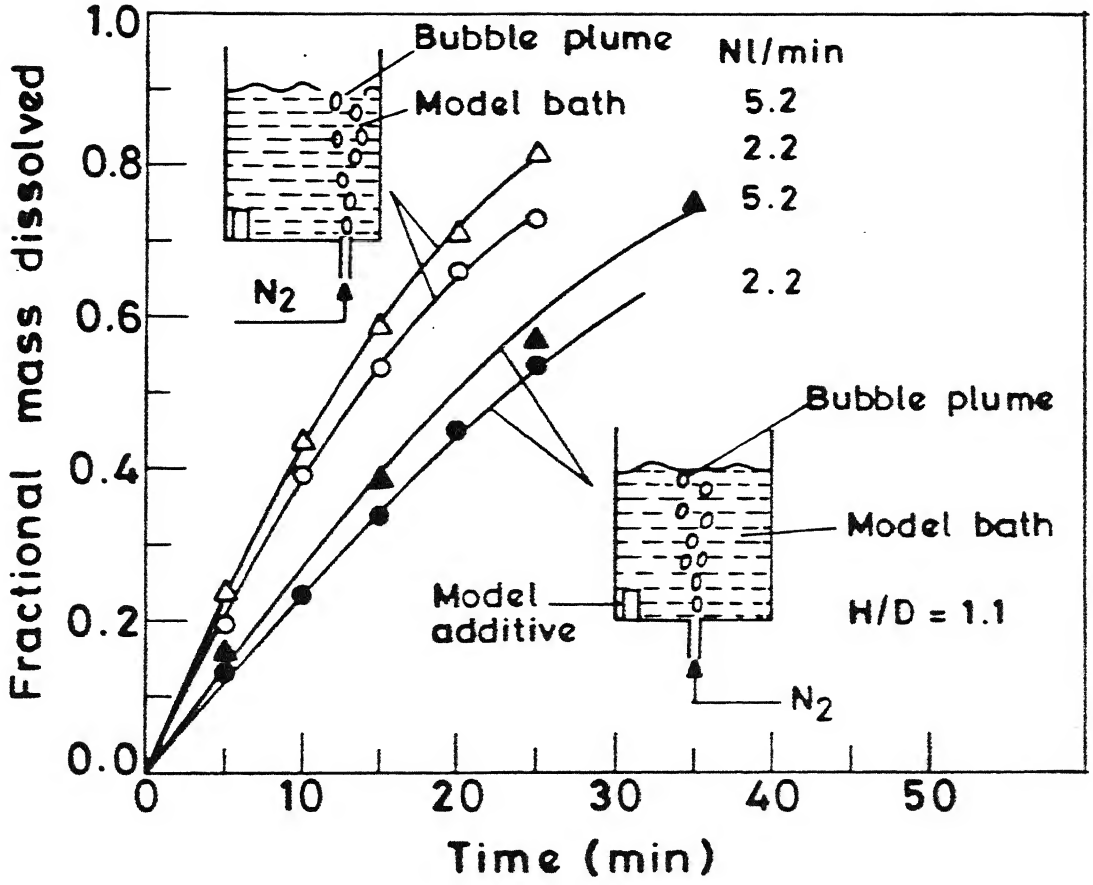

Fig. 8. Changing of fractional mass dissolved with time at different positions of nozzle.

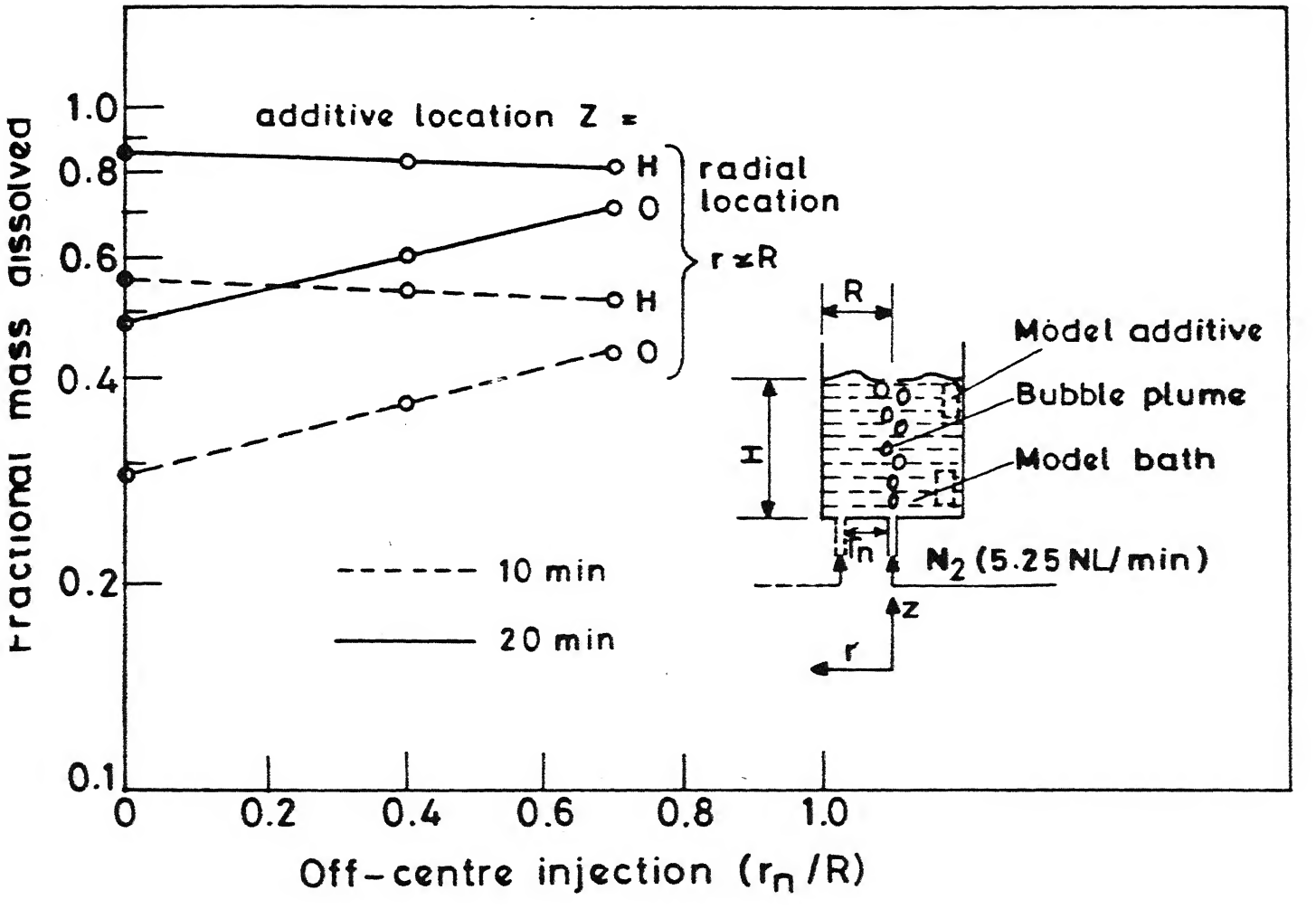

Fig. 9. Variation of fractional mass dissolved as a function of off-centre injection. off-centre injection is expressed by radial position of the nozzle (r_n)/ vessel radius (R).

5.3.2 Influence of different types of additive

Fig.10 shows the fractional mass dissolved as a function of time for different types of additives. The location of the additive is shown on the figure. It can be seen on the figure that the fractional mass dissolved of oxalic acid is greatest compared with boric acid succinic acid and benzoic acid. These results suggest that dissolution of the additive depends upon difusion coeficient and solubility of the additive. Diffusion coefficient and solubility of oxalic acid are higher than all other acids used in the present investigation.

5.3.3 Influence of initial weight of the additive

Figure 11 shows the fractional mass dissolved as a function of time for various initial weight of the additive. The diameter of additive was kept constant but its high was changed. (h/d varies from 0.35 to 2.3; the initial weight varies from 5 grams to 32 grams). The location of the additive is shown on the figure. It can be seen on the figure that the fractional mass dissolved depends on the initial weight of the additive. Smaller sized compact dissolves ~~vesmuch~~ very much faster than a larger compact at any time.

5.3.4 Influence of Temperature

Figure 12 shows the fractional mass dissolved of oxalic acid compact vs time at different temperatures of the water bath. An increase in temperature increases the fractional mass dissolved of acid in water bath irrespective of the hydrodynamic conditions of the bath (stagnant or gas stirring).

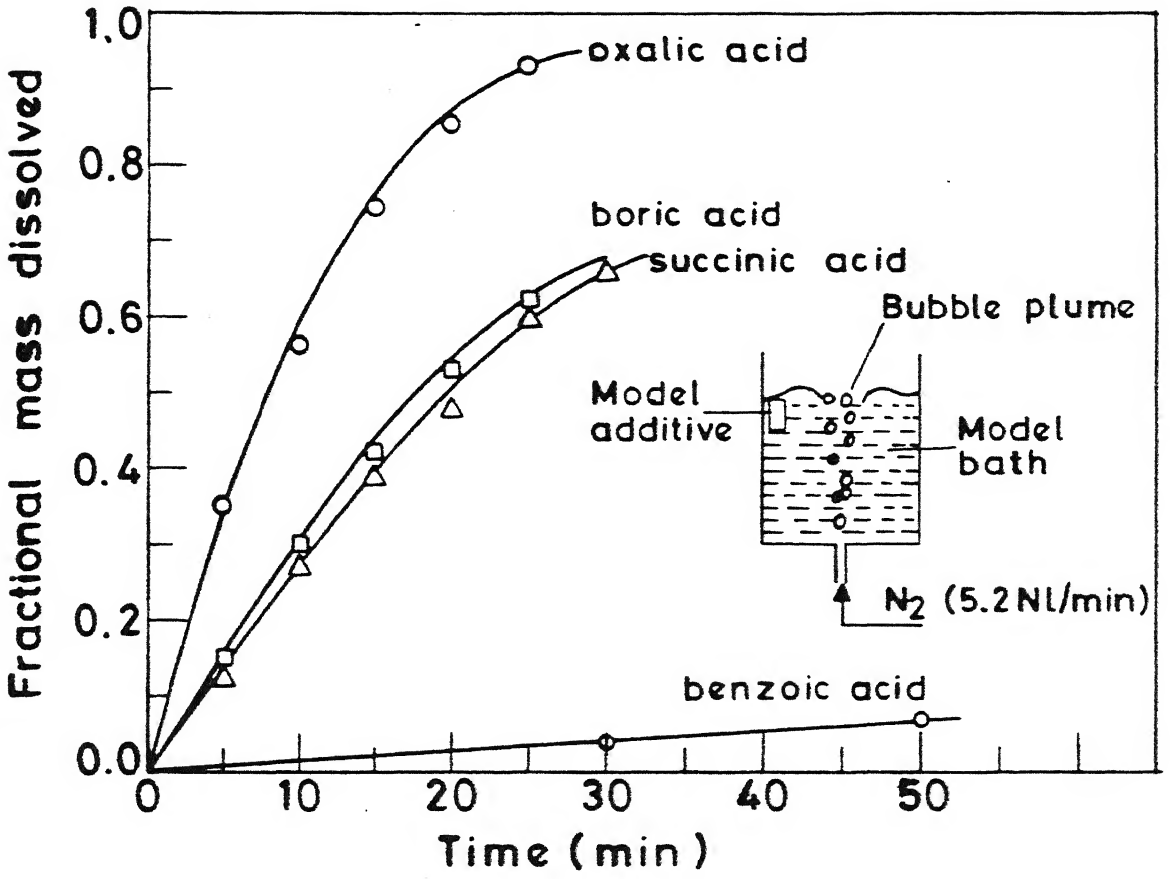

Fig. 10. Variation of fractional mass dissolved vs, time with different types of additive (acids).

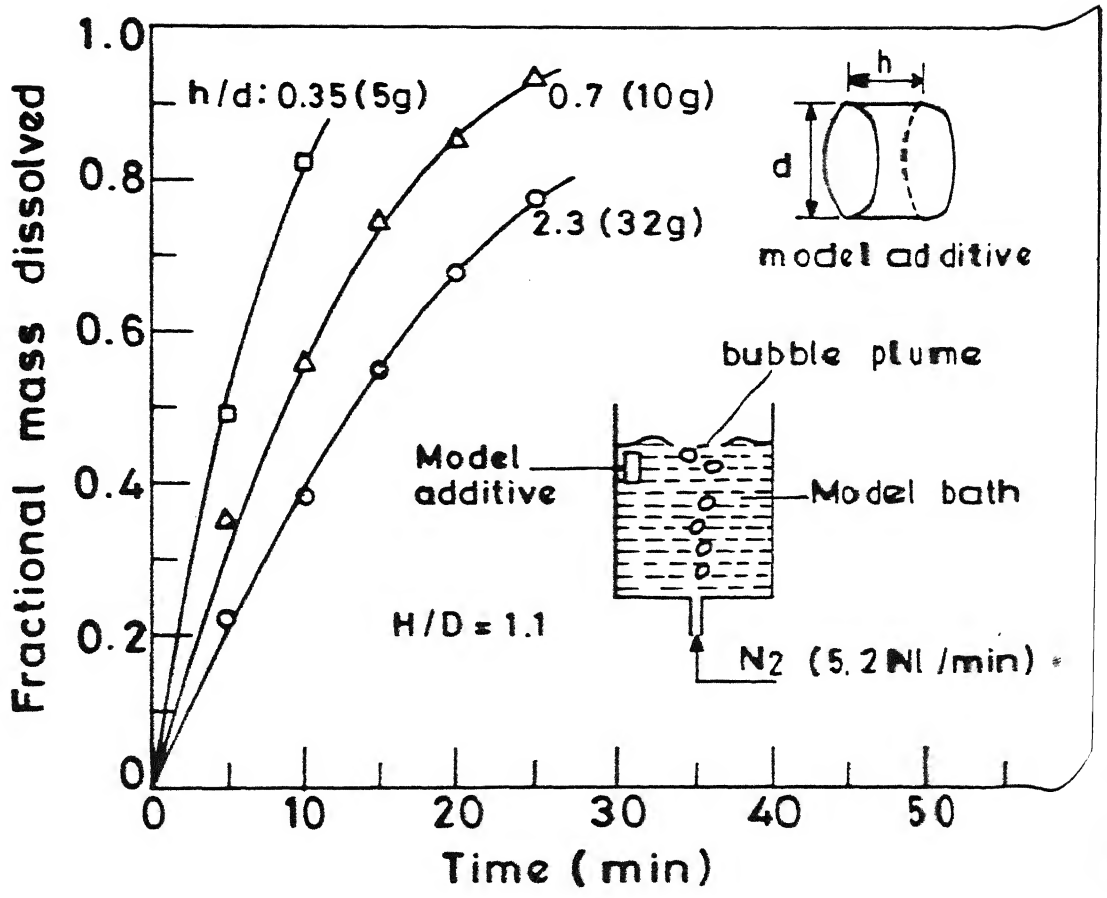

Fig. 11. Changing of fractional mass dissolved vs. time with different initial weights of additive.

5.3.5 Influence of location of additive for center injection:

In figure 13 the fractional mass dissolved of oxalic acid is ploted as a function of time for different location of the additive (shown in the figure) in the bath.

Fig. 14 evaluates the fractional mass dissolved in 10 min (by dotted line) and in 20 min (by solid line) at different axial location of introduction of additive in the model bath for two radial locations, namely $r \simeq 0$ (i.e. the plume region) and $r \simeq R$ (annulus zone). Axial location is expressed by the ratio Z/H. The value of the coordinates $Z/H = 0$ to 1 and $r \simeq 0$ represents the location of the additive in the plume region whereas $Z/H = 0$ to 1 and $r \simeq R$ in the annulus region of the bath. These locations are clearly defined in the Fig.14.

It can be seen in the figure 13 and 14 that for a given radial location the fractional mass dissolved increases as the axial location of the additive increases from $Z = 0$ i.e. at the bottom of the bath to a position $Z = H$ i.e. at the free surface of the bath. The dissolution of the additive is maximum when it is introduced in the 'eye' of the plume (i.e. $Z/H = 1$ and $r \simeq 0$) and minimum when the additive lies at the bottom of the annulus zone (i.e. $Z/H = 0$ and $r \simeq R$).

The above results suggest that the dissolution of the additive depends strongly on the intensity of agitation induced by a gas-liquid rising plume in the liquid bath. Since a centrally rising gas-liquid plume produces a very weak agitation in the bottom of the

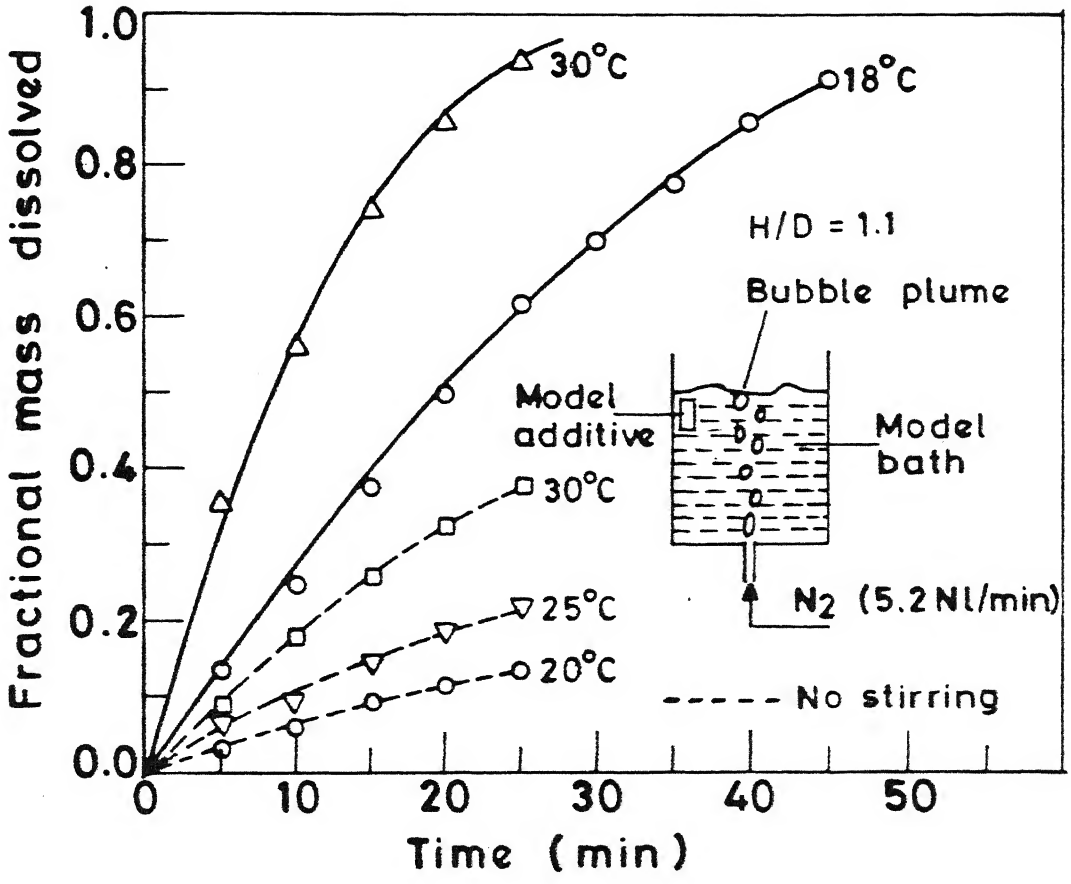

Fig. 12. Variation of fractional mass dissolved with time at different temperatures of the bath.

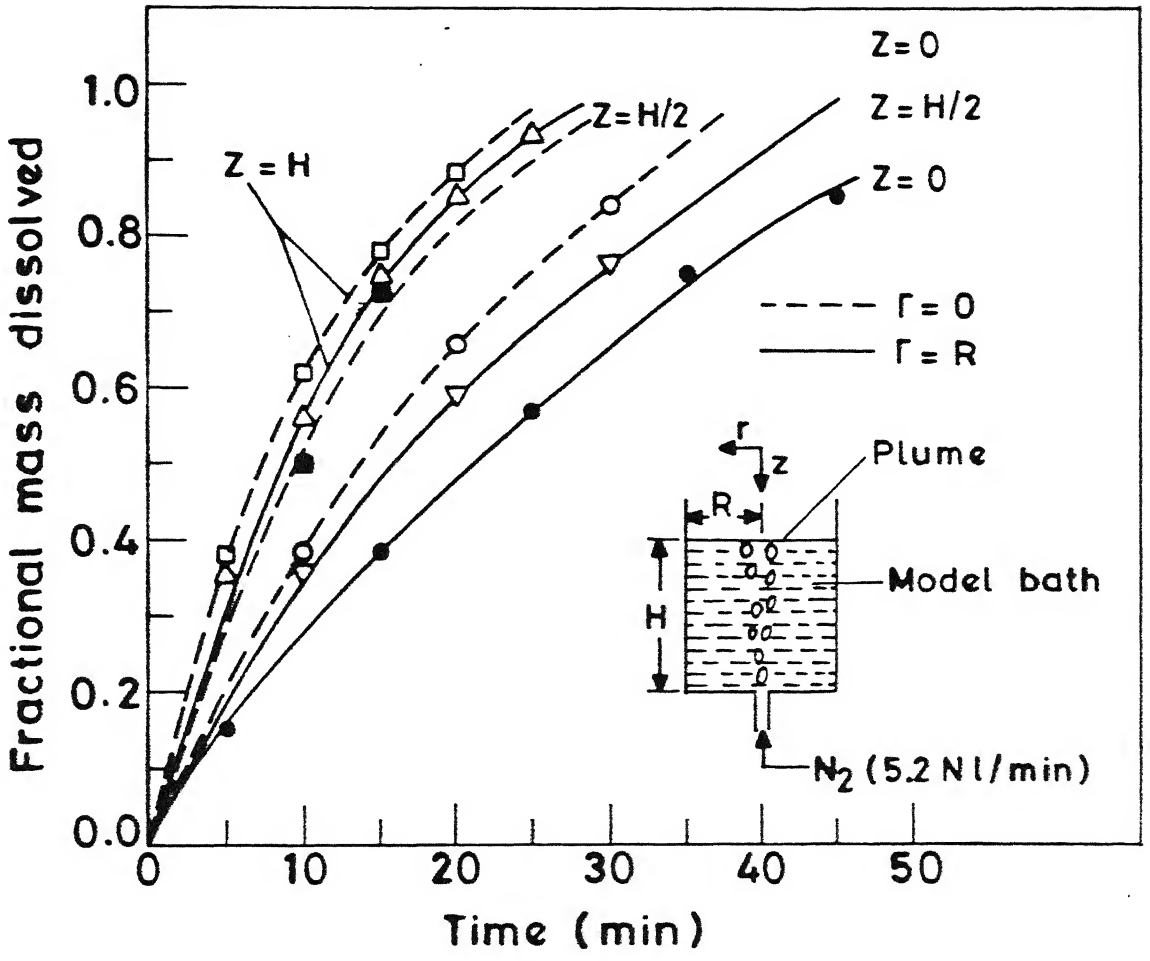

Fig. 13. Variation of fractional mass dissolved vs time at different positions of additive in the bath.

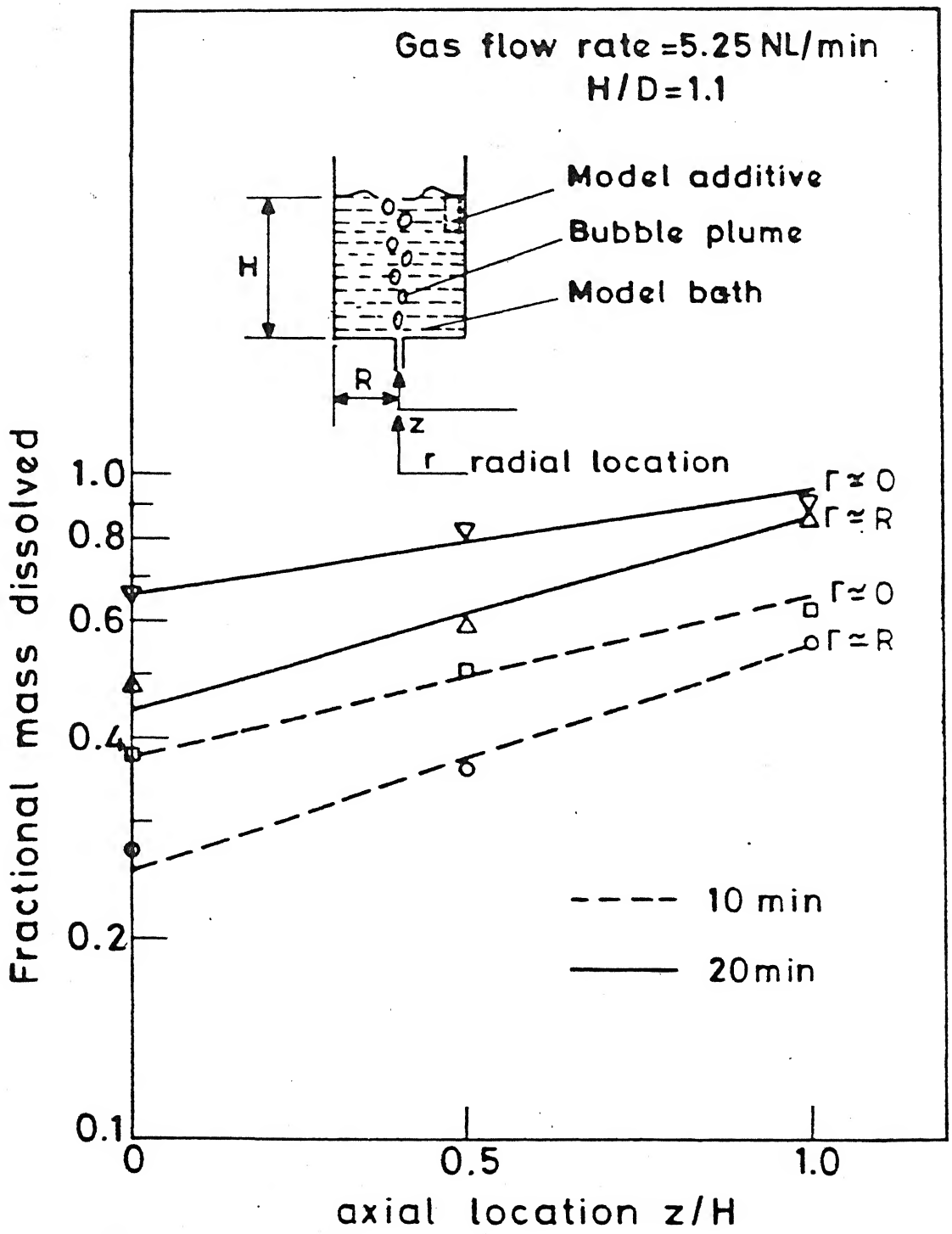

Fig. 14. Variation of fractional mass dissolved in a 2.5L model bath at a function of the location of introduction of the additive. Locations of the additive is given by axial and radial coordinate.

nnulus zone of the bath as compared to in the plume region and closed to the surface[12,20-22,29], therefore, dissolution of the additive at the location Z/H = 0 and r≃R (i.e. bottom of the annulus zone of the bath) must also be minimum as compared to any other location as the results presented in Fig. 13 and 14 also show.

5.4 Top Injection

5.4.1 Influence of depth of submergence of lance

Fig.15. shows the variation in fractional weight of acid in water vs. time for difference values of depth of submergence of the gas injecting top lance. The experimental arrangement and the position of the additive are shown on the figure. Increase in time, increases the fractional mass dissolved at both the positionsof the additive that is at the surface and at the bottom. Increase in depth of submergence of the lance, increases the fraction mass of acid dissolved in water.

The results presented in the figure show the dissolution of acid depends on position of the additive as observed for bottom injection.

5.4.2 Influence of off-centre injection

Following the experimental results of bottom injection (see section 5.3.1) similar experimentsare performed by varying the radial location of the lance at a constant depth of submergence of the lance equal to 0.64 the radial location of the lance is expressed by the ratio $\frac{r_n}{R}$. The experimental results on $\frac{\text{fractional}}{\text{mass dissolved}}$ are presented in figure 16.

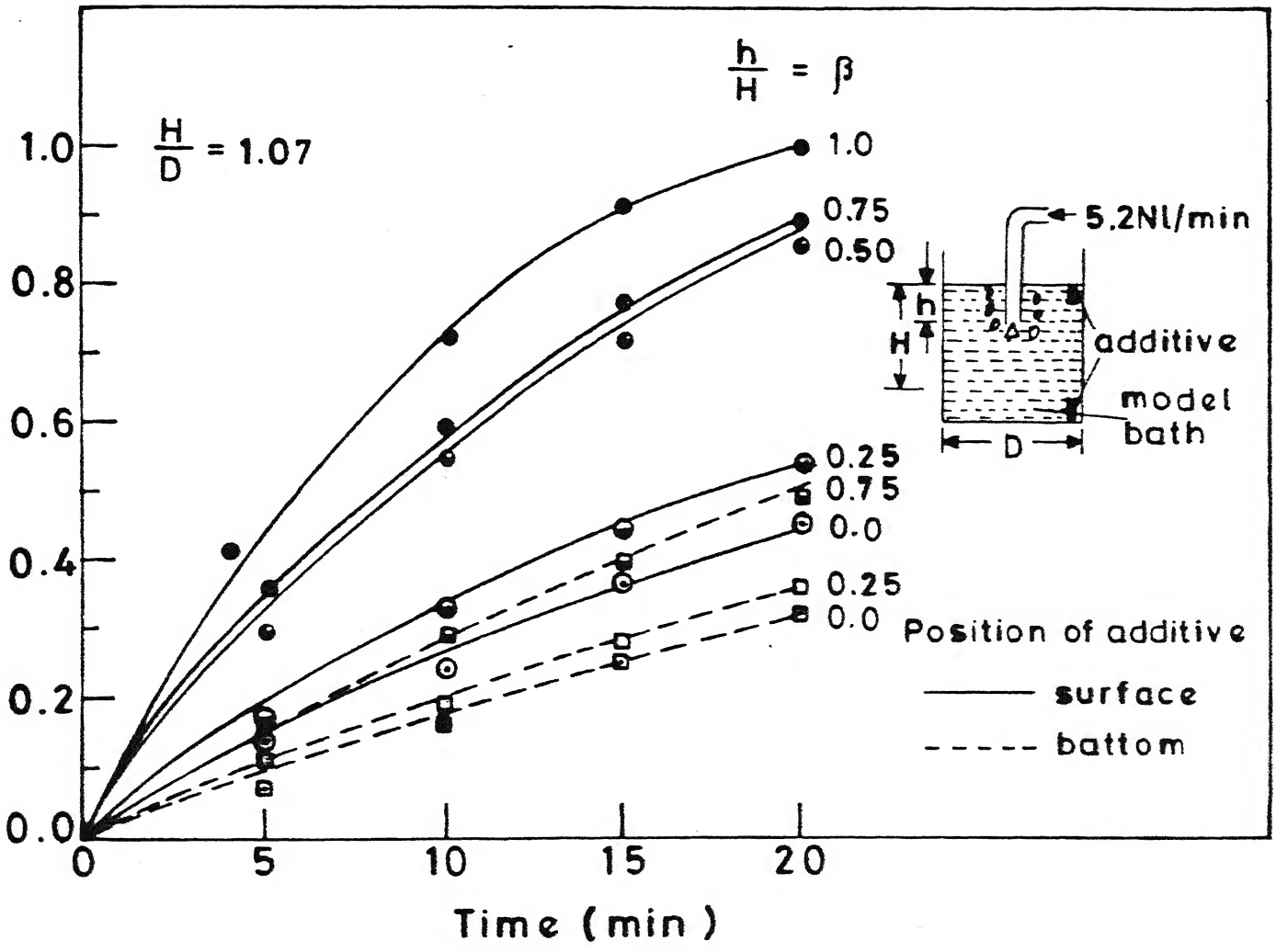

Fig. 15. Variation of fractional mass dissolved vs. time at different depths submergence of the lance (for top injection).

It can be seen on the figure that an off-center injection increases the dissolution of the additive introduce at the bottom of the bath. It is interesting to note that off center injection has a tendency to decrease the dissolution of the additive introduced at the surface of the bath.

The above observation are similar to the one reported for bottom (see section 5.3.1).

A combined analysis of the experimental result for top and bottom injection gives the following information:-

1- Dissolution of the additive from the bottom of the bath is slower than from surface of the bath irrespective of the center location of the gas injecting lance.

2- Off center injection increases the dissolution of the additive introduced at the bottom of the bath. This is valid for top injection and bottom injection.

5.5 Area vs. weight relationship

Figs. 17 (for bottom injection) and 18 (for top injection) show the ratio surface area of the solid at any time t (A) and original surface area (A_o) of all type of acids with their corresponding masses ($\frac{m}{mo}$). The straight line represents the relationship:

$$\frac{A}{Ao} = \left(\frac{m}{mo}\right)^{\frac{2}{3}} \qquad (13)$$

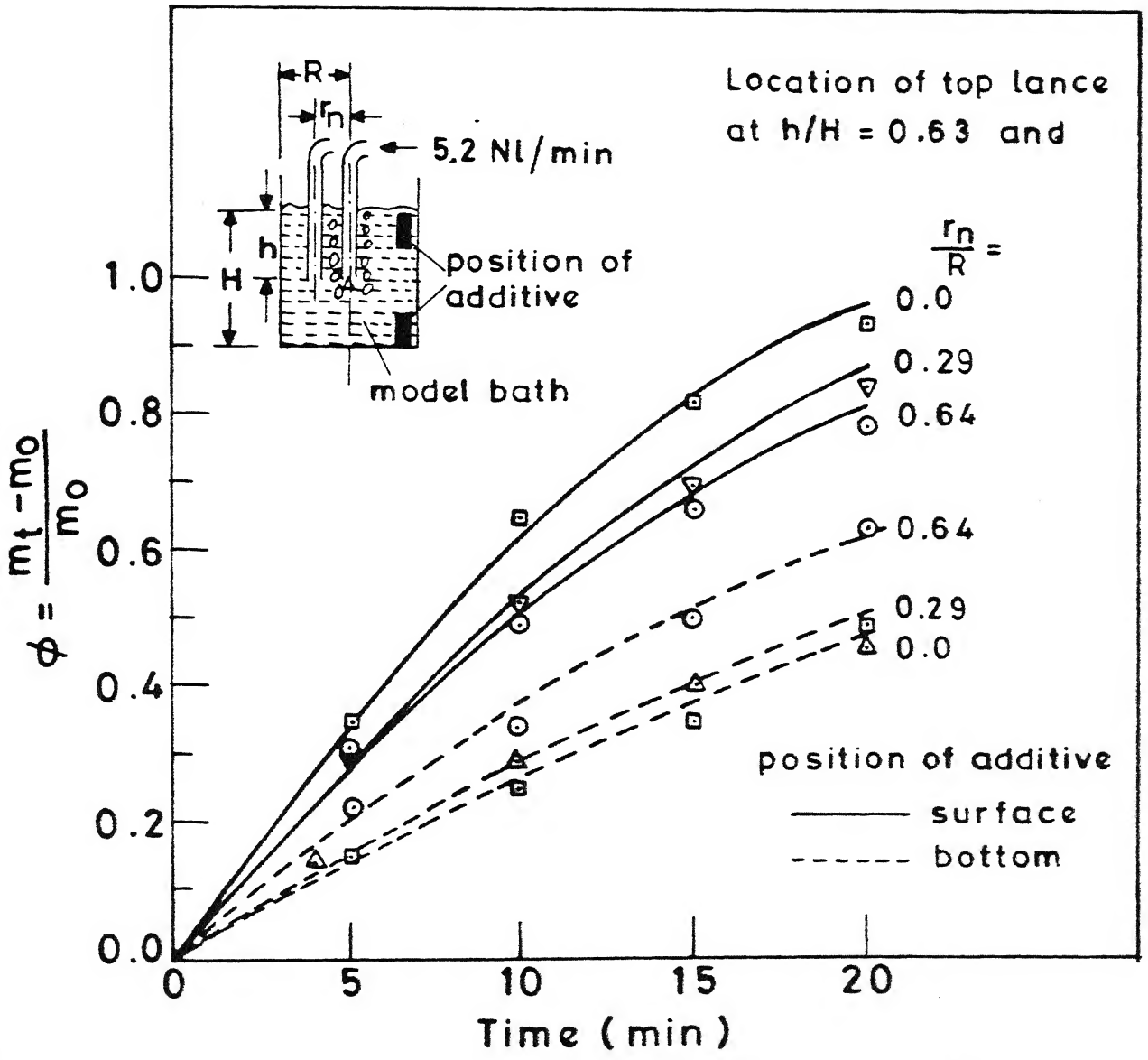

Fig. 16. Changing of fractional mass dissolved vs. time at different positions of the lance (centre and off-centre injection).

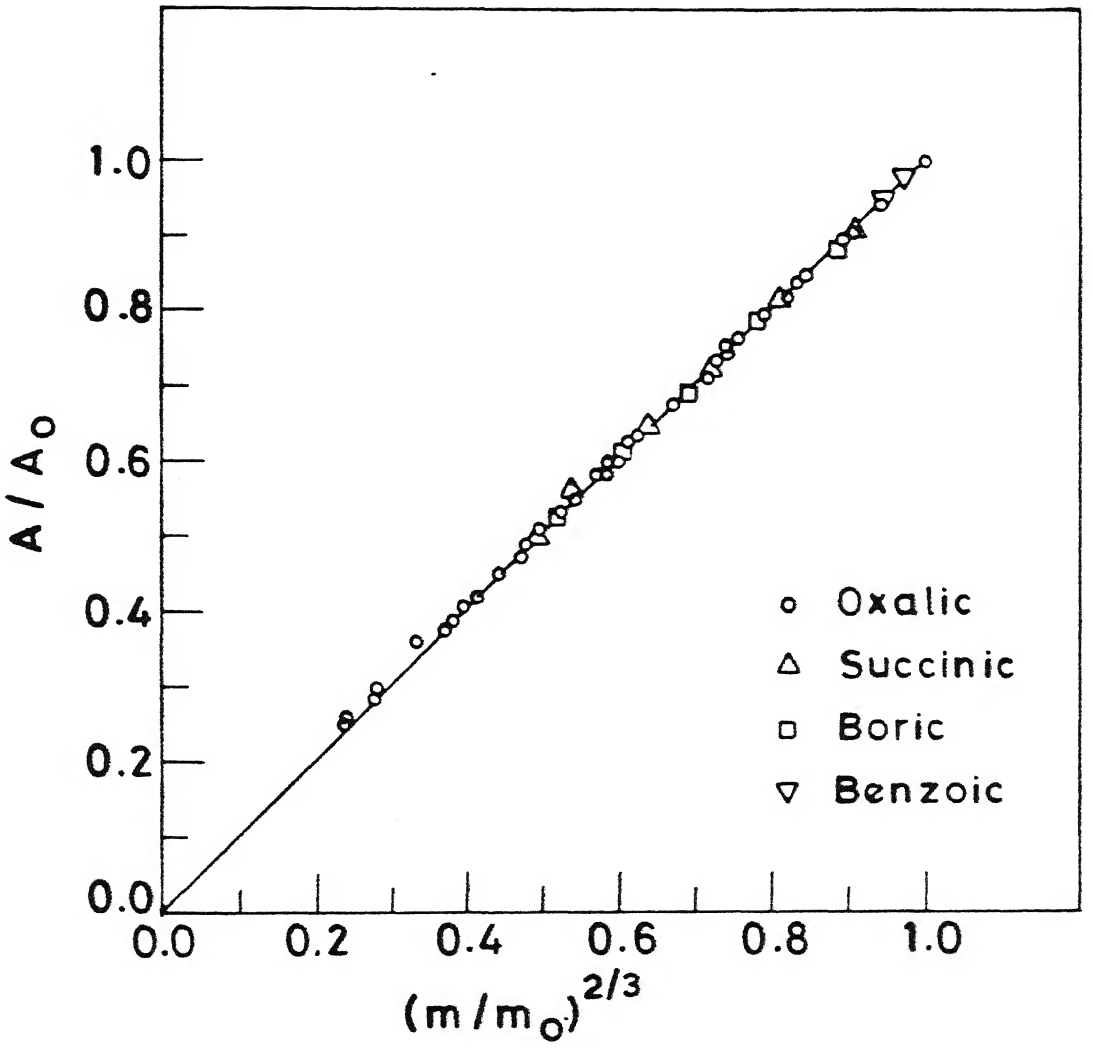

Fig. 17. Area vs. weight relationship (for bottom injection).

This relationship follows from property of similar geometrical solids provided the form of the solid does not change . In the present experiments the form of the compact is not observed to change.

The experimental results presented in figure 17 and 18 confirm the validity of the relationship 13. This is an important finding in the present investigation.

5.6 Determination of rate constant

The rate of dissolution is given by[11]

$$- \frac{dm}{dt} = k_A (C_s - C), \qquad (14)$$

Where C_s is saturation concentration, k dissolution rate constant and C is concentration. When $C_s >> C$ as in the present case (dissolved amount of acid is very much less than saturation amount), then concentration changesin the liquid is negligibly small and $C_s - C \simeq C_s$.

Therefore eq.14 follows

$$- \frac{dm}{dt} = k_A C_s \qquad (15)$$

putting eq.13 into 15 we get

$$- \frac{dm}{dt} = k A_o \left(\frac{m}{mo} \right)^{\frac{2}{3}} C_s \qquad (16)$$

Integrating eq.16 within the limits m = mo at t = 0 and m = m at t = t and rearranging the terms we get

$$\left(m_o^{\frac{1}{3}} - m^{\frac{1}{3}} \right) = \frac{A_o}{m_o^{\frac{2}{3}} C_s} \cdot \frac{kt}{3} \qquad (17)$$

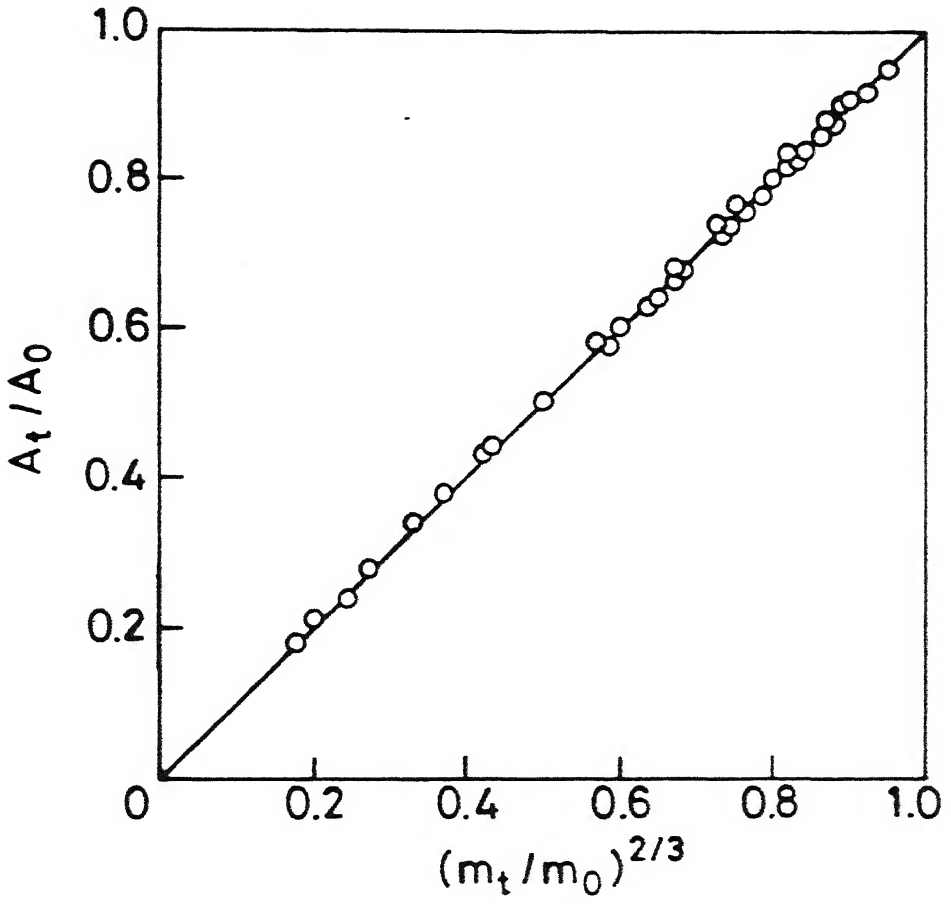

Fig. 18. Area vs. weight relationship (for top injection)

The equation 17 is a cubic rate law. Thus a plot of $m_o^{\frac{1}{3}} - m^{\frac{1}{3}}$ gainst t should give a straight line if the experimental results ollows eq.17.

Figures 19 to 25 are plotedfor bottom injection and from 26 o 27 for top injection following the eq.17.

The experimental results follow the equation 17 very well hich suggest that cubic rate law discribes the process of dissolution f solid in liquid in the present investigation. Straight line are rawn on the figures 19 to 27 by the least square analysis and k is etermined by slope of the line using equation 17.

All the values of k determined by the above procedure are isted in table 3 and 4.

TABLE 3 : Slopes and k values for bottom injection

Table No.	Slope	$k \times 10^{-3}$ (cm sec.)
1	0.03927	2.27128
2	0.04520	2.61372
3	0.05183	3.02216
4	0.05580	3.24825
5	0.02008	1.17015
6	0.02257	1.30903
7	0.02345	1.36954
8	0.00413	0.53223
9	0.00788	0.63710
10	0.01383	0.80646
11	0.02360	4.20964
12	0.02168	-
13	0.00097	-
14	0.04937	2.86223
15	0.05332	3.08830
16	0.05549	3.20759
17	0.032078	1.84349
18	0.03637	2.10316
19	0.05003	2.89741
20	0.05696	3.30582
21	0.04745	2.75260
22	0.03155	1.82179
23	0.02702	1.56763
24	0.07540	3.92856
25	0.05002	2.70200

TABLE 4 : Sopes and k values for top injection

Table No.	Slopes	$k \times 10^{-3}$ (cm sec.)
1	0.01986	1.13000
2	0.01301	0.74713
3	0.02510	1.43900
4	0.01480	0.85030
5	0.05100	2.93320
6	0.01990	1.13730
7	0.05476	3.31400
8	0.02199	1.26200
9	0.07776	4.44600
10	0.01979	1.13300
11	0.04376	2.51100
12	0.02071	1.17825
13	0.04383	2.52400
14	0.02960	1.69540

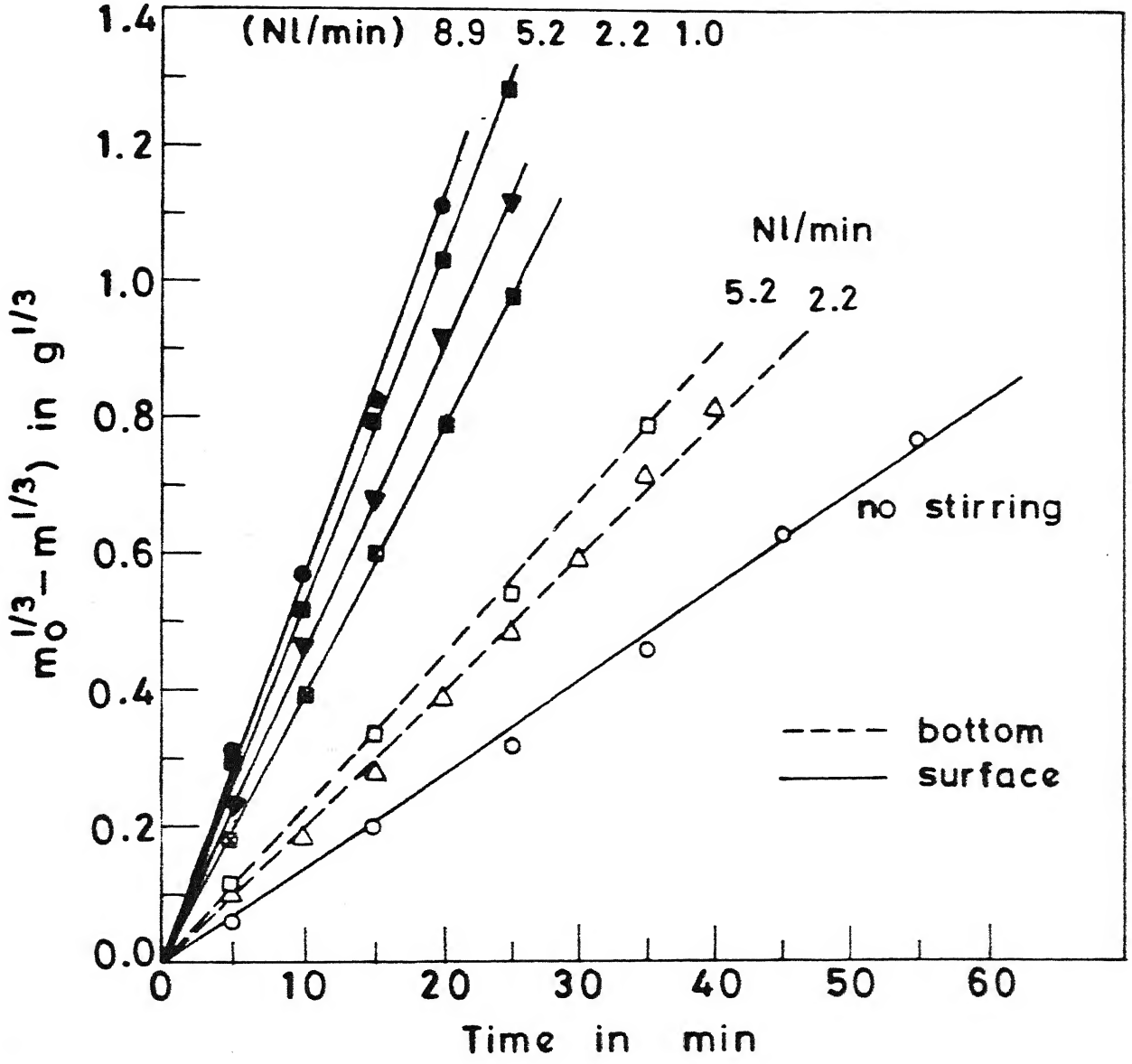

Fig. 19. $m_o^{1/3} - m^{1/3}$ vs. time at different gas flow rates.

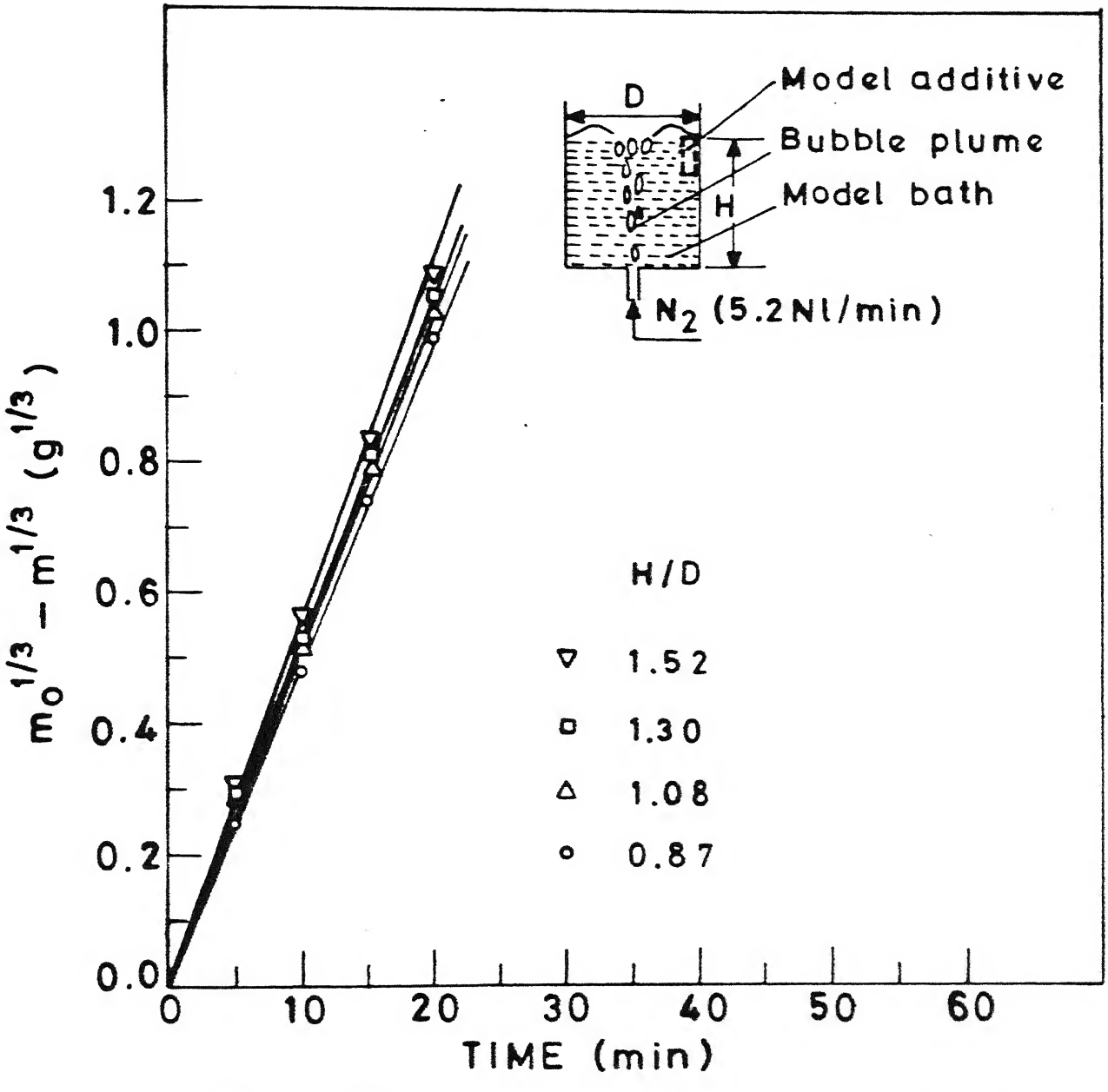

Fig. 20. $m_o^{1/3} - m^{1/3}$ vs. time with different aspect ratios of the bath.

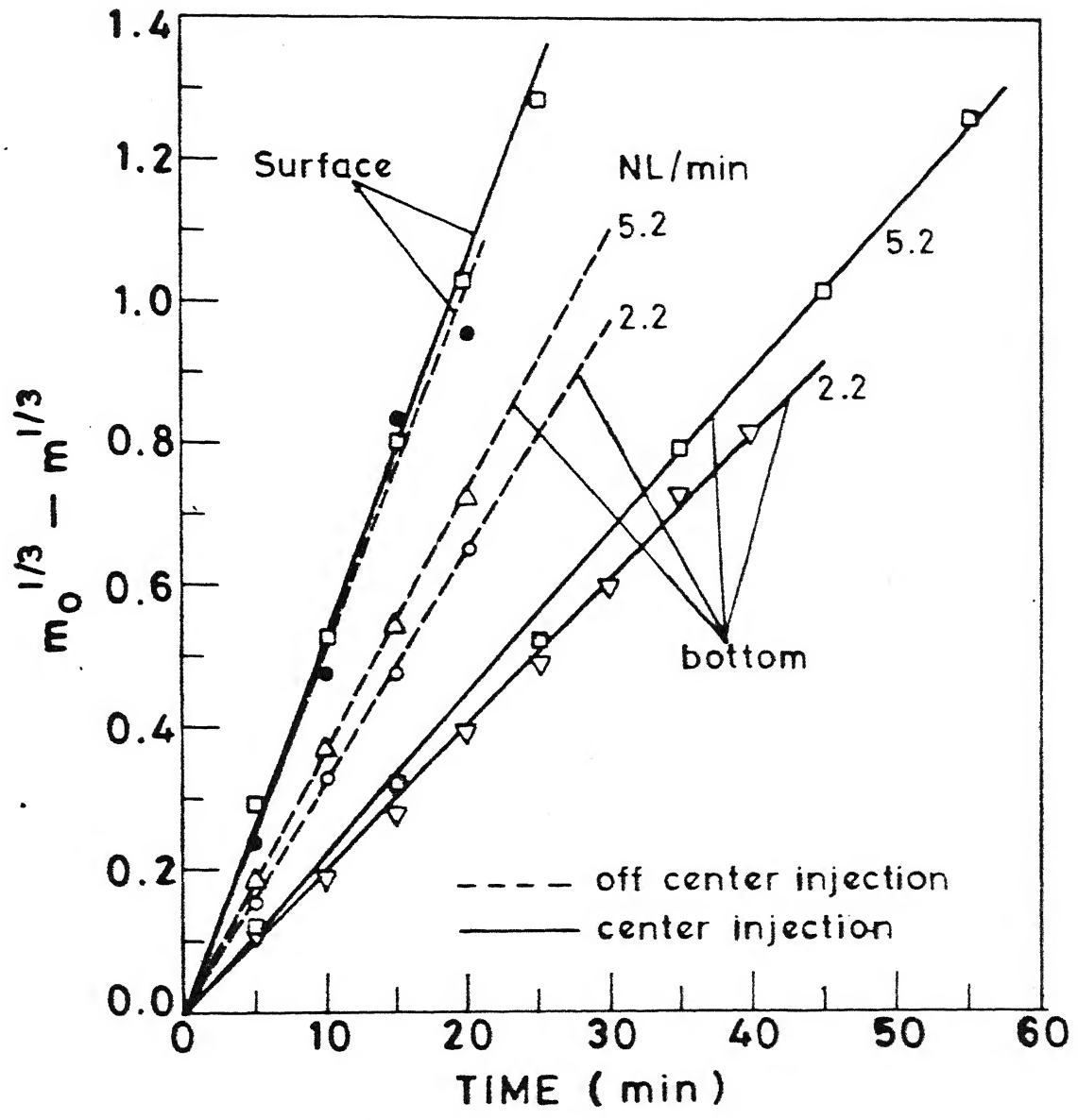

Fig. 21. $m_o^{1/3} - m^{1/3}$ vs. time at different positions of nozzle (centre and off-centre injection gas).

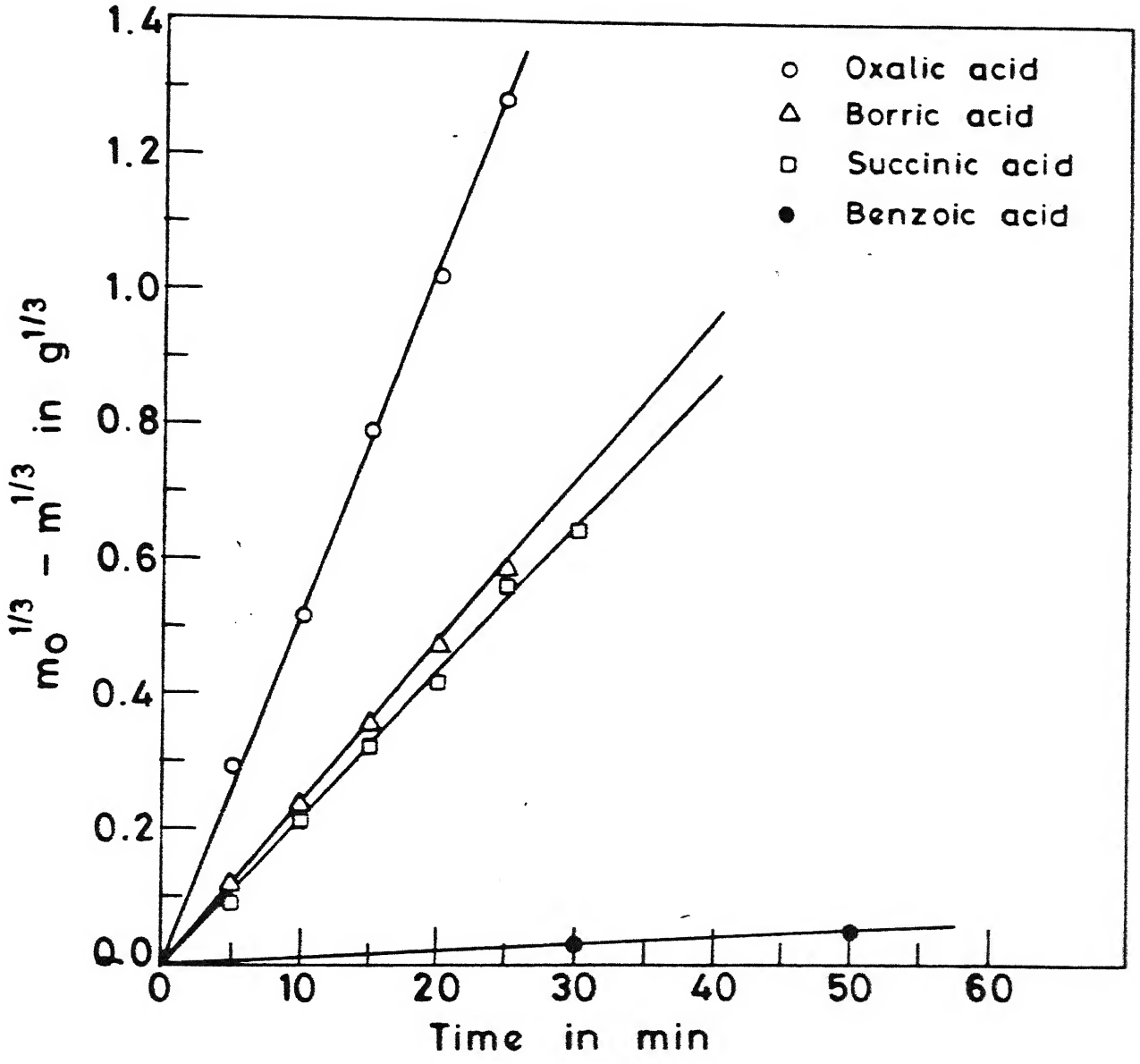

Fig. 22. $m_o^{1/3} - m^{1/3}$ vs. time with different types of additives (acids).

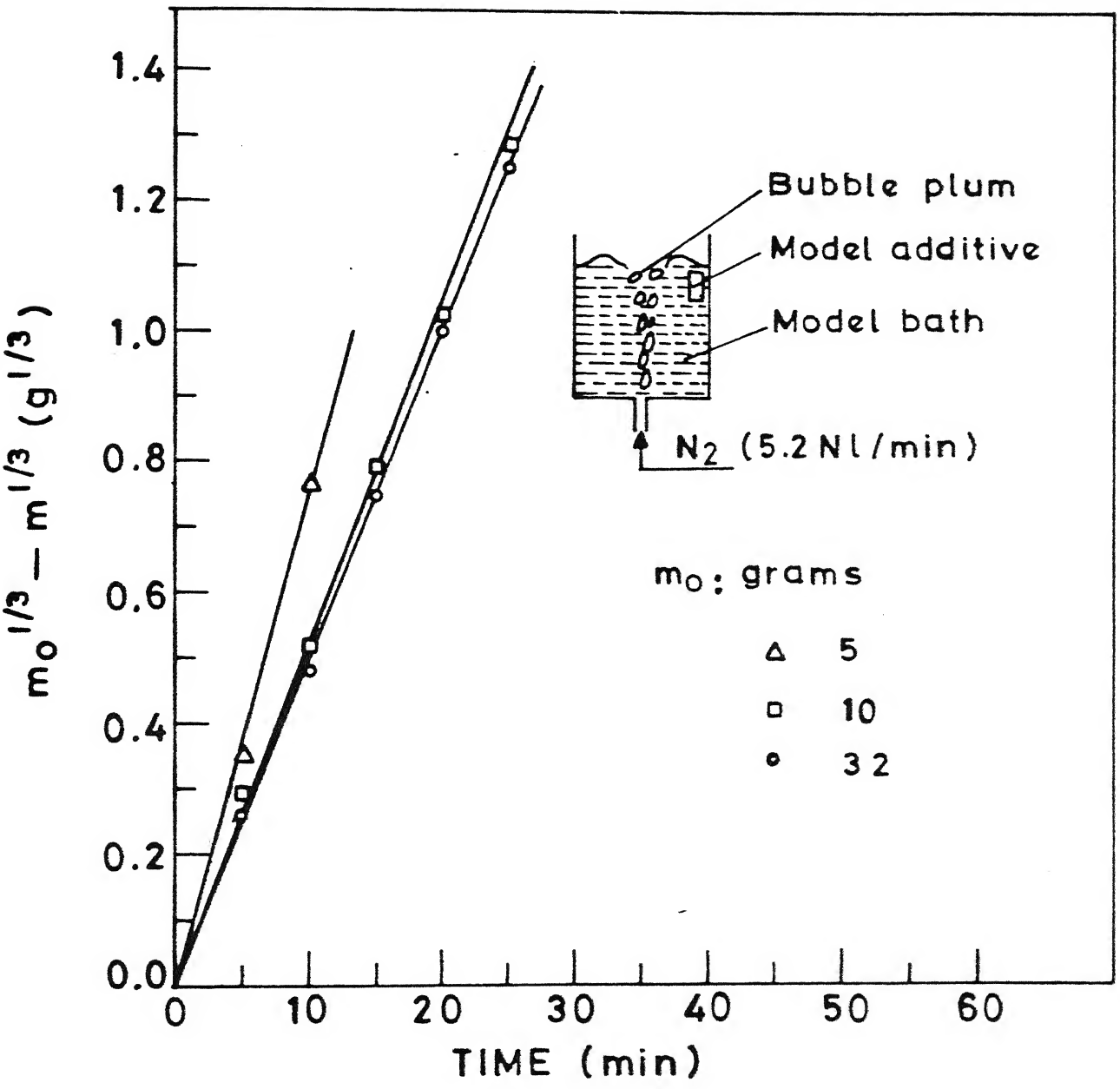

Fig. 23. $m_o^{1/3} - m^{1/3}$ vs. time at different initial weights of additive.

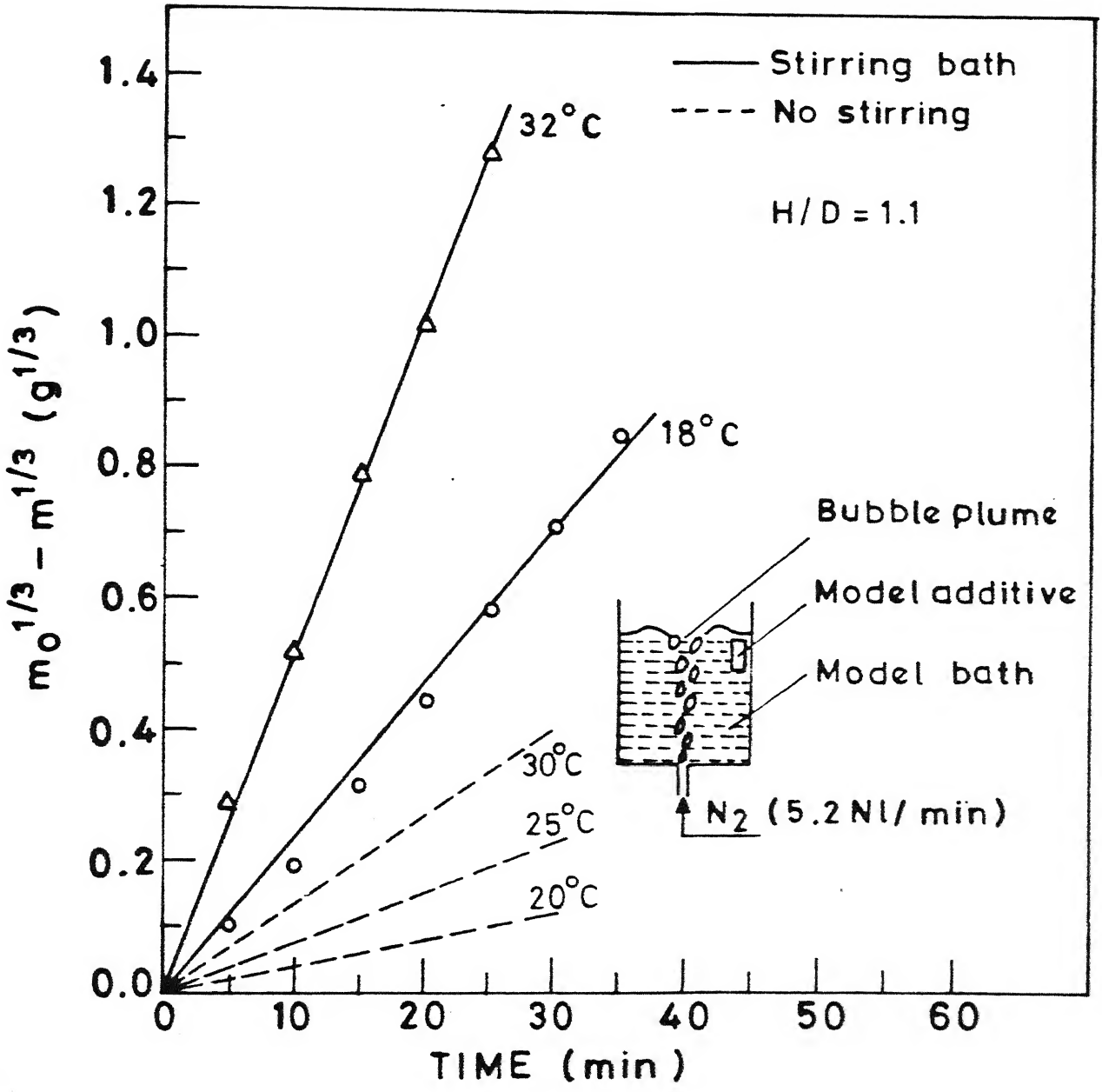

Fig. 24. $m_o^{1/3} - m^{1/3}$ vs. time at different temperatures of the bath.

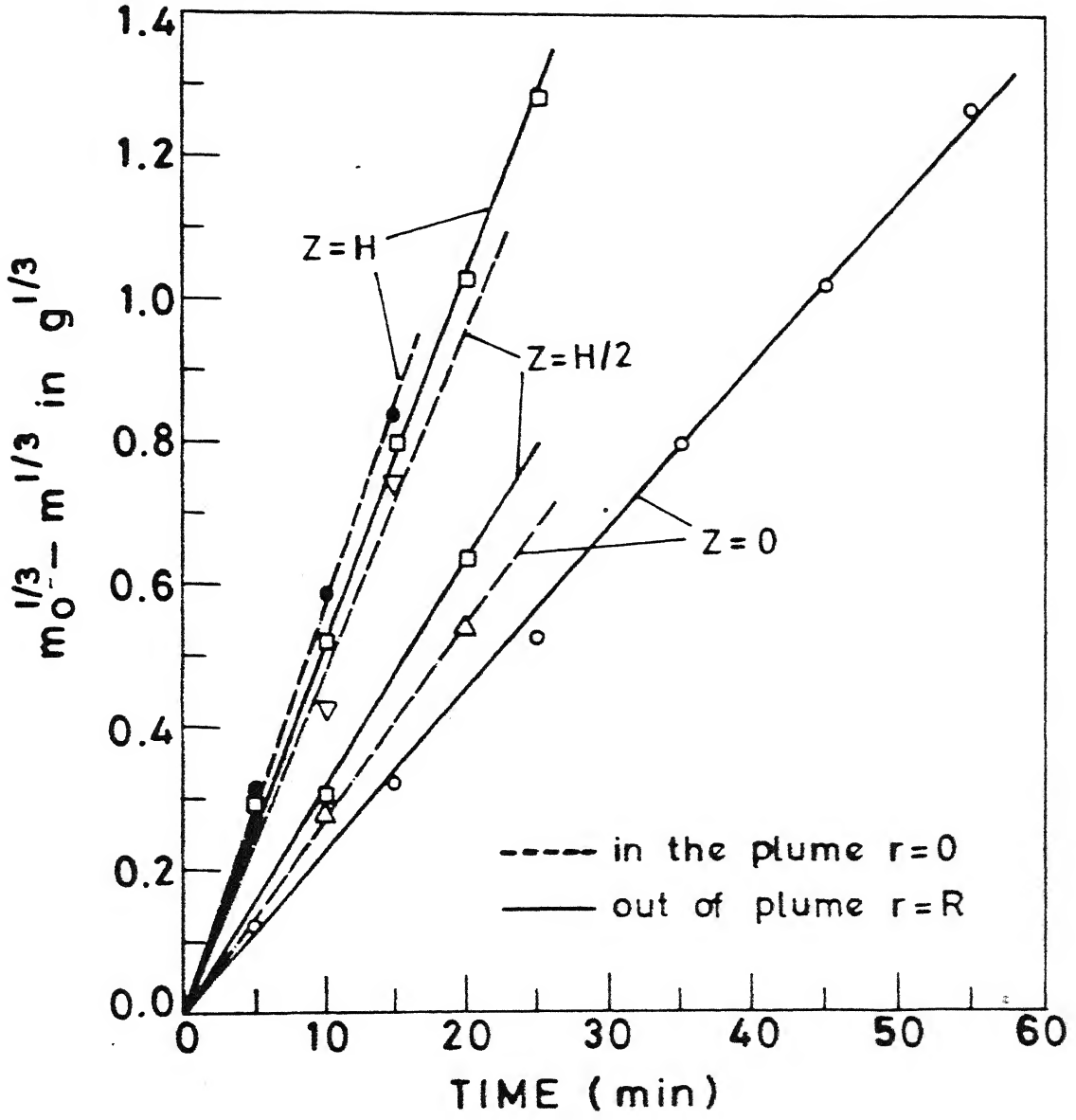

Fig. 25. $m_o^{1/3} - m^{1/3}$ vs. time at different positions of additive in the plume and out of plume.

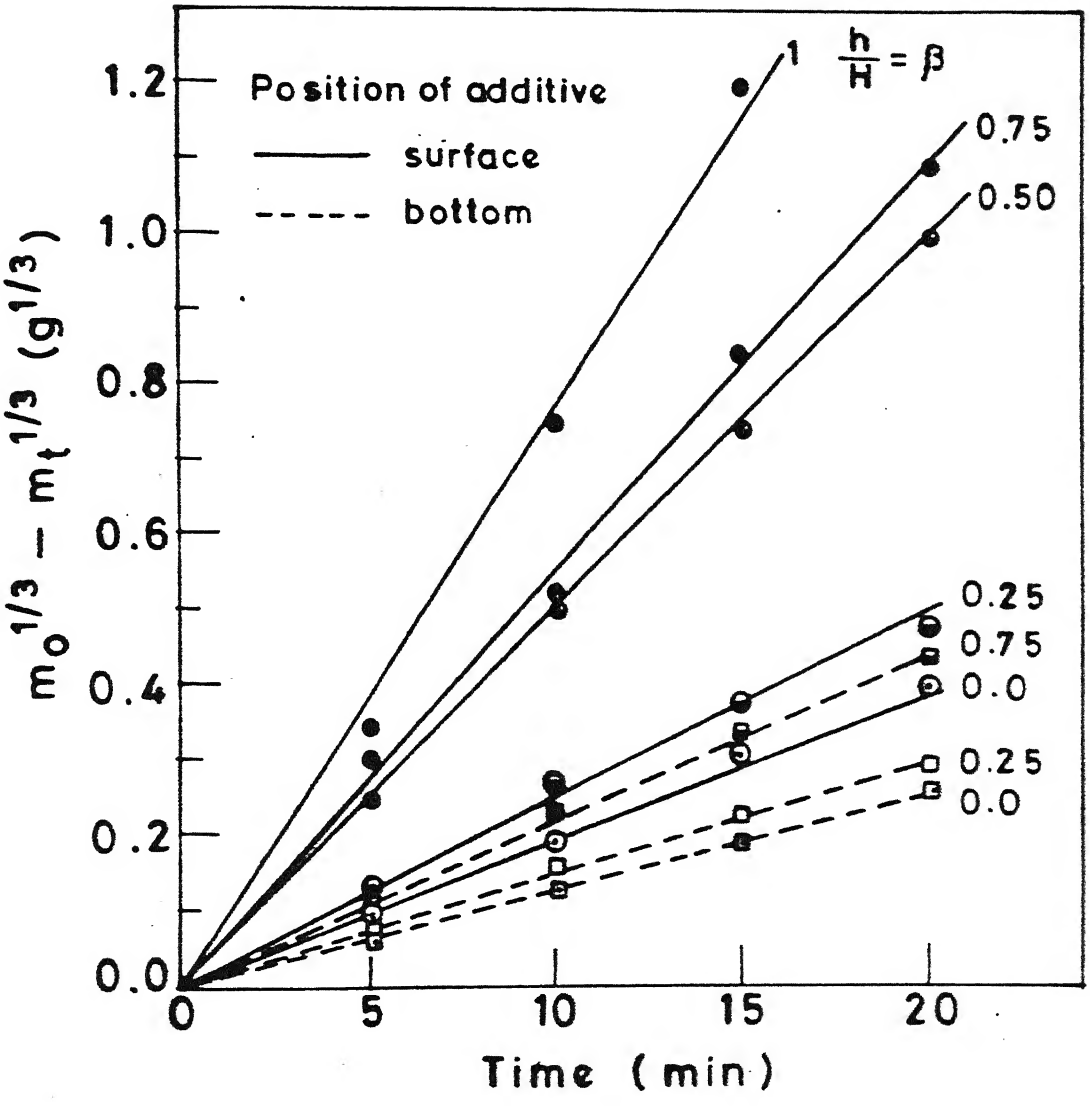

Fig. 27. $m_o^{1/3} - m^{1/3}$ vs. time at different depths submergence of the lance.

Chapter 6

DISCUSION OF RESULTS

6.1 Comparison of k-value with other investigators

The experimental results of the present investigation show that the process of dissolution of solid is very well described by the cubic rate law (eq.17) this finding implies that any effect caused by decrease in surface area of the solid on the dissolution is taken into account while determiningk-value using eq.15. Therefore k-value determined in the present investigation must be comparable with the values calculated by available correlations.

Most of the investigators have determined mass transfer coefficient of a solid of constant surface area dissolving in liquid and proposed various empirical correlations for natural and forced convective mass transfer[7,10,15]. Since the expression 17 takes into account the effects of changing surface area on the rate of dissolution, therefore, k value determined in the present investigation must be comparable with those calculated by appropriate correlation available in the literature. Figure 28 compares the observed k($k = k_N$ for stagnant bath and $k = k_c$ for gas stirred bath) values with calculated ones for bottom and top injection. The following correlations are used to calculate k_N or k_c:

For the dissolution of acid compacts in stagnant water bath mass transfer occurs due to radial diffusion and natural convection. For this case the value of k_N is calculated by [32].

$$\frac{k_N L}{D} = 0.11 \left(\frac{\rho^2 \beta \Delta C L^3}{\eta^2} \frac{\eta}{\rho D} \right)^{\frac{1}{3}} \qquad (18)$$

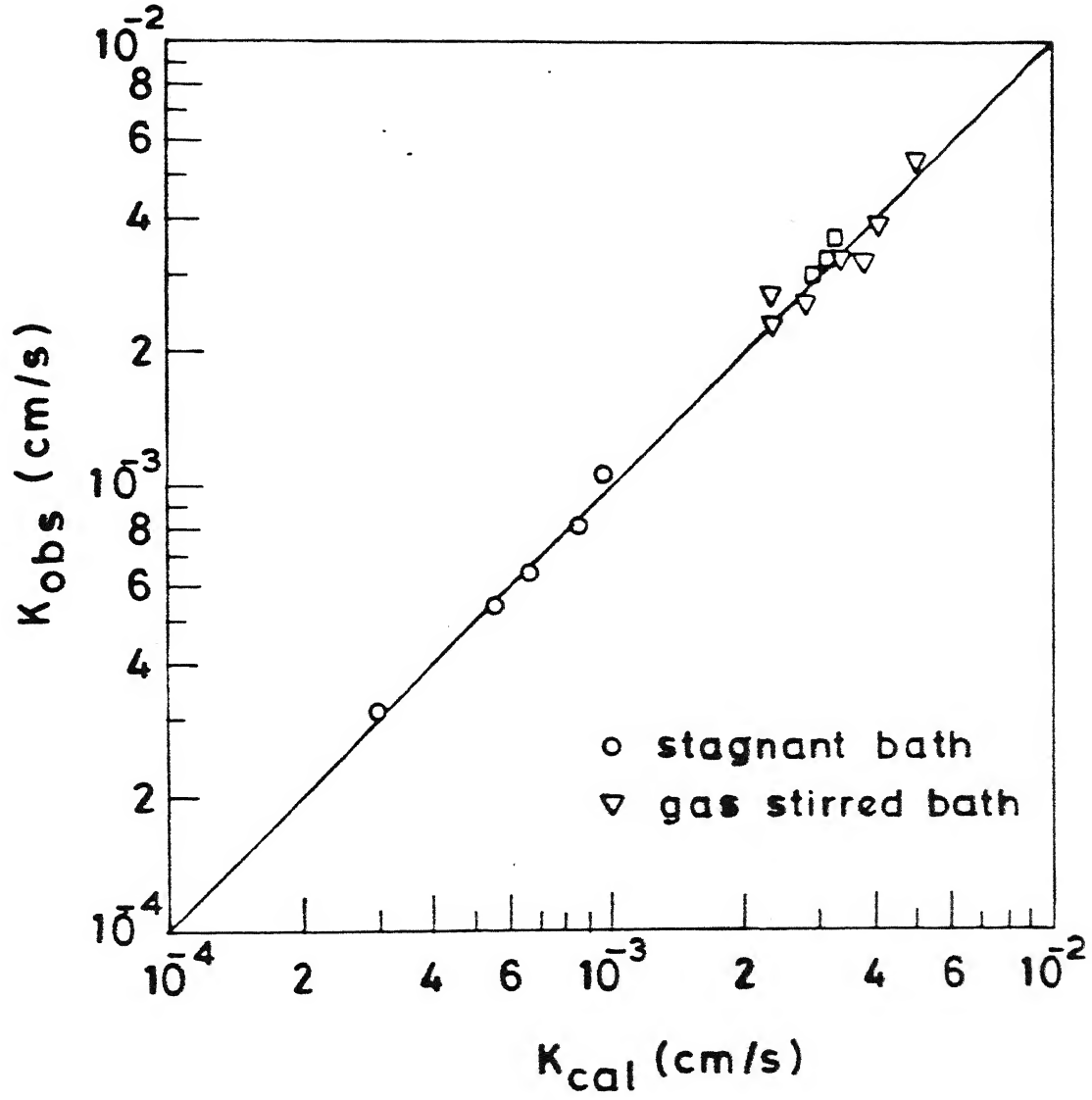

Fig. 28. Comparision of the mass transfer coefficient (between k observation and k calculation).

in the present investigation. k_N is natural convective mass transfer coefficient, D is diffusion coefficient of acid in water, ρ is density of water, β is coefficient of density change with concentration, ΔC is change in concentration ($\Delta C = C_s - C_B$) and L is characteristic length and η is viscosity of water.

In a gas stirred water bath the dissolution occurs by combined natural and forced convective mass transfer and k_c is determined by[7]

$$\frac{k_c L}{D} = 0.079 \left(\frac{LU\rho}{\eta}\right)^{0.7} \left(\frac{\eta}{\rho D}\right)^{0.356} \qquad (19)$$

In the correlation 19, U is liquid velocity past the solid surface. It is determined by[21]

$$U_B = \frac{k' \dot{V}_g \, H^{0.25}}{R^{\frac{1}{3}}} \qquad (20)$$

For bottom injection. In the eq.20, k' is a constant ($4.19\ m^{\frac{1}{2}}\ s^{-\frac{2}{3}}$)[21] $\dot{V}_g$ is volumetric flow rate in Nm^3/s, H is height of bath in m and R is vessel radius in m. For top injection U_T is determined by [21]

$$U_T = \beta^{\frac{1}{3}} U_B \qquad (21)$$

where β is depth of submergence of the lance.

The eq.20 and 21 determine the velocity of liquid at the top surface of the bath. At other locations in the bath no such correlation to calculate U is available in the literature. Therefore k_c for top and bottom injection could be calculated by expression 19 only for the compact dissolving at the top surface of the bath (see fig.3 for location).

The agreement between observed and calculated k (k_N or k_c) values suggests once again that the dissolution of solid of changing surface area is described very well by ~~cube root~~ cubic rate law i.e. expression 17.

5.2 Variation of k

Fig.29 shows the variation of k at constant gas injection rate with the axial location of introduction of the additive Z/H when the additive is in the plume (r = 0) and outside the plume (r = R). The experimental results are presented by the following least square lines:

$$\left.\begin{aligned} k &= e^{0.596Z/H} - 6.269 \qquad \text{for } r = 0 \\ k &= e^{0.836Z/H} - 6.717 \qquad \text{for } r = R \end{aligned}\right\} \qquad (22)$$

The experimental results show that k depends on the axial and radial locations of the additive: k is highest at Z/H = 1 and r = 0 and lowest at Z/H = 0 and r = R. This is due to the fact that in central gas injection the liquid velocity is maximum at the top surface of the plume and minimum at the bottom outside of the plume[1-4].

Fig 30 shows the variation of k with the location of the gas injecting nozzle at the base of the vessel. The location of the additive is r = R, Z/H = 1 and r = R; Z/H $\simeq$ 0. It can be seen in the figure that off location of gas injecting nozzle considerably improves the value of k of the solid dissolving from the bottom of the bath whereas k is almost independent of off location of nozzle for solid dissolving from the surface of the bath.

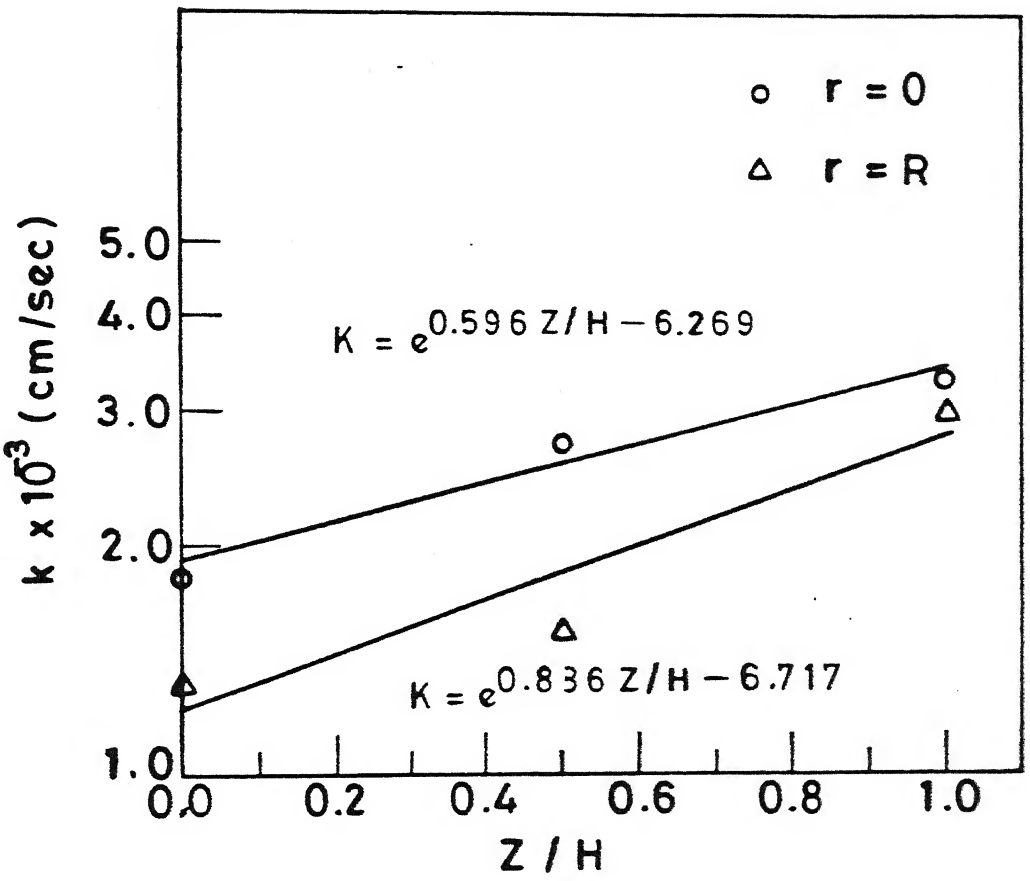

Fig. 29. Variation of k values at constant gas injection rate with different positions of additive (in the plume and out of plume).

The experimental results are presented by the following last square lines:

$$\left.\begin{aligned} k &= e^{0.6848\frac{r_n}{R}} - 6.633 \;;\quad r = R;\quad Z/H \simeq 0 \\ k &= e^{-0.0592\,\frac{r_n}{R}} - 5.802;\quad r = R;\quad Z/H = 1 \end{aligned}\right\} \qquad (23)$$

In Fig.31 the variation of k with aspect ratio of the bath (H/D) is presented by the following last square line:

$$k = 2.94 \times 10^{-3}(H/D)^{0.1983} \qquad (24)$$

The k - value is almost independent of H/D within the range of the present investigation. This is due to the fact that liquid velocity induced by gas injection in the bath was not varying significantly with the bath height[1-4].

All the above variation of k with the respective parameters suggest that k depends on the velocity of the liquid past the solid surface. Since the liquid velocity induced by gas injection depends on H/D, location of gas injecting nozzle and location of additive[1-4], therefore, k varies accordingly.

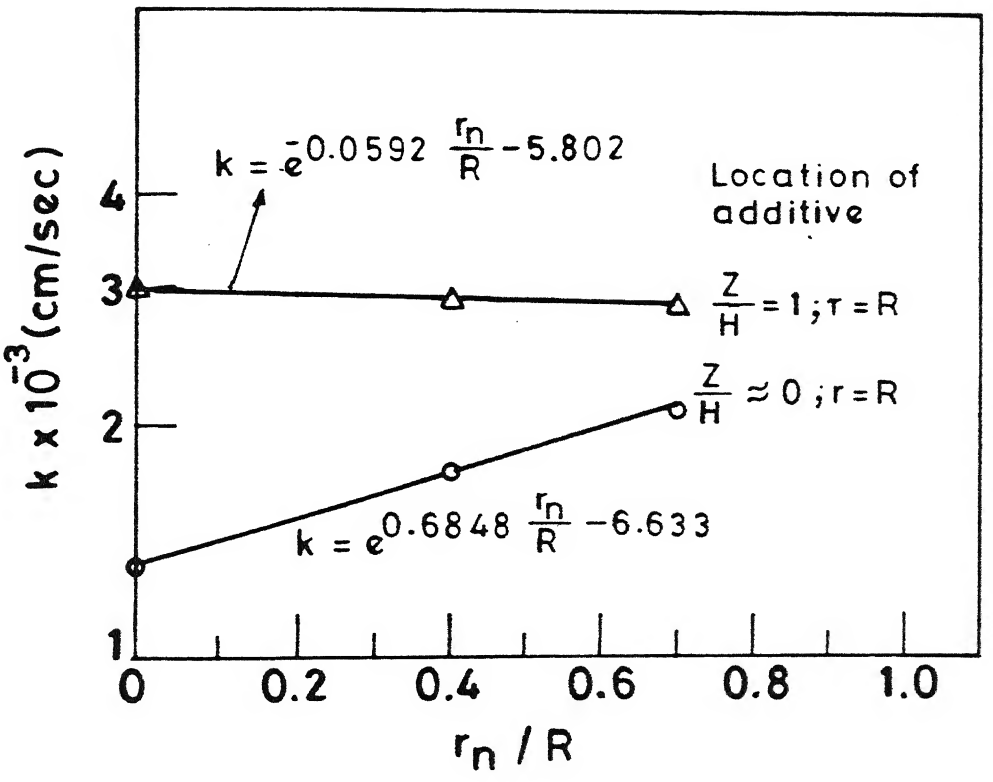

Fig. 30. Variation of k values with different positions of nozzle (centre and off-centre injection gas)

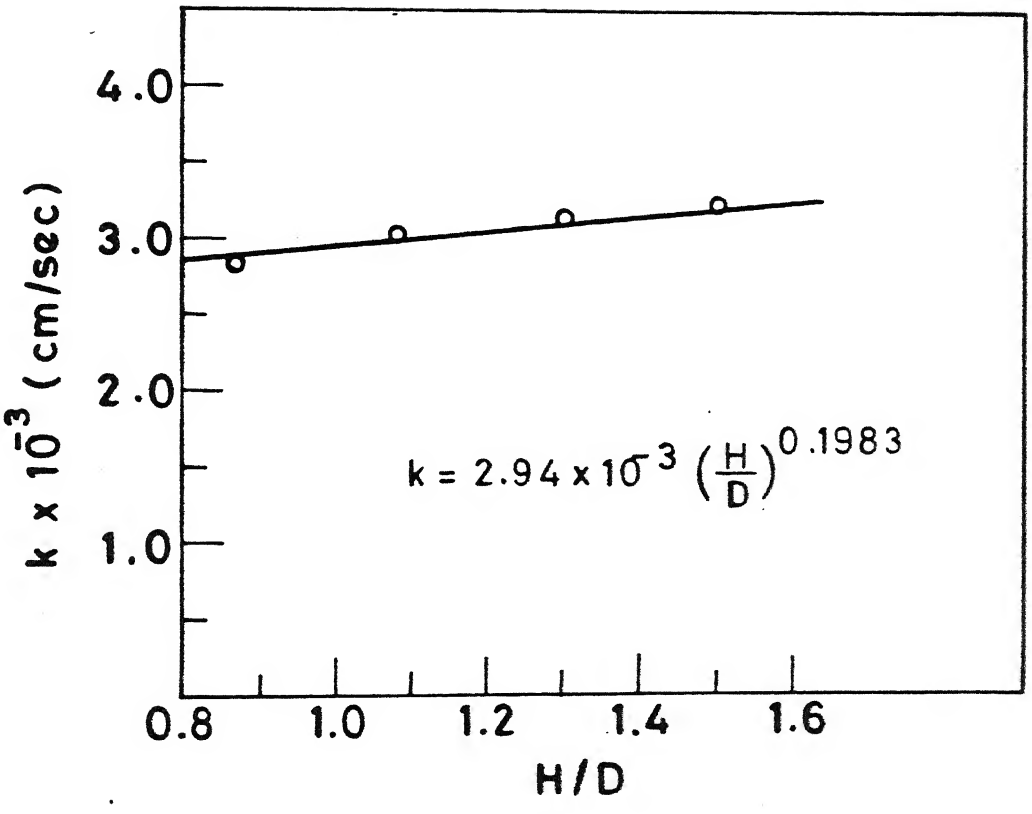

Fig. 31. Variation of k values with aspect ratios.

Chapter 7

APPLICATION TO INDUSTRIAL SYSTEMS

As the experiments are performed by maintaining a close similarity with the industrial system steel melt solid additive (see Table 2), the results of the experiments can be discussed in terms of applicability to the above system. The limitation of the low temperature mass transfer system, as one here, should be kept clearly in mind as far as heat transfer simulation is concerned. Nevertheless, the experimental results do indicate that the practice of gas stirring of steel melts in ladles can be easily extended to alloying of steel, composition adjustments, refining and other purposes. In this connection the following derived information may be relevent.

7.1 Gas Injection Rate and Location of Additive

The experimental results suggest that only small amount of gas is needed to increase the dissolution of the additions made at any location in the bath (the amount dissolved will depend on the location). At higher gas injection rates the amount dissolved does not increase appreciably. From the value of optimum gas injection rate (see Fig.5 in which optimum gas injection rate is 2.2 Nl/min.) the modified Froude number by Eq.11 is determined in the present investigation: its value is $0.897 \simeq 0.9$. This observation is important and could be used to determine the optimum gas injection rate in submerged injection treatment of liquid steel in ladles:

Consider the expression 11 in which $N_{Fr} \geq 0.9$, one obtains

$$(Q^2)_{opt} = \frac{0.9Hd^4 \rho_l}{0.0826 \rho_g} \qquad (25)$$

In the expression 25 d as a function of D is not known. From geometrical similarity consideration d/D should be constant[25,26] i.e.

$$\frac{d}{D} = K \qquad (26)$$

The value of K is determined by the data of the reference[22] in the present investigation as 4.33×10^{-3}. Substituting this value of K in expression 26 and with the help of eq.25 one obtains after simplification the following expression for Argon/liquid steel system:

$$Q_{opt} = 3.877 \times 10^{-3} \left(\frac{H}{D}\right)^{0.5} D^{2.5} \qquad (27)$$

In the expression 27 D is in (m) in order to get Q_{opt} in Nm^3/s. The optimum gas injection rate varies strongly with the ladle diameter. The eq.27 is represented in Fig.32. From this figure the optimum amount of gas can be determined from a knowledge of bath dimensions for the ratio $d/D = 4.3 \times 10^{-3}$. For other d/D ratios eq.25 should be used.

Another important finding of the present investigation is that the amount of additive dissolved depend very much on the location of introduction of the additive irrespective of the nozzle position at the base of the vessel. For this purpose Fig.33 is prepared in which the fractional amount dissolved (in pct.) in 10 min. is shown at various

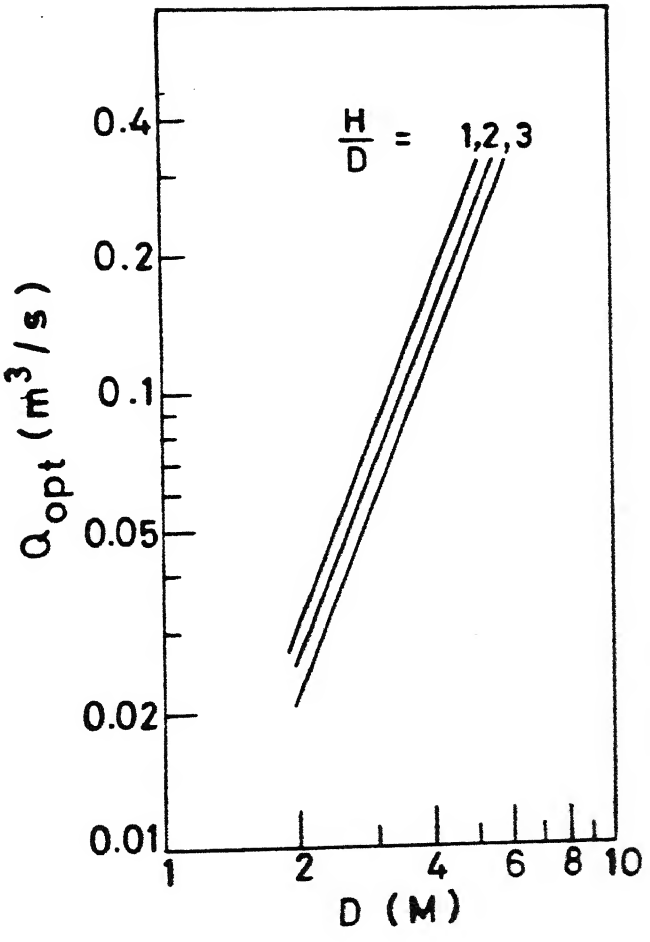

Fig. 32. Optimum gas flow rate as a function of vessel diameter for liquid steel/Argon system.

Despite the limitations of low temperature mass transfer system Fig.33 does show the most favourable position of the introduction of the solid additive in the actual gas stirred melts in ladles. The most favourable position is the 'eye' of the plume or closed to the surface of the annulus zone by plunging the additive. The practice of plunging the solid additive at the above locations will ensure quick assimilation of the additive into the bath which results in high recovery and reduced losses by oxidation.

7.2 Calculation of dissolution time of metallic material in steel melt

The eq.17 provides an easy estimation of total dissolution time (t_T). For the metallic materials whose melting points are higher than liquid steel, initial thermal time is much less than the free dissolution period[7,29]. The total dissolution time (for a free dissolution period) is given by eq.17 in that m = 0:

$$t_T = \frac{3\ m_o}{S_o K C_s} \qquad (28)$$

where $k = k_N$ or k_c depending on the hydrodynamic conditions of the steel bath. The total dissolution time of molybdenum sphere of different diameters in stagnant liquid steel bath is calculated by eq. 28. k_N is determined by correlation 18. The various values of physical constants are taken from[7,29]. The results of calculations are shown in Fig.34 with theoretical predictions of Guthrie and Coworker[29].

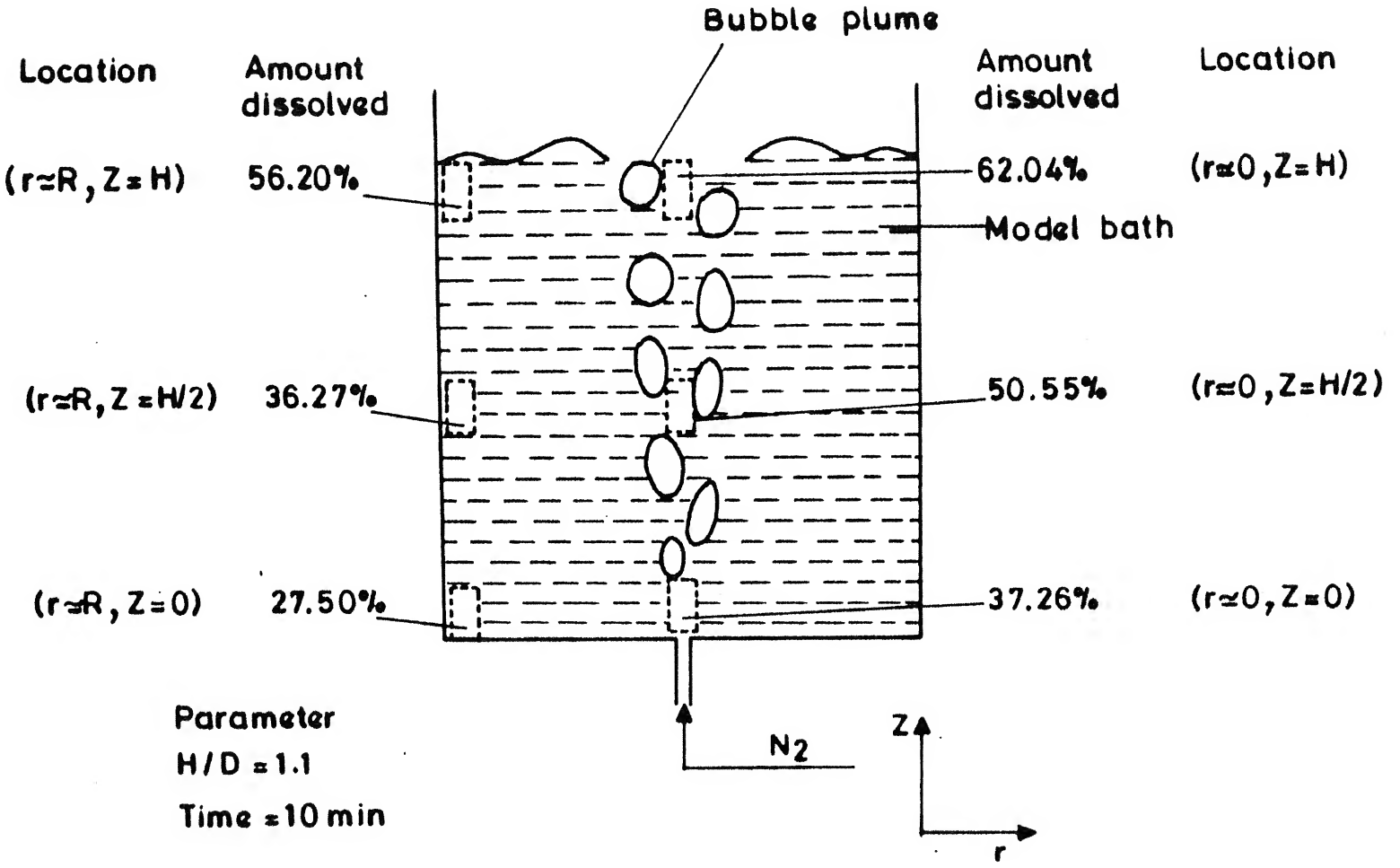

Fig. 33. Representation of a centrally gas stirred ladle in terms of the dissolution of an addition. The amount dissolved corresponds to the value of the modified Froude number 5.02.

The comparison shows that equation 28 determines larger dissolution times (about 7 percent) than theoretical predictions of Guthrie and Coworker[29]. This is to be expected in view of the limitations of low temperature mass transfer system (heat transfer effects are not considered) as that of present investigation. Despite, the agreement between the two is surprisingly good. (See Appendix E).

Some experiments are performed at high temperature to know influence of agitation on the dissolution. For this purpose commercial grade of Cu is dissolved in liquid aluminium. In some experiments bath is stirred with N_2 whereas in other bath is not stirred. The results are given in table 1 of Appendix-D and ploted in Fig. 35.

Influence of agitation on dissolutions of Cu in liquid aluminium is clearly visible in Fig. 35. For no stirring conditions the dissolution is very slow than when bath is stirred.

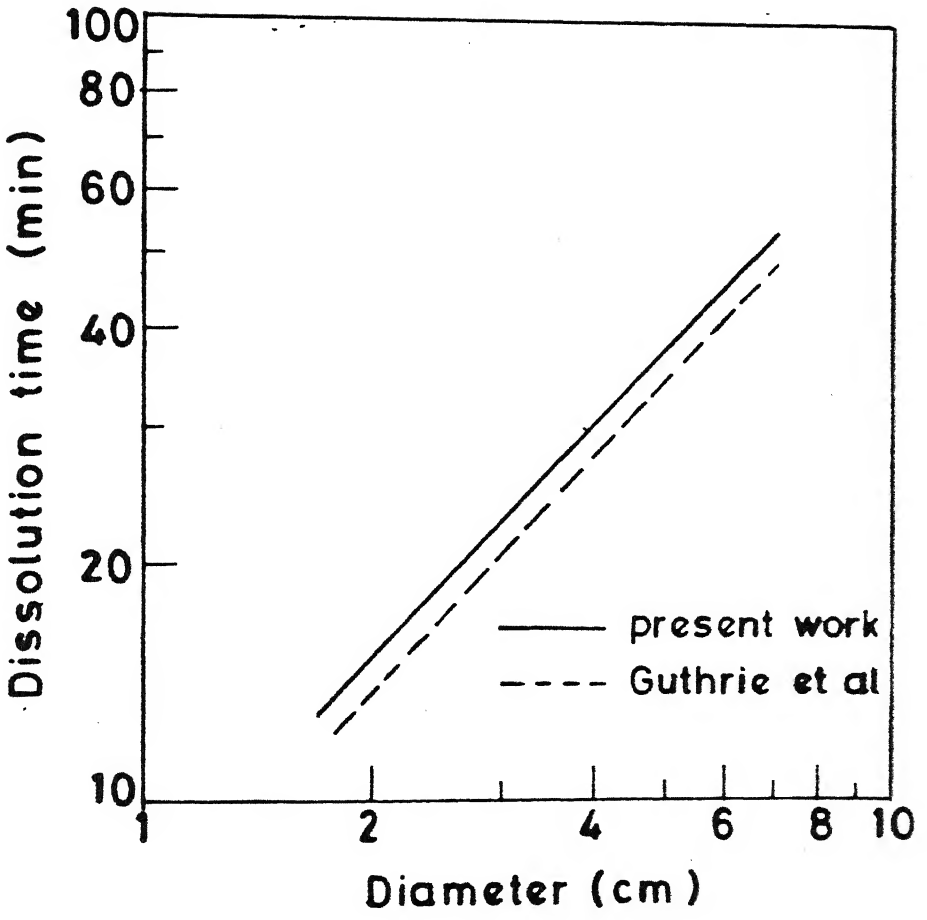

Fig. 34. Dissolution time of Molybdenum sphere in steel melt vs. different diameters.

Chapter 8

CONCLUSION:

An experimental study is conducted to study the dissolution of dense solid additives in gas stirred steel melts by using a low temperature mass transfer system. The following conclusion are derived:

1 - Slight amount of gas injection considerably increases the amount of additive dissolved in the liquid and further increase in gas injection rate causes only a small increase in the dissolution.

2 - The most favourable location for the introduction of the additive is found to be << eye >> of the plume.

3 - It is observed that off-centre injection significantly improves the dissolution of the addition made at the bottom of the vessel. From these results the optimum gas injection rate is determined for submerged gas injection treatment of liquid steel in ladles.

4 - A cubic rate law has discribed the process of dissolution.

Chapter 9

SUGGESTIONS FOR FURTHER WORKS

Further work may be done along the following lines:

1 - Study on dissolution of solid in liquid at high temperature.

2 - Study on injection of powder in liquid melts for alloying purpose.

3 - Study on dissolution of large solid cylinder in low temperature and high temperature liquid.

Appendix : A

GENERAL INFORMATIONSOF BOTTOM GAS INJECTION

1 - Vessel dimensions : ϕ 143 m.m.; L = 400 m.m.

2 - High of the bath with 2.0 l of water : 114.4 m.m.

3 - High of the bath with 2.5 l of water : 155 m.m.

4 - High of the bath with 3.0 l of water : 186.7 m.m.

5 - High of the bath with 3.5 l of water : 217.9 m.m.

6 - Temperature for all experiment : 30^{o}C
Except some cases for variable of Temperature.

7 - Nozzle diameter : 1 m.m.

8 - Gas injection : Nitrogen.

TABLE 1 : Variation of gas flowrate : 1 NL/min

additive position . : Surface

Time (min)	L (cm)	D (cm)	A (cm^2)	m (grams)	$m^{1/3}$	$m_o^{1/3} - m^{1/3}$	At/Ao	m/m_o	$1 - \frac{m}{m_o}$
0	1.52	2.33	19.69	9.72	2.13	0	1	1	0
5	1.36	2.15	16.48	7.41	1.95	0.18	0.84	0.73	0.27
10	1.18	1.96	13.30	5.32	1.75	0.39	0.67	0.55	0.45
15	1.00	1.76	10.39	3.63	1.54	0.60	0.53	0.37	0.63

TABLE 2 : Variation of gas flowrate : 2.23 NL/min

Additive position : Surface

TIME (min)	L (cm)	D (cm)	A (cm^2)	m (grams)	$m^{1/3}$	$m_o^{1/3} - m^{1/3}$	At/Ao	m/m_o	$1 - \frac{m}{m_o}$
0	1.60	2.33	20.23	10.12	2.16	0	1	1	0
5	1.34	2.14	16.20	7.15	1.93	0.23	0.80	0.71	0.29
10	1.10	1.96	12.80	4.92	1.70	0.46	0.63	0.49	0.51
15	0.91	1.77	9.98	3.32	1.49	0.67	0.49	0.33	0.67
20	0.64	1.61	7.31	1.93	1.24	0.92	0.36	0.19	0.81
25	0.50	1.40	5.27	1.14	1.04	1.12	0.26	0.11	0.89

TABLE 3 : Variation of gas flowrate : 5.25 NL/min
Additive position : Surface

TIME (min)	L (cm)	D (cm)	A (cm^2)	m (grams)	$m^{1/3}$	$m_o^{1/3} - m^{1/3}$	At/A_o	m/m_o	$1 - \frac{m}{m_o}$
0	1.58	2.33	20.09	10.14	2.16	0	1	1	0
5	1.29	2.07	15.17	6.57	1.87	0.29	0.75	0.65	0.35
10	1.06	1.88	11.84	4.45	1.64	0.52	0.59	0.44	0.56
15	0.80	1.64	8.37	2.56	1.37	0.79	0.42	0.25	0.75
20	0.58	1.46	6.06	1.48	1.14	1.02	0.30	0.15	0.85
25	0.35	1.27	3.95	0.67	0.87	1.29	0.19	0.06	0.94

TABLE 4 : Variation of gas flow rate : 8.9 NL/min
Additive position : Surface

TIME (min)	L (cm)	D (cm)	A (cm^2)	m (grams)	$m^{1/3}$	$m_o^{1/3} - m^{1/3}$	At/A_o	m/m_o	$1 - \frac{m}{m_o}$
0	1.58	2.33	20.09	10.12	2.16	0	1	1	0
5	1.28	2.06	15.03	6.46	1.86	0.30	0.75	0.64	0.36
10	1.00	1.85	11.18	4.03	1.59	0.57	0.56	0.40	0.60
15	0.76	1.62	8.01	2.36	1.33	0.83	0.40	0.23	0.77
20	0.50	1.40	5.31	1.16	1.05	1.11	0.26	0.11	0.89

TABLE 5 : Variation of gas flow rate : 2.23 NL/min

Additive position : bottom

TIME (min)	L (cm)	D (cm)	A (cm^2)	m (grams)	$m^{1/3}$	$m_c^{1/3} - m^{1/3}$	At/A_o	m/m_o	$1 - \frac{m}{m_o}$
0	1.58	2.33	20.09	10.13	2.16	0	1	1	0
5	1.48	2.24	18.29	8.77	2.06	0.10	0.91	0.86	0.14
10	1.39	2.17	16.93	7.77	1.98	0.18	0.84	0.76	0.24
15	1.30	2.08	15.37	6.70	1.88	0.28	0.76	0.66	0.34
20	1.20	1.98	13.62	5.56	1.77	0.39	0.68	0.55	0.45
25	1.12	1.88	12.2	4.70	1.67	0.49	0.61	0.46	0.54
30	1.03	1.78	10.73	3.86	1.57	0.59	0.53	0.38	0.62
35	0.92	1.66	9.12	2.99	1.44	0.72	0.45	0.29	0.71

TABLE 6 : Variation of gas flowrate : 5.25 NL/min.

Additive position : bottom

TIME (min)	L (cm)	D (cm)	A (cm^2)	m (grams)	$m^{1/3}$	$m_c^{1/3} - m^{1/3}$	At/A_o	m/m_o	$1 - \frac{m}{m_o}$
0	1.52	2.33	19.69	9.76	2.14	0	1	1	0
5	1.41	2.23	17.69	8.26	2.02	0.11	0.90	0.85	0.15
15	1.21	2.05	14.39	5.99	1.82	0.32	0.73	0.61	0.39
25	1.02	1.87	11.48	4.20	1.61	0.52	0.58	0.43	0.57
35	0.81	1.59	8.02	2.41	1.34	0.80	0.41	0.25	0.75
45	0.63	1.38	5.72	1.41	1.12	1.01	0.29	0.14	0.86
55	0.43	1.15	3.63	0.67	0.87	1.26	0.18	0.07	0.93

TABLE 7 : Variation of bath temperature : 18°C
gas flow rate : 5.25 NL/min
Additive position : Surface

TIME (min)	L (cm)	D (cm)	A (cm^2)	m (grams)	$m^{1/3}$	$m_c^{1/3} - m^{1/3}$	At/A_o	m/m_o	$1 - \frac{m}{m_o}$
0	1.57	2.33	20.05	10.14	2.16	0	1	1	0
5	1.48	2.24	18.30	8.81	2.06	0.10	0.91	0.87	0.13
10	1.37	2.17	16.73	7.65	1.97	0.19	0.83	0.75	0.25
15	1.24	2.07	14.80	6.30	1.85	0.32	0.74	0.62	0.38
20	1.12	1.96	12.93	5.10	1.72	0.44	0.64	0.50	0.50
25	0.97	1.84	11.12	3.92	1.58	0.59	0.55	0.38	0.62
30	0.85	1.74	9.40	3.05	1.45	0.71	0.47	0.30	0.70
35	0.72	1.62	7.81	2.26	1.31	0.85	0.39	0.22	0.78

TABLE 8 : Variation of bath temperature : 20°C
Gas flow rate : 0

TIME (min)	L (cm)	D (cm)	A (cm^2)	m (grams)	$m^{1/3}$	$m_c^{1/3} - m^{1/3}$	At/A_o	m/m_o	$1 - \frac{m}{m_o}$
0	1.52	2.33	19.65	9.72	2.13	0	1	1	0
5	1.49	2.32	19.31	9.44	2.11	0.02	0.98	0.97	0.03
10	1.47	2.30	18.93	9.16	2.09	0.04	0.96	0.94	0.06

TABLE 9 : Variation of bath temperature : 25°C
Gas flow rate : 0

TIME (min)	L (cm)	D (cm)	A (cm^2)	m (grams)	$m^{1/3}$	$m_c^{1/3} - m^{1/3}$	At/A_o	m/m_o	$1 - \frac{m}{m_o}$
0	1.58	2.33	20.09	10.10	2.16	0	1	1	-
5	1.53	2.29	19.28	9.48	2.12	0.04	0.96	0.94	0.06
10	1.51	2.26	18.77	9.11	2.08	0.07	0.93	0.90	0.10

TIME 10 : Variation of bath temperature : 30°C
Gas flow rate : 0

TIME (min)	L (cm)	D (cm)	A (cm^2)	m (grams)	$m^{1/3}$	$m_c^{1/3} - m^{1/3}$	At/A_o	m/m_o	$1 - \frac{m}{m_o}$
0	1.58	2.33	20.09	10.13	2.16	0	1	1	0
5	1.52	2.27	18.99	9.29	2.10	0.06	0.94	0.92	0.08
15	1.4	2.14	16.60	7.57	1.96	0.20	0.82	0.75	0.25
25	1.27	2.05	14.81	6.33	1.85	0.31	0.74	0.62	0.38
35	1.14	1.91	12.57	4.91	1.70	0.46	0.62	0.48	0.52
45	0.98	1.75	10.22	3.56	1.53	0.63	0.51	0.35	0.65
55	0.87	1.61	8.47	2.66	1.38	0.77	0.42	0.26	0.74

TABLE 11:

- Variation of different types of additives: Borric acid
- Additive position: Surface
- Gas flow rate : 5.25 NL/min
- bath Temperature : 30°C

TIME (min)	L (cm)	D (cm)	A (cm^2)	m (grams)	$m^{\frac{1}{3}}$	$m_o^{\frac{1}{3}} - m^{\frac{1}{3}}$	$\frac{At}{A_o}$	$\frac{m}{m_o}$	$1-\frac{m}{m_o}$
0	1.57	2.33	20.05	9.68	2.13	0	1	1	0
5	1.47	2.22	18.03	8.23	2.02	0.11	0.90	0.90	0.10
10	1.35	2.11	15.94	6.80	1.89	0.23	0.79	0.79	0.21
15	1.23	2.00	14.01	5.57	1.77	0.36	0.70	0.69	0.31
20	1.12	1.90	12.35	4.58	1.66	0.47	0.62	0.61	0.39
25	1.00	1.80	10.74	3.67	1.54	0.59	0.53	0.52	0.48

TABLE 12: - Variation of different types of additives Succinic acid
- Additive Position : Surface
- Gas flow rate : 5.25 NL/min
- bath Temperature : 30°C

TIME (min)	L (cm)	D (cm)	A (cm^2)	m (grams)	$m^{\frac{1}{3}}$	$m_o^{\frac{1}{3}} - m^{\frac{1}{3}}$	$\frac{At}{A_o}$	$\frac{m}{m_o}$	$1 - \frac{m}{m_o}$
0	1.58	2.33	20.09	9.73	2.13	0	1	1	0
5	1.50	2.24	18.44	8.54	2.04	0.09	0.92	0.92	0.08
10	1.38	2.13	16.36	7.10	1.92	0.21	0.81	0.81	0.19
15	1.25	2.05	14.65	5.96	1.81	0.32	0.73	0.72	0.28
20	1.17	1.95	13.14	5.04	1.71	0.42	0.65	0.65	0.35
25	1.05	1.80	11.27	3.86	1.57	0.56	0.56	0.54	0.46
30	0.95	1.75	10.03	3.30	1.49	0.65	0.50	0.49	0.51

TABLE 13:

- Variation of different types of additive: Benzoic acid
- Additive Position : Surface
- Gas flow rate : 5.25 NL/min
- bath Temperature : 30°C

TIME (min)	L (cm)	D (cm)	A (cm^2)	m (grams)	$m^{\frac{1}{3}}$	$m_o^{\frac{1}{3}} - m^{\frac{1}{3}}$	$\frac{AT}{A_o}$	$\frac{m}{m_o}$	$1 - \frac{m}{m_o}$
0	1.76	2.33	21.41	9.71	2.13	0	1	1	0
30	1.72	2.31	20.93	9.37	2.11	0.02	0.98	0.97	0.03
50	1.68	2.30	20.45	9.03	2.08	0.05	0.95	0.95	0.05

TABLE 14 : - Variation of the bath's aspect ratio : $\frac{H}{D}$ = 0.87
- Additive Position : Surface
- Gas Flow rate : 5.25 NL/min.

TIME (min)	L (cm)	D (cm)	A (cm^2)	m (grams)	$m^{\frac{1}{3}}$	$m_o^{\frac{1}{3}} - m^{\frac{1}{3}}$	$\frac{At}{A_o}$	$\frac{m}{m_o}$	$1 - \frac{m}{m_o}$
0	1.52	2.33	19.65	9.73	2.13	0	1	1	0
5	1.30	2.09	15.40	6.69	1.88	0.25	0.78	0.69	0.31
10	1.08	1.88	11.93	4.50	1.65	0.48	0.61	0.46	0.54
15	0.87	1.62	8.55	2.69	1.39	0.74	0.43	0.28	0.72
20	0.66	1.39	5.92	1.50	1.14	0.99	0.30	0.15	0.85

TABLE 15 : - Variation of the bath's aspect ratio : $\frac{H}{D}$ = 1.30
- Additive Position : Surface
- Gas flow rate : 5.25 NL/min.

TIME (min)	L (cm)	D (cm)	A (cm^2)	m (grams)	$m^{\frac{1}{3}}$	$m_o^{\frac{1}{3}} - m^{\frac{1}{3}}$	$\frac{At}{A_o}$	$\frac{m}{m_o}$	$1 - \frac{m}{m_o}$
0	1.53	2.33	19.73	9.77	2.14	0	1	1	0
5	1.25	2.05	14.65	6.18	1.83	0.30	0.74	0.63	0.37
10	1.02	1.85	11.30	4.10	1.60	0.54	0.57	0.42	0.58
15	0.79	1.60	7.99	2.38	1.33	0.80	0.40	0.24	0.76
20	0.57	1.38	5.46	1.28	1.08	1.05	0.28	0.13	0.87

TABLE 16 : - Variation of the bath's aspect ratio : $\frac{H}{D}$ = 1.52
- Additive Position : Surface
- Gas flow rate : 5.25 NL/min

TIME (min)	L (cm)	D (cm)	A (cm^2)	m (grams)	$m^{\frac{1}{3}}$	$m_o^{\frac{1}{3}} - m^{\frac{1}{3}}$	$\frac{At}{A_o}$	$\frac{m}{m_o}$	$1 - \frac{m}{m_o}$
0	1.53	2.33	19.73	9.74	2.13	0	1	1	0
5	1.23	2.04	14.42	6.00	1.82	0.32	0.73	0.62	0.38
10	1.00	1.82	10.92	3.88	1.57	0.56	0.55	0.40	0.60
15	0.77	1.56	7.60	2.20	1.30	0.83	0.38	0.22	0.78
20	0.53	1.35	4.37	1.13	1.04	1.09	0.22	0.12	0.88

TABLE 17 : - Variation of the nozzle's location : non-central injection
- Additive Position : bottom
- Gas flow rate : 2.23 NL/min.

TIME (min)	L (cm)	D (cm)	A (cm^2)	m (grams)	$m^{\frac{1}{3}}$	$m_o^{\frac{1}{3}} - m^{\frac{1}{3}}$	$\frac{At}{A_o}$	$\frac{m}{m_o}$	$1 - \frac{m}{m_o}$
0	1.54	2.33	19.80	9.75	2.14	0	1	1	0
5	1.39	2.20	17.21	7.84	1.99	0.15	0.87	0.80	0.20
10	1.22	2.04	14.35	5.92	1.81	0.33	0.72	0.61	0.39
15	1.12	1.87	12.10	4.59	1.66	0.47	0.61	0.47	0.53
20	0.97	1.71	9.80	3.31	1.49	0.65	0.49	0.34	0.66

TABLE 18 : - Variation of the nozzle's location : non-central injection
- Additive Position : Bottom
- Gas flow rate : 5.25 NL/min.

TIME (min)	L (cm)	D (cm)	A (cm^2)	m (grams)	$m^{\frac{1}{3}}$	$m_o^{\frac{1}{3}} - m^{\frac{1}{3}}$	$\frac{At}{A_o}$	$\frac{m}{m_o}$	$1 - \frac{m}{m_o}$
0	1.52	2.33	19.65	9.72	2.13	0	1	1	0
5	1.36	2.15	16.44	7.41	1.95	0.18	0.84	0.76	0.24
10	1.20	1.97	13.52	5.49	1.76	0.37	0.69	0.56	0.44
15	1.06	1.79	11.00	4.00	1.59	0.55	0.56	0.41	0.59
20	0.90	1.63	8.78	2.82	1.41	0.72	0.45	0.30	0.70

TABLE 19 : - Variation of the nozzle's location : non central injection
- Additive Position : Surface
- Gas flow rate : 5.25 NL/min

TIME (min)	L (cm)	D (cm)	A (cm^2)	m (grams)	$m^{\frac{1}{3}}$	$m_o^{\frac{1}{3}} - m^{\frac{1}{3}}$	$\frac{At}{A_o}$	$\frac{m}{m_o}$	$1 - \frac{m}{m_o}$
0	1.52	2.33	19.69	9.74	2.13	0	1	1	0
5	1.30	2.12	15.72	6.87	1.90	0.23	0.80	0.70	0.30
10	1.07	1.91	12.15	4.59	1.66	0.47	0.62	0.47	0.53
15	0.87	1.69	9.10	2.92	1.43	0.84	0.46	0.30	0.70
20	0.66	1.46	6.37	1.65	1.18	0.95	0.32	0.17	0.83

- Gas flow rate : 5.25 NL/min.

- variation of the additive's location : r = 0 ; Z = H

TIME (min)	L (cm)	D (cm)	A (cm^2)	m (grams)	$m^{\frac{1}{3}}$	$m_o^{\frac{1}{3}} - m^{\frac{1}{3}}$	$\frac{At}{A_o}$	$\frac{m}{m_o}$	$1 - \frac{m}{m_o}$
0	1.52	2.33	19.65	9.74	2.14	0	1	1	0
5	1.25	2.03	14.44	6.08	1.82	0.31	0.73	0.62	0.38
10	1.00	1.77	10.48	3.70	1.55	0.59	0.53	0.38	0.62
15	0.77	1.56	7.59	2.21	1.30	0.83	0.39	0.23	0.77

TABLE 21 : - Variation of the additive's location: r = 0; Z = $\frac{H}{2}$

- Gas flow rate : 5.25 NL/min

TIME (min)	L (cm)	D (cm)	A (cm^2)	m (grams)	$m^{\frac{1}{3}}$	$m_o^{\frac{1}{3}} - m^{\frac{1}{3}}$	$\frac{At}{A_o}$	$\frac{m}{m_o}$	$1 - \frac{m}{m_o}$
0	1.52	2.33	19.65	9.74	2.13	0	1	1	0
10	1.09	1.94	12.51	4.82	1.69	0.43	0.64	0.49	0.51
15	0.78	1.68	8.51	2.58	1.37	0.74	0.43	0.26	0.74

Table 22 : - Variation of the additive's location : r = o; z = o
- gas flow rate : 5.25 NL/min

TIME (min)	L (cm)	D (cm)	A (cm^2)	m (grams)	$m^{\frac{1}{3}}$	$m_o^{\frac{1}{3}} - m^{\frac{1}{3}}$	$\frac{At}{A_o}$	$\frac{m}{m_o}$	$1 - \frac{m}{m_o}$
0	1.53	2.33	19.73	9.72	2.13	0	1	1	0
10	1.24	2.05	14.59	6.10	1.82	0.31	0.74	0.63	0.37
20	0.94	1.75	9.99	3.37	1.50	0.63	0.51	0.35	0.65

TABLE 23 :

- Variation of the additive's location: r = R, $Z = \frac{H}{2}$
- Gas flow rate : 5.25 NL/min.

TIME (min)	L (cm)	D (cm)	A (cm^2)	m (grams)	$m^{\frac{1}{3}}$	$m_o^{\frac{1}{3}} - m^{\frac{1}{3}}$	$\frac{At}{A_o}$	$\frac{m}{m_o}$	$1 - \frac{m}{m_o}$
0	1.52	2.33	19.65	9.74	2.13	0	1	1	0
10	1.27	2.03	14.62	6.21	1.84	0.28	0.74	0.64	0.36
20	1.03	1.79	10.90	3.94	1.58	0.54	0.55	0.40	0.60

- Additive Position : Surface
- Gas flow rate : 5.25 NL/min (91)
- Variation of the additive's initial weight : 5 grams

TIME (min)	L (cm)	D (cm)	A (cm^2)	m (grams)	$m^{\frac{1}{3}}$	$m_o^{\frac{1}{3}} - m^{\frac{1}{3}}$	$\frac{At}{A_o}$	$\frac{m}{m_o}$	$1 - \frac{m}{m_o}$
0	0.81	2.33	14.46	5.23	1.74	0	1	1	0
5	0.52	2.06	10.06	2.65	1.38	0.35	0.70	0.51	0.49
10	0.25	1.75	6.18	0.91	0.97	0.77	0.43	0.17	0.83

TABLE 25 : -Variation of the additive's initial weight: 32 grams
-Additive Position : Surface
-Gas flow rate : 5.25 NL/min

TIME (min)	L (cm)	D (cm)	A (cm^2)	m (grams)	$m^{\frac{1}{3}}$	$m_o^{\frac{1}{3}} - m^{\frac{1}{3}}$	$\frac{At}{A_o}$	$\frac{m}{m_o}$	$1 - \frac{m}{m_o}$
0	5.28	2.33	47.18	32.55	3.19	0	1	1	0
5	5.03	2.10	40.11	25.18	2.93	0.26	0.85	0.77	0.23
10	4.47	1.92	32.75	19.97	2.71	0.48	0.69	0.61	0.39
15	4.45	1.70	28.30	14.60	2.44	0.75	0.60	0.45	0.55
20	4.21	1.48	23.01	10.46	2.19	1.01	0.49	0.32	0.68
25	3.92	1.28	18.34	7.29	1.94	1.25	0.39	0.22	0.78

TABLE 26 : Changing of the additives area with it's weight.

$\frac{At}{A_o}$	$(\frac{m}{m_o})^{\frac{2}{3}}$	$\frac{At}{A_o}$	$(\frac{m}{m_o})^{\frac{2}{3}}$
1	1	0.589	0.577
0.945	0.943	0.583	0.570
0.910	0.908	0.556	0.542
0.898	0.895	0.534	0.524
0.842	0.837	0.509	0.498
0.826	0.823	0.493	0.476
0.800	0.793	0.454	0.443
0.765	0.759	0.421	0.410
0.755	0.748	0.416	0.399
0.748	0.741	0.407	0.394
0.731	0.722	0.397	0.387
0.678	0.669	0.361	0.332
0.633	0.618	0.301	0.277
0.625	0.617	0.290	0.276
0.607	0.598	0.264	0.236
0.592	0.593	0.260	0.234

Appendix : B

GENERAL INFORMATION FOR TOP GAS INJECTION

1 - Vessel dimension : ϕ 143 m.m.

L = 400 m.m.

2 - High of the bath with 2.5 l of water: 155 m.m.

3 - Lance inside diameter : ϕ 1 m.m.

L = 400 m.m.

4 - Gas Injection : Nitrogen

5 - Gas flow rate : 5.25 NL/min.

Table 1 : Variation for depth Submerged of the lance : h/H = 0
aditive position: Surface

Time (min.)	L (cm)	D (cm)	A (cm^2)	m (gm)	$m^{1/3}$	$m^{1/3} - m^{1/3}$	At/Ao	m/m_o	$1-m/m_o$
0	1.58	2.34	20.21	9.98	2.153	0	1	1	0
5	1.47	2.25	18.34	8.59	2.048	0.10	0.91	0.86	0.14
10	1.38	2.18	16.97	7.57	1.96	0.19	0.84	0.76	0.24
15	1.29	2.05	14.91	6.26	1.84	0.31	0.74	0.63	0.37
20	1.18	2.00	13.73	5.47	1.76	0.39	0.68	0.54	0.45

Table 2 : Variation for depth submergence of the lance : h/H = 0
additive position : bottom

Time (min.)	L (cm)	D (cm)	A (cm^2)	m (gm)	$m^{1/3}$	$m^{1/3} - m^{1/3}$	A_t/A_o	m/m_o	$1-m/m_o$
0	1.57	2.34	20.14	9.95	2.15	0	1	1	0
5	1.54	2.27	19.07	9.18	2.09	0.05	0.95	0.92	0.07
10	1.48	2.20	17.88	8.33	2.03	0.12	0.89	0.84	0.16
15	1.42	2.13	16.63	7.45	1.95	0.20	0.82	0.75	0.25
20	1.38	2.05	15.49	6.71	1.88	0.26	0.77	0.67	0.32

TABLE 3 : Variation for depth submergence of the lance : h/H = 0.25
additive position : Surface

Time (min.)	L (cm)	D (cm)	A (cm^2)	m (gm)	$m^{1/3}$	$m^{1/3} - m^{1/3}$	A_t/A_o	m/m_o	$1-m/m_o$
0	1.57	2.34	20.14	9.94	2.15	0	1	1	0
5	1.47	2.21	17.83	8.27	2.02	0.13	0.88	0.83	0.17
10	1.35	2.06	15.40	6.63	1.88	0.27	0.76	0.67	0.33
15	1.26	1.95	13.72	5.56	1.77	0.38	0.68	0.56	0.44
20	1.16	1.85	12.12	4.59	1.66	0.49	0.60	0.46	0.54

Table 4 : Variation for depth submergence of the lance : h/H = 0.25
additive position : bottom

Time (min.)	L (cm)	D (cm)	A (cm^2)	m (gm)	$m^{1/3}$	$m_o^{1/3} - m^{1/3}$	A_t/A_o	m/m_o	$1-m/m_o$
0	1.58	2.34	20.22	10.00	2.15	0	1	1	0
5	1.51	2.26	18.74	8.92	2.07	0.08	0.93	0.89	0.11
10	1.46	2.18	17.46	8.02	2.00	0.15	0.86	0.80	0.20
15	1.42	2.10	16.29	7.24	1.93	0.22	0.80	0.72	0.28
20	1.38	2.01	15.06	6.45	1.86	0.29	0.74	0.64	0.35

Table 5 : Variation fof depth submergence of the lance : h/H = 0.5
additive position : Surface

Time (min.)	L (cm)	D (cm)	A (cm^2)	m (gm)	$m^{1/3}$	$m_o^{1/3} - m^{1/3}$	A_t/A_o	m/m_o	$1- m/m_o$
0	1.57	2.33	20.02	9.93	2.15	0	1	1	0
5	1.33	2.11	15.81	6.89	1.90	0.24	0.79	0.69	0.30
10	1.09	1.87	11.89	4.44	1.64	0.51	0.59	0.45	0.55
15	0.84	1.68	8.86	2.76	1.40	0.75	0.44	0.28	0.72
20	0.62	1.38	5.73	1.39	1.12	1.03	0.28	1.14	0.86

Table 6 : Variation for depth submergence of the lance : h/H = 0.5
additive position : bottom

Time (min.)	L (cm)	D (m)	A (cm^2)	m (gm)	$m^{1/3}$	$m_o^{1/3} - m^{1/3}$	A_t/A_o	m/m_o	$1 - m/m_o$
0	1.58	2.34	20.21	9.93	2.15	0	1	1	0
5	1.52	2.23	18.46	8.68	2.05	0.09	0.91	0.87	0.13
10	1.43	2.12	16.58	7.38	1.95	0.20	0.82	0.74	0.26
15	1.36	2.00	14.83	6.25	1.84	0.29	0.73	0.63	0.37
20	1.30	1.91	13.53	5.44	1.76	0.31	0.66	0.55	0.45

Table 7 : Variation for depth submergence of the lance : h/H = 0.75
additive position : Surface

Time (min.)	L (cm)	D (cm)	A (cm^2)	m (gm)	$m^{1/3}$	$m_o^{1/3} - m^{1/3}$	A_t/A_o	m/m_o	$1 - m/m_o$
0	1.58	2.34	20.21	9.94	2.15	0	1	1	0
5	1.33	2.23	14.95	6.3	1.84	0.30	0.74	0.63	0.36
10	1.13	1.84	11.85	4.39	1.64	0.51	0.58	0.44	0.56
15	0.93	1.46	7.61	2.28	1.32	0.83	0.37	0.23	0.77
20	0.72	1.19	4.92	1.17	1.05	1.09	0.24	0.12	0.88

Table 8 : Variation for depth Submergence of the lance : h/H = 0.75
additive position : bottom

Time (min.)	L (cm)	D (cm)	A (cm^2)	m (gm)	$m^{1/3}$	$m_o^{1/3} - m^{1/3}$	A_t/A_o	m/m_o	$1-m/m_o$
0	1.57	2.34	20.14	9.94	2.15	0	1	1	0
5	1.51	2.20	18.04	8.45	2.04	0.11	0.89	0.85	0.15
10	1.42	2.07	15.96	7.04	1.92	0.23	0.79	0.71	0.29
15	1.36	1.97	14.51	6.10	1.83	0.32	0.72	0.61	0.38
20	1.31	1.82	12.69	5.02	1.71	0.40	0.63	0.50	0.49

Table 9 : Variation for depth submergence of the lance : h/H = 1
additive position : Surface

Time (min.)	L (cm)	D (cm)	A (cm^2)	m (gm)	$m^{1/3}$	$m_o^{1/3} - m^{1/3}$	A_t/A_o	m/m_o	$1-m/m_o$
0	1.58	2.34	20.21	9.94	2.15	0	1	1	0
5	1.25	2.02	14.34	5.86	1.80	0.35	0.71	0.59	0.41
10	0.87	1.66	8.86	2.75	1.40	0.75	0.44	0.28	0.72
15	0.5	1.22	4.23	0.85	0.95	1.2	0.21	0.08	0.91
20	0	0	0	0	0	2.15	0	0	1

Table 13 : Variation for off centre injection : $r_n/R = 0.64$
depth submergence of the lance : $h/H = 0.625$
additive position : Surface

Time (min.)	L (cm)	D (cm)	A (cm^2)	m (gm)	$m^{1/3}$	$m_o^{1/3} - m^{1/3}$	A_t/A_o	m/m_o	$1 - m/m_o$
0	1.56	2.34	20.07	9.94	2.15	0	1	1	0
5	1.33	2.11	15.81	6.89	1.90	0.25	0.79	0.69	0.31
10	1.14	1.94	12.86	4.99	1.71	0.44	0.64	0.50	0.50
15	1.03	1.67	9.78	3.34	1.49	0.65	0.49	0.33	0.66
20	0.8	1.50	7.30	2.09	1.28	0.87	0.36	0.21	0.79

Table 14 : Variation for off centre injection : $r_n/R = 0.64$
depth submergence of the lances : $h/H = 0.625$
additive position : bottom

Time (min.)	L (cm)	D (cm)	A (cm^2)	m (gm)	$m^{1/3}$	$m_o^{1/3} - m^{1/3}$	A_t/A_o	m/m_o	$1 - m/m_o$
0	1.58	2.34	20.21	9.95	2.15	0	1	1	0
5	1.48	2.14	17.14	7.79	1.98	0.17	0.85	0.78	0.22
10	1.38	2.03	15.27	6.54	1.87	0.28	0.75	0.66	0.34
15	1.26	1.87	12.89	5.07	1.72	0.43	0.64	0.51	0.49
20	1.10	1.71	10.50	3.70	1.54	0.60	0.52	0.37	0.63

Appendix : C

BASIS PARAMETERS FOR CALCULATION

Diffusion coefficience of different type of additives

Acid	DA_B : (cm/sec)		
	20°C	25°C	30°C
Oxalic	1.53×10^{-5}	1.67×10^{-5}	1.895×10^{-5}
Succinic	8.229×10^{-6}	0.94×10^{-5}	1.067×10^{-4}
Borric	-	1.21×10^{-5}	1.3736×10^{-5}
Benzoic	-	-	0.8341×10^{-5}

Saturation Coefficients of different type of additive

Acid	C_S : g/l		
	20°C	25°C	30°C
Oxalic	0.09	0.144	0.20
Succinic	0.06	-	-
Borric	-	-	0.0635
Benzoic	0.0034	-	-

Viscosity of water at different temperature

Water	μ_{H_2O} (g/cm.sec)		
	20°C	25°C	30°C
	0.01	0.008904	0.007975

Appendix : D

GENERAL INFORMATION FOR HIGH TEMPERATURE EXPERIMENTS

1 - Copper dissolved in Aluminium bath

2 - Graphite Crusible dimensions: ϕ_{mean} : 54.5 m.m.
High : 81.5 m.m.

3 - Type of furnace : Resistance coil

4 - Lance dimension : ϕ_{in} : 1 m.m.
L = 400 m.m.

5 - Gas Injection : Nitrogen

6.- Instrument to measure Temperature: Digital millivoltmeter

7 - Bath Temperature = [mv out side crusible + mv. room temperature + erro of instrument] - 5.36.

5.36 is number of mv. different between inside and out side crusible.

TABLE: I

Experimental No.	Room Temperature	Error of Digital & Voltmeter (mV)	mV outside crucible	T°C melt (mean)	Time (min.)	m_o (gms)	m_t (gms)	wt% of Cu dissolved in Al bath	Melt weight (gms)	mV inside crucible	T° melt
1.	20	0.95	31.85/ 32.05	681	15	5.59	5.5312	1.0518	300	28.24/ 28.44	679/683
2.	20	0.94	33.9/ 34.15	730	15	5.97	5.75	3.68	276	30.28/ 30.53	727/733
3	26	0.66	35.88/ 36.17	777.5	15	5.12	4.73	7.617	283	32.22/ 32.51	774/781
4	27	0.66	37.92/ 38.3	829.5	15	4.4	4.00	9.09	325	34.3/ 34.68	825/834
5	27	0.66	37.86/ 38.4	829.5	15	5.7	5.02	11.929	351	34.24/ 34.78	823/836
6	30	0.66	31.92/ 32.23	686.5	3	5.228	4.814	7.918	354	28:42/ 28.73	683/690
7	30	0.66	33.75/ 34.22	732	3	5.80	5.082	12.38	352	30.25/ 30.72	726/738
8	30	0.66	35.91/ 36.18	781.5	3	5.325	4.575	14.084	345	32.41/ 32.68	778/785
9	30	0.66	37.83/ 38.35	831.5	3	5.91	5.001	15.38	349.4	34.33/ 34.85	825/838

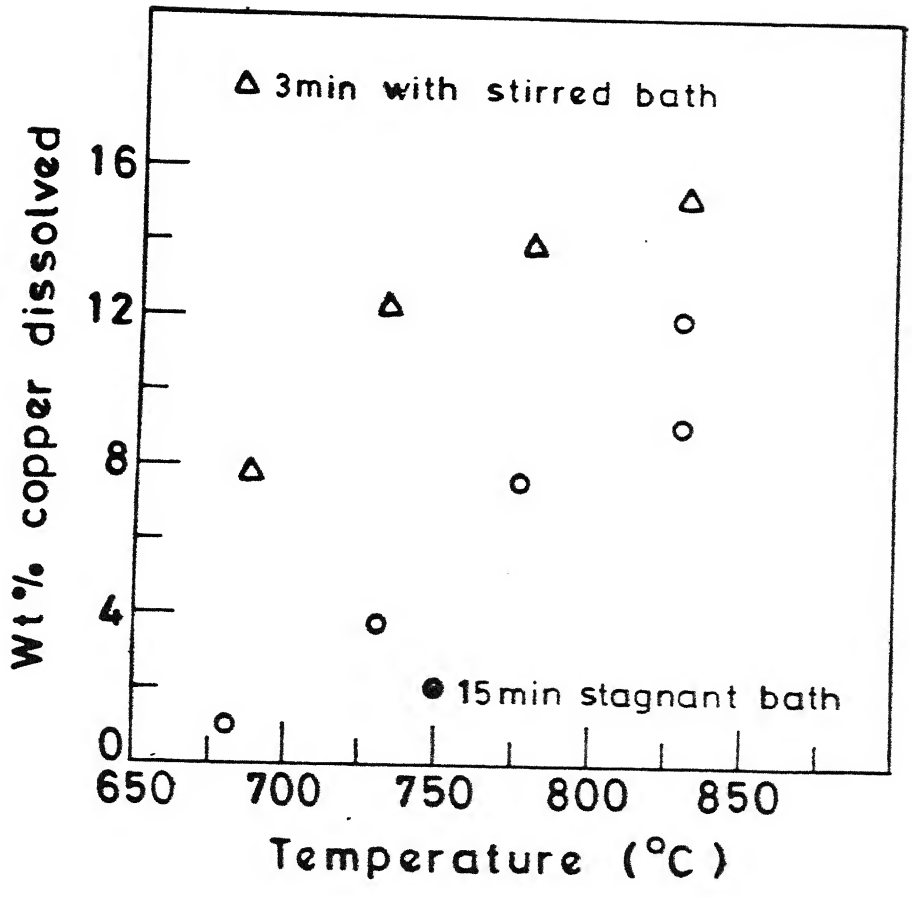

Fig. 35. Wt% copper dissolved in Aluminium bath vs. different temperatures (with Stirred bath and Stagnant bath).

Appendix E

Calculation of time required for dissclution of Molybdenum sphere in liquid steel

$$Sh_o = 0.1\ (G_{TM} \cdot S_c)^{1/3} \qquad (1)$$

Sh_o is SHRWOOD Number in stagnant bath

where G_{TM} is Grasshof Number

$$G_{TM} = \frac{\rho_L \cdot \beta \cdot g \cdot \Delta x \cdot L^3}{2} \qquad (2)$$

ρ_L is density of liquid steel = 7.1 (g/ cm^3)

ρ_{Mo} is density of molybdenum 10.0 (g/cm^3)

$$= \frac{\rho_{Mo} - \rho_L}{1\ mol} = \frac{10.0 - 7.1}{1} = 2.9$$

g is acceleration activity

= 981 (cm/sec^2)

ΔX is concentration difference

$\Delta X = 0.38$

L is diameter of Molybdenum pellet (in cm)

μ is viscosity of liquid steel = 0.064 (poise)

$$G_{TM} = \frac{7.1 \times 2.9 \times 981 \times 0.38 \times L^3}{(0.064)^2} = 1873911\ L^3$$

S_c is Schemidt number

$$S_c = \frac{\mu_{Steel}}{\rho_{steel} \cdot D_{Mo-Fe}} \qquad (3)$$

where D_{Mo-Fe} is diffusion coefficient of Molybdenum in iron bath

$$D_{Mo-Fe} = 3.2.10^{-5}\ (cm^2/sec)$$

$$S_c = \frac{0.064}{7.1 \times 3.2 \times 10^{-5}} \simeq 282$$

$$Sh_o = 0.1\ (G_{TM} \cdot S_c)^{1/3}$$

$$= 0.1\ (1873911 \cdot L^3 \cdot 282)^{1/3} = 81.L$$

The total dissolution time of M_o in iron bath is calculated following

$$t_T = \frac{r_o \cdot Mo}{K_N \cdot C_S} \qquad (4)$$

where r_o is radius of M_o pellet

C_S is saturation of M_o in iron bath at 1600°C

$C_S = 0.044 \times 96 = 4.224\ (g/cm^3)$

K_N is mass transfer coefficient

$$K_N = \frac{D_{Mo-Fe}\ Sh_o}{L} \qquad (5)$$

Putting K_N in eq. 5 into eq. (4) we get:

$$t_T = 147964 \cdot \frac{r_o^2}{Sh_o}$$

$$\text{or}\quad t_T = \frac{147964 \cdot r_o^2}{81.L} = \frac{147964 \cdot r_o^2}{81 \times 2\ r_o}$$

$$t_T = 913.36 \cdot r_o \cdot (\text{Sec.})$$

$$\text{or}\quad t_T = 15.22 \times r_o\ (\text{min.})$$

M_o pellet radius (cm) r_o	Sh_o	t_T (in min.)
1	162	15.22
2	324	30.44
3	486	45.66
4	648	60.89
5	810	76.11
6	972	91.33

APPENDIX G : PHOTOGRAPHS

Photograph 1 : Influence of the positions of additives to the fractional mass dissolved gas flow rate = 2.2 NL/min. T^{o} = 30 °C ; r = R ; Z = 0 and Z = H/2.

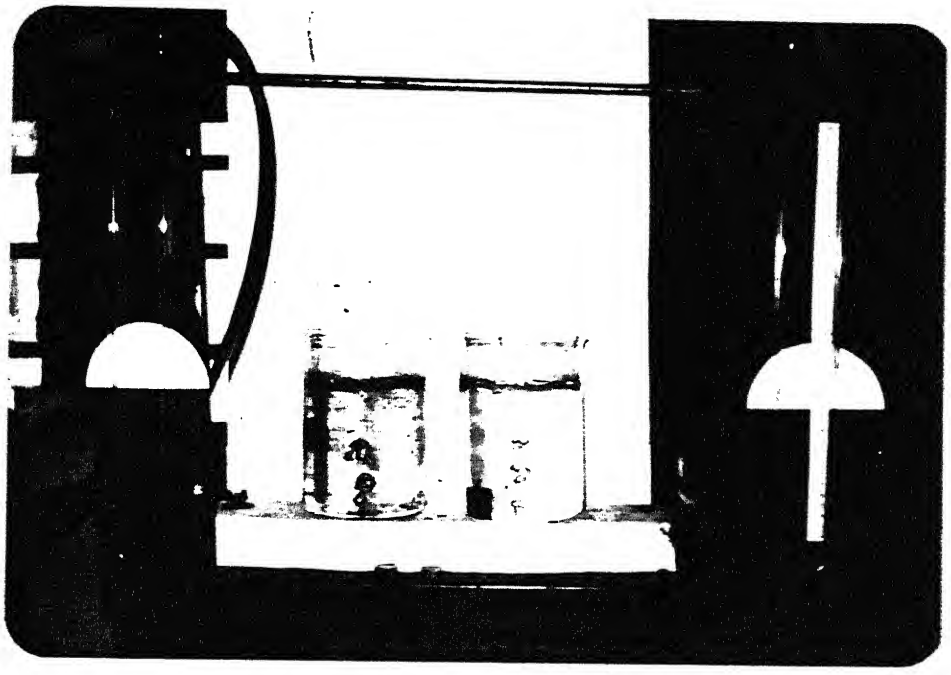

Photograph 2 : Influence of the positions of additives to the fractional mass dissolved gas flow rate = 2.2 NL/min. T^{o} = 30 °C ; r = R ; Z = H/2 and Z = H.

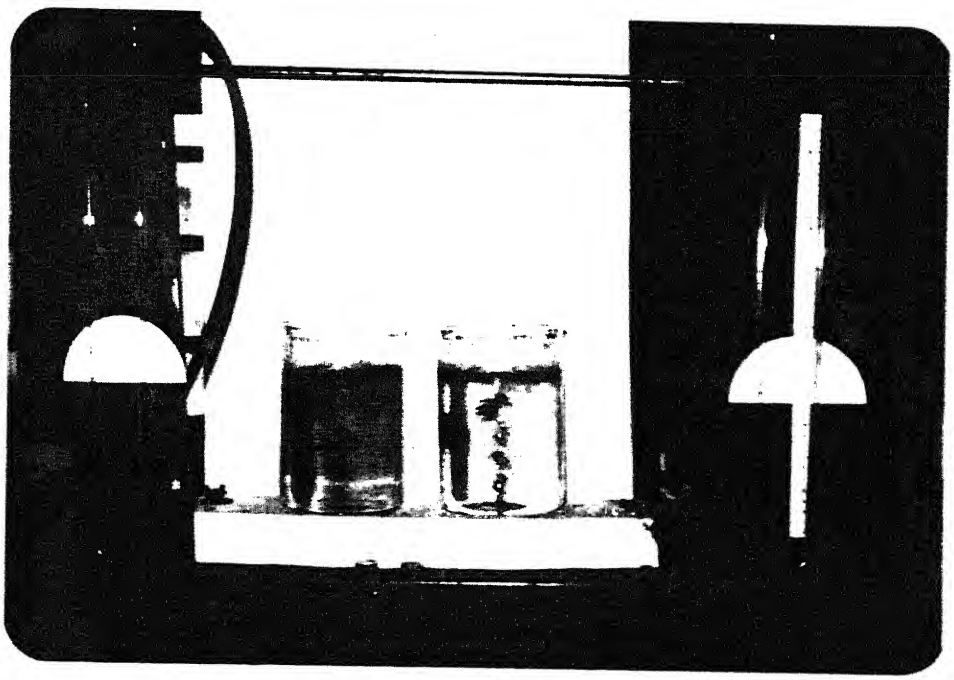

Photograph 3 : Influence of the positions of additives to the fractional mass dissolved; Gas flow rate = 2.2 NL/min.
T^{o} = 30°C; r = 0; Z = 0 and Z = H/2.

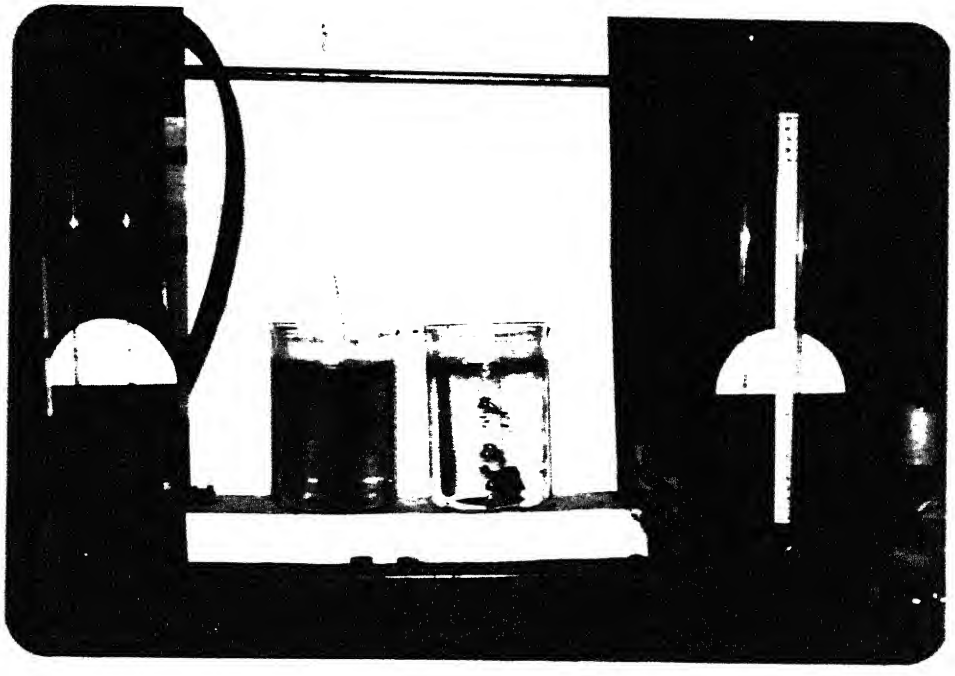

Photograph 4 : Influence of the position additive to the fractional mass dissolved; Gas flow rate = 2.2 NL/min.
T^{o} = 30°C; r = 0; Z = H/2. and Z = H.

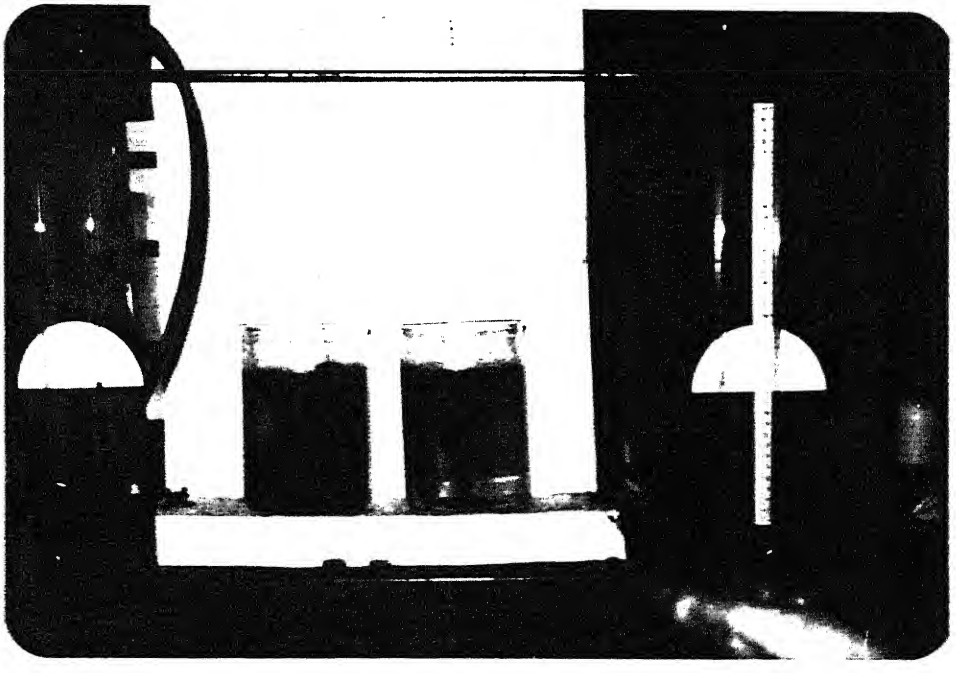

Photograph 5 : Influence of the positions of additives to the fractional mass dissolved; Gas flow rate = 2.2 NL/min T^{o} = 30°C, r = 0 and r = R; Z = H.

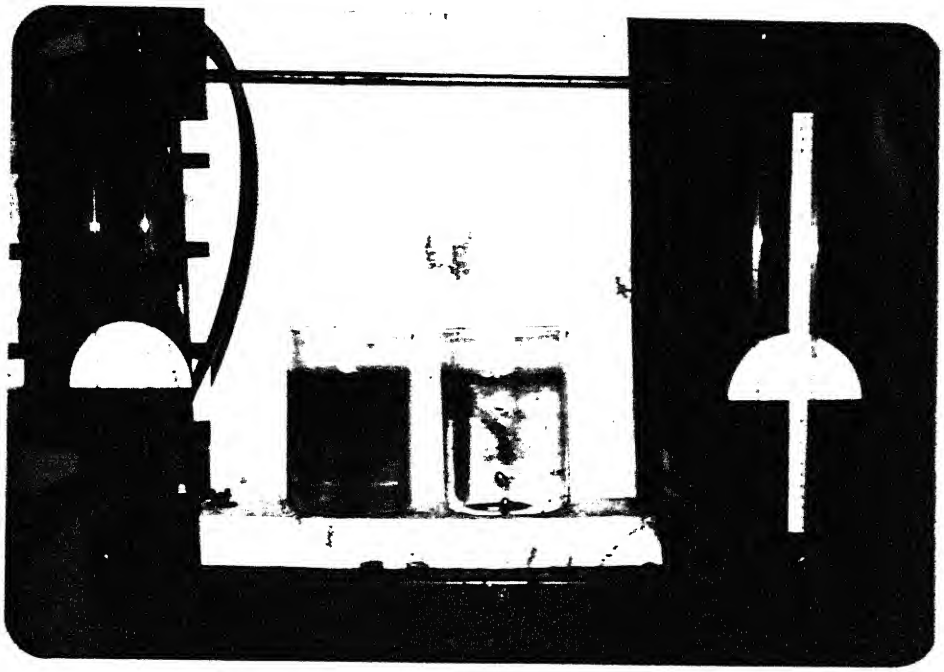

Photograph 6 : Influence of the initial weight of additives to the fractional mass dissolved; Gas flow rate = 2.2 NL/min. T^{o} = 30°C, r = R; Z = H; Wt_{o_1} = 5 grams; Wt_{o_2} = 10 grams.

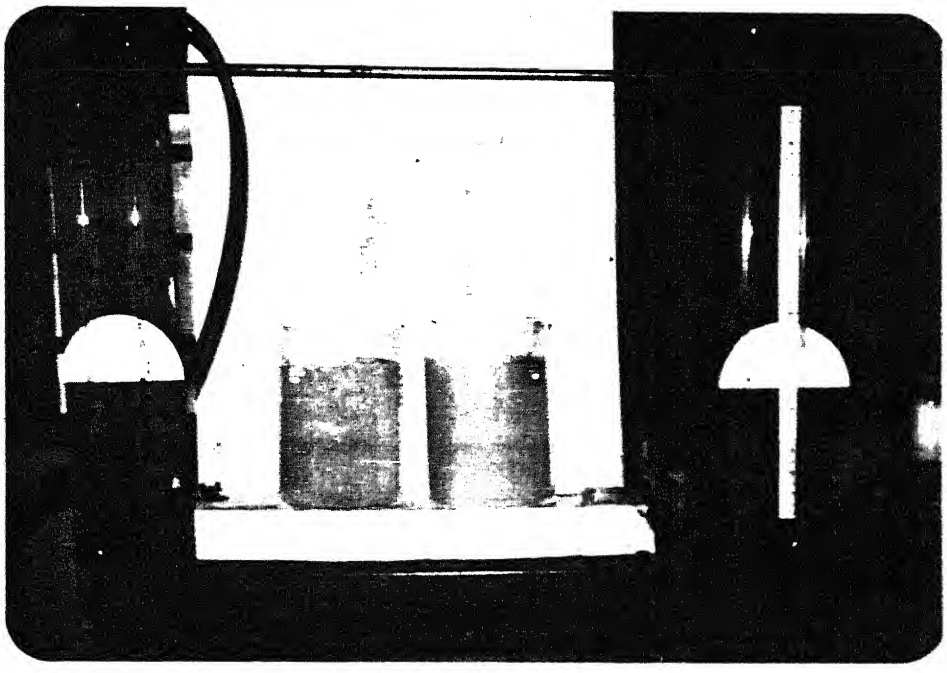

REFERENCES

1. S.A. Argyropoulos and R.I.L. Guthrie: 65th Steelmaking Conference Proceedings, ISS-AIME (1982) pp. 156-171.

2. S.A. Argyropoulos, and R.I.L. Guthrie: Met. Trans. 15B (1984) pp.47-58.

3. L. Gourtsoyannis, R.I.L. Guthrie and G.A. Ratz: 65th Steelmaking Conference proceedings, ISS-AIME, (1982) pp.119-132.

4. R.I.L. Guthrie: SCANINJECT, 2nd Internation Conference on Injection Metallurgy, MEFOS and Jernkentert (1980) pp.6.1-6.31.

5. R.I.L. Guthrie and P. Stubbs: Can. Met. Quarterly 12(1973) pp. 465-473.

6. S.C. Koria and C.D. Khai: To be published in Trans. Indian Institute of Metals (1987).

7. M.Eisenberg, C.W. Tobias and C.R. Wilke: A.I. Ch.E. Symp. Ser, 51(1951) pp 1-16.

8. P.L.T. Brian and H.B. Hales: AICHE Journal. Vol 15, No.3 (1969) pp.419-425.

9. A.W. Hixson and J.H. Crowell, Ind. and Eng. Chemistry vol.23, No.8 (1931) pp.923-930.

10. J.J. Baker and R.E. Treybal: AICHE Journal vol.6 No.2 (1960) pp.289-295.

11. M. Sevinc and J.F. Elliot: Ironmaking and Steelmaking 3(1976) pp.268-278.

12. J.Szekely, T. Lehner and C.W. Chang: Ironmaking and Steelmaking 6(1979) pp. 285-293.

13. Y.S.C. Uchida and T. Ariga: Metall. Trans. Vol 13B(1982) pp.339-444.

14. S. Orsten and F. Oeters: Proceedings Fifth intern.Iron and Steel Congress: Process Techn. Washington DC vol.6(1986) pp.143-155.

15. D.A. Stevenson and J. Wulff. Trans. of the Metall. Soc. of AIME Vol 221 (1961) pp. 279-285.

16. T. Ishida Trans. JIM Vol. 14(1973) pp. 37 - 44.

17. T. Ishida Metall. Trans. B Vol. 17B (1986) pp. 281-305.

18. R.Ohno, M. Kagawa and T. Hasmin Trans. JIM vol 14 (1973) pp. 140-147.

19. S.A. Argyropoulos and R.I.L. Guthrie: Metall.Trans.B Vol 15B (1984) pp.48-57.

20. D.Majumdar and R.I.L. Guthrie: Ironmaking and steelmaking 12(1985) pp 256-264.

21. D.Majumdar and R.I.L. Guthrie: Met.Trans. 16B (1985) pp 83-90.

22. Y.Sahai and R.I.L. Guthrie: Met.Trans. 13B (1982) pp.192-211.

23. Y.Sahai and R.I.L. Guthrie: Int. Symp. on Modern Developments in Steelmaking, Jamshedpur, India (1981) pp.1.5.1 to 1.5.24.

24. H.Abratis and H-J Langhammer: SCANINJECT, 2nd International Conference on Injection Metallurgy, MEFOS and Jernkontert (1980) pp.27.1-27.18.

25. S.C. Koria and K.W. Lange: Met.Trans. 15B (1984) pp.109-116.

26. S.C. Koria and K.W. Lange: Arch. Eisenhuttenwes. 55(1984) pp 97-100.

27. S.C. Koria and K.W. Lange: Proc 6th Japan-Germany Seminar, Tokyo, (1984) pp. 91-101.

28. T.Miyahara, H.Terkakado and T.Takaharhi: J. of Chemical Engg. Japan 16(1983) pp.454-458.

29. S. Asai, M. Kawachi and I. Muchi: SCANINJECT, 3rd International Conf. on Injection Metallurgy, MEFOS and Jernkontoret (1980) pp.11.1-11.30.

30. D.A. Steversen and J. Wulff: Trans. Met. Soc.AIME 221 (1961) pp.279-285.

31. R.L. Steinberger and R.E. Treybal: A.I.Ch.E.Jl.V.6 (1960) pp.227-232.

32. M. Kosaka and S. Minowa: J. Iron Steel Inst. Japan V. 53 (1967) pp. 983-987.

Date Slip

This book is to be returned on the date last stamped.

.....	.....	...
.....	.....	...
.....	.....	...
.....	.....	...
.....	.....	...
.....	.....	...
.....	.....	...
.....	.....	...
.....	.....	...
.....	.....	...
.....	.....	..
.....	.....	...